UNIVERSIDADE FEDERAL DO RIO GRANDE DO SUL

INSTITUTO DE CIÊNCIAS BÁSICAS DA SAÚDE

PROGRAMA DE PÓS-GRADUAÇÃO EM CIÊNCIAS BIOLÓGICAS:

BIOQUÍMICA

CARACTERIZAÇÃO FUNCIONAL DE MODELOS DE CULTURA DE ASTRÓCITOS E MECANISMO DE INTERNALIZAÇÃO DA PROTEÍNA S100B

Fabiana Andrea Barrera Galland

Orientadora: Profa. Dra. Marina Concli Leite

Porto Alegre

2017

CARACTERIZAÇÃO FUNCIONAL DE MODELOS DE CULTURA DE ASTRÓCITOS E MECANISMO DE INTERNALIZAÇÃO DA PROTEÍNA S100B

Fabiana Andrea Barrera Galland

Orientadora: Profa. Dra. Marina Concli Leite

Tese apresentada ao Programa de Pós-Graduação em Ciências Biológicas: Bioquímica da Universidade Federal do Rio Grande do Sul, como requisito parcial à obtenção de grau de Doutor em Bioquímica.

Porto Alegre

2017

CIP - Catalogação na Publicação

Barrera Galland, Fabiana Andrea
Caracterização Funcional de Modelos de Cultura de Astrócitos e Mecanismo de Internalização da Proteína S100B / Fabiana Andrea Barrera Galland. -- 2017.
163 f.

Orientadora: Marina Concli Leite.

Tese (Doutorado) -- Universidade Federal do Rio Grande do Sul, Instituto de Ciências Básicas da Saúde, Programa de Pós-Graduação em Ciências Biológicas: Bioquímica, Porto Alegre, BR-RS, 2017.

1. Astrócitos. 2. Endocitose. 3. S100B. 4. Glutamina Sintetase. I. Concli Leite, Marina, orient. II. Título.

Elaborada pelo Sistema de Geração Automática de Ficha Catalográfica da UFRGS com os dados fornecidos pelo(a) autor(a).

Dedico esta tese aos meus pais, que são minha maior referência

“A ciência nunca resolve um problema sem criar pelo menos outros dez”.

(George Bernard Shaw)

Agradecimentos

Aos meus pais Andres e Griselda pelo amor incondicional, pela torcida e incentivo constante, por serem meus exemplos de vida!

Às minhas irmãs Lê e Eli por serem meus orgulhos, minhas inspirações e as melhores amigas que a vida poderia ter me dado! E por me dar o presente de ser tia de dois pitoquinhos que estão a caminho para alegrar ainda mais essa família!

Ao meu amor Maicon por todo apoio e incentivo. Por me ensinar a lutar por aquilo que quero fazendo-me mais forte e tornando a minha jornada mais leve e divertida! Te amo!

À Mara por ser minha segunda mãe, por torcer muito por mim sempre!

À minha amiga da vida, Maíra, por estar sempre do meu lado e ter me dado de presente a minha afilhada linda, Melissa!

Aos meus sogros Nice e Seu Machado pelo carinho e torcida!

Ao pessoal da Eslovênia que contribuiu para fazer do meu Doutorado Sanduíche inesquecível!

Às minhas amigas/colegas do laboratório (Caroll, Fezinha, Jéssica, Jé, Marina e Gabriel) por fazer meus dias mais divertidos e ser um ótimo grupo de trabalho! Em especial às que se dedicaram a esta tese com muito empenho e dedicação, Marina Seady e a Jéssica Taday! Sem vocês a realização deste trabalho teria sido muito mais difícil!

À todo o pessoal do laboratório 33, bolsistas e pós graduandos por nos incluir, e compartilhar formando um super grupo de trabalho alegre e divertido! Em especial a Fê Hansen, pela grande amizade, troca de conhecimentos e confiança!

Ao CA por ser um super co-orientador, com toda sua experiência, sabedoria encarando os problemas sempre de forma tão leve! Obrigada por toda ajuda!

Por fim, à quem não poderia faltar, a Marina, minha querida orientadora! Obrigada por todos os teus ensinamentos, desde os tempos de IC, pela tua paciência, dedicação, pelas horas de conversa sérias, mas também por aquelas de diversão! Obrigada principalmente pela tua confiança. Certamente, tu és uma inspiração a seguir na minha vida acadêmica!

Índice

Lista de Abreviaturas 3
1. Introdução 4
1.1. Astrócitos 4
1.1.1. Origem 4
1.1.2. Morfologia 5
1.1.3. Proteínas marcadoras 6
1.1.4. Funções 7
1.1.4.1. Papel no desenvolvimento cerebral 8
1.1.4.2. Regulação do fluxo sanguíneo, barreira hematoencefálica (BHE) e angiogênese 8
1.1.4.3. Manutenção do ambiente extracelular: fluído, íons e pH 9
1.1.4.4. Papel dos astrócitos na função sináptica 11
1.1.4.5. Metabolismo energético nos astrócitos 13
1.1.4.6. Astrogliose e doenças neurodegenerativas 14
1.2. S100B 15
1.2.1. Efeitos intracelulares da S100B 16
1.2.2. Efeitos extracelulares da S100B 17
1.2.3. Mecanismos de internalização 20
1.3. Glutamina Sintetase 22
1.4. Modelos de astrócitos 26
2. Justificativa 30
2.1. Objetivo Geral 31
2.2. Objetivos Específicos 31
3. Resultados 32
3.1. Capítulo I 32
Molecular and functional characterization of primary culture of astrocytes, immortalized astrocytes and C6 glioma cells. 32
3.2. Capítulo II 65
Time-dependent uptake and trafficking of vesicles capturing extracellular S100B in cultured rat astrocytes 65
3.3. Capítulo III 81
Standardization of a routine protocol for glutamine synthetase activity in astrocytes and cerebral tissue, using glutamyl-transferase activity 81
4. Discussão 105

4.1. Caracterização molecular e funcional de cultura primária de astrócitos, astrócitos imortalizados e glioma C6. 105
4.1.1. Avaliação da morfologia basal e plasticidade após estímulo 105
4.1.2. Perfil molecular dos diferentes modelos de astrócitos 106
4.1.3. Caracterização funcional do metabolismo do glutamato em modelo de astrócitos 108
4.1.4. Comparação do metabolismo energético e comunicação por junção gap em modelos de astrócitos 110
4.1.5. Avaliação de resposta nos modelos de cultura de astrócitos 111
4.1.6. Escolha do modelo de cultura de astrócitos 113
4.2. Internalização tempo-dependente da S100B extracelular e análise da movimentação de vesículas em cultura de astrócitos 115
4.2.1. Mecanismo de internalização da S100B em cultura de astrócitos 115
4.2.3. A mobilidade das vesículas S100B-Alexa^{488} é alterada pelo estímulo com ATP 119
4.2.4. Regulação da S100B por endocitose 121
4.3. Padronização de ensaio colorimétrico para dosagem de atividade da GS 124
5. Conclusões 127
6. Perspectivas 130
7. Referências Bibliográficas 131

Resumo

Os astrócitos são células gliais do sistema nervoso central (SNC) que, entre diversas funções, tem um importante papel na manutenção do ambiente extracelular, removendo neurotransmissores e íons os quais podem ser tóxicos em altas concentrações. Estas células estão envolvidas em diversas doenças neurodegenerativas e representam um importante alvo de estudo para o desenvolvimento de estratégias terapêuticas. A técnica de cultura primária (CP) de astrócitos de ratos é amplamente utilizada como modelo para o estudo de características mecânicas e bioquímicas dessa célula em um sistema isolado. Alternativamente, astrócitos imortalizados por transfecção (AI) e a linhagem C6 de rato (C6) são usados como modelo astrocítico, uma vez que são células mais homogêneas, além de serem de fácil e rápida manipulação. No entanto, apesar de resultados divergentes serem encontrados na literatura, existe uma carência de estudos comparativos entre estes três modelos experimentais. A escolha de um modelo adequado para o estudo destas células nos permitiria estudar de forma mais precisa as funções extracelulares de proteínas como a S100B. Essa proteína pode ser liberada ou secretada principalmente por astrócitos no SNC e, apesar de possuir efeitos tróficos, exerce funções tóxicas, quando em altas concentrações no meio extracelular. Apesar disso, pouco se sabe sobre o processo de remoção da S100B extracelular. Em vista disso, o objetivo desta tese foi comparar e caracterizar funcionalmente a CP, AI e C6 no que diz respeito a diferenças morfológicas, marcadores proteicos e funções clássicas astrocíticas, bem como estudar a capacidade destas células de internalizar a proteína S100B, avaliando-se o mecanismo deste processo. Além disso, foi realizada a padronização de um ensaio colorimétrico utilizando a atividade glutamil-transferase da glutamina sintetase (GS), visto a carência deste ensaio em cultura de astrócitos e em diferentes estruturas cerebrais. Esta enzima é considerada um marcador astrocítico e sua disfunção pode comprometer o ciclo glutamina-glutamato, processo relacionado ao quadro de excitotoxicidade glutamatérgica, observado em doenças neurodegenerativas. O ensaio mostrou-se preciso, sensível, linear, específico e com alta aplicabilidade no SNC e nos modelos de cultura celular. Nossos resultados mostraram que as duas linhagens celulares (AI e C6) foram positivas para proteínas características de astrócitos, bem como funcionais no metabolismo glutamatérgico e energético. No entanto, estes parâmetros mostraram-se reduzidos em estado basal em comparação com a CP. Frente a estímulos específicos, os AI não se mostraram como um modelo reprodutível das funções astrocíticas clássicas, ao contrário da linhagem C6, a qual apresentou resposta similar aos astrócitos de CP. De forma geral a linhagem C6 representou um modelo válido para estudo das características astrocíticas estudadas, porém sempre com valores basais reduzidos quando comparados com a CP que, em nossa avaliação, representou um melhor modelo para o estudo da internalização da proteína S100B. Estas células foram capazes de endocitar a S100B extracelular por um mecanismo dependente de RAGE e dinamina. Uma vez internalizada, a S100B seguiu pela via endocítica, colocalizando com importantes marcadores, como Dextran e Lysotracker. As vesículas de S100B mostraram um aumento de direcionalidade ao longo do tempo de incubação, afetado pela variação de cálcio intracelular. Estes dados mostram a importância da escolha de um modelo *in vitro* adequado de cultura de astrócitos, bem como evidenciam o importante papel destas células na remoção de concentrações tóxicas da proteína S100B do meio extracelular, auxiliando na compreensão dos mecanismos de sinalização desta proteína.

Abstract

Astrocytes are glial cells that participate in a variety of function of central nervous system (CNS) such as the maintenance of the extracellular environment, removing toxic concentration of ions and neurotransmitters. These cells are involved in several neurodegenerative diseases and are important targets for the development of therapeutic strategies. Astrocyte primary culture (PC) is a potent instrument to study these cells in an isolated system, allowing the elucidation of mechanistic features specific for this type of cell. An alternative to this model is the use of cell lines, such as immortalized astrocytes (IA) or C6 glioma cells (C6). These linages have the advantage to present more homogeneous features, are easily, faster and lower cost to manipulate. Despite these facilities, cell lines present highly proliferative features and some different characteristics in comparison to PC, which put into question the validity of them as an astrocytic model. The selection of a suitable model to the study of astrocytes would allow us to evaluate protein extracellular effects, such as S100B with greater reliability. This protein is released and secreted mainly by astrocytes in the CNS, exerting trophic and toxic effect in a RAGE dependent manner. S100B toxic effects are shown in high extracellular concentrations, although the clearance of this protein from the extracellular space is poorly understood. In view of this, the goal of this research was to show a comparative analysis of PC, IA and C6 regarding morphological features, protein profile and classical astrocytic functions. Furthermore, we evaluated the mechanism of S100B internalization, characterization of internalized vesicles and intracellular dynamics in astrocytes. In addition, the standardization of a colorimetric assay to measure the glutamyl-transferase activity of glutamine synthetase (GS) was performed, considering the lack of this study in culture of astrocytes and different brain structures. This enzyme is considered an astrocytic marker and any dysfunction may compromise the glutamine-glutamate cycle, which is observed in many neurodegenerative diseases. The assay was accurate, sensitive, linear, specific and with high applicability in the CNS. Our results showed that the two cell lines (IA and C6) were positive for characteristic proteins of astrocytes, although expressing less quantities then PC. Similarly, the glutamatergic and energetic metabolism and cellular communication by gap junction also showed to be reduced in lineages cells. IA did not reveal a reproducible model of classic astrocytic functions, in opposite to C6 cells that presented a similar response to PC when submitted to the same stimulus. Nevertheless, PC showed pronounced astrocytic characteristics, representing the best model for the study of S100B protein internalization. The results in this study revealed that cultured astrocytes efficiently remove fluorescently labeled extracellular S100B in a time-dependent manner by vesicle endocytosis. The internalization was RAGE and dynamine dependent. In time, vesicles capturing S100B exhibit directional mobility, meaning that vesicles get functionally attached to the cytoskeleton. Moreover, the mobility of vesicles capturing S100B was affected by changes in $[Ca^{2+}]$. These data support to the understanding of the mechanism of extracellular signaling of S100B protein, as well as the role of astrocytes in this regulation.

Lista de Abreviaturas

ANP – peptídeo natriurético atrial

AMPc - monofosfato cíclico de adenosina

AQP4 – aquaporina-4

ALDH1L1- membro da família L1 da aldeido desidrogenase 1 (*aldehyde dehydrogenase 1 family member L1)*

BDNF - fator neurotrófico derivado do cérebro

BHE – barreira hematoencefálica

Cx43 – conexina-43

EAAT – transportador de aminoácidos excitatórios

ERO – espécies reativas de oxigênio

GABA – ácido gamaaminobutírico

GFAP – proteína ácida fibrilar

GLAST- transportador glutamato-aspartato

GLUT1 – transportador de glicose

GS – glutamina sintetase

IL – interleucina

iNOS – óxido nítrico sintase induzível

LCR - líquor

MSO – monoamina oxidase

NGF – fator de crescimento nervoso

RAGE – receptor para produtos finais de glicação avançada

SNC – sistema nervoso central

TNF-α – fator de necrose tumoral α

1. Introdução

1.1. Astrócitos

O sistema nervoso central (SNC) é formado pelas células neuronais e gliais. Por sua vez, as células gliais são divididas em micróglia e macroglia. Ainda, a macroglia é composta por outros três tipos células: os oligodendrócitos, células de Schwann e astrócitos.

Entre as células gliais, os astrócitos são as mais abundantes. A razão astrócitos/neurônio aumenta com a evolução das espécies, assim como a estrutura, morfologia e diversidade entre espécies, indicando a importância destas células no desenvolvimento de sistemas neurais mais sofisticados (Leuba & Garey 1989, Vasile *et al.* 2017). O nome deriva da palavra grega para estrela (*astron*) junto com (*cyte*) de célula, devido ao fato de semelhar-se a uma estrela quando descoberta no início do século 20. Primeiramente foi descrita como uma célula passiva, servindo como suporte estrutural de neurônios. Atualmente, é considerada como participante ativa nos circuitos cerebrais e no processamento, apresentando um grande espectro de funções a nível celular, tais como a formação, maturação e eliminação de sinapses, homeostase iônica, depuração de neurotransmissores, regulação do volume no espaço extracelular e modulação da atividade sináptica e plasticidade neuronal (Kimelberg & Nedergaard 2010, Vasile et al. 2017).

1.1.1. Origem

A gliogênese inicia-se tarde no desenvolvimento embrionário após o início da formação neuronal. Os astrócitos originam-se de três fontes distintas: de células glia-radial da zona ventricular durante a vida perinatal, progenitores da zona subventricular durante a vida embrionária, e progenitores glia-restritos durante a vida pós-natal e na

vida adulta. Durante a vida perinatal as células tronco neurais sofrem uma mudança no desenvolvimento passando a fazer parte da gliogênese e não mais da neurogênese. Nesta mudança passam a expressar alguns marcadores astrocíticos como o GLAST (*glutamate aspartate transport*), transportador de glutamato. Estas células parecem migrar ao longo da glia radial até certo estágio do desenvolvimento, onde acredita-se que outra leva de precursores astrocíticos passem a regular o processo. No entanto, os processos moleculares e celulares que ocorrem nesta fase ainda são desconhecidos. (Molofsky & Deneen 2015). O processo de diferenciação em astrócitos é de difícil estudo, devido a variedade de marcadores moleculares característicos deste tipo celular, os quais são expressos em um subtipo de astrócito, porém não em outros. Sabe-se que após a migração e antes da maturação funcional e morfológica os astrócitos passam a expressar algumas proteínas marcadoras como GFAP, S100B, ALDH1-L1. Esta diversidade de linhagens astrocíticas, sugere que os astrócitos não são formados da mesma maneira, o que explicaria a diversidade destas células em relação à localização, morfologia e expressão gênica (Wang & Bordey 2008).

1.1.2. Morfologia

Assim como sua origem, os astrócitos maduros apresentam morfologia heterogênea, com três principais variantes: a forma esférica espessa em processos, chamado de protoplasmáticos, presentes na substância cinzenta, representando a forma mais abundante; a forma menos carregada em processos, chamados de fibrosos da substância branca e; a forma alongada com poucos processos, representados pelas células de Bergmann no cerebelo e as células de Müller na retina. Os processos finos e longos dos astrócitos fibrosos envelopam os nódulos de Ranvier, enquanto que os processos presentes nos astrócitos protoplasmáticos estão em contato com os vasos

sanguíneos (pés-terminais), assim como com os neurônios. Os processos astrocíticos se infiltram, na forma de lamelas e fibras, entre a intrincada rede de processos neurais incluindo terminais sinápticos, dendritos e espinhos dendríticos. Observou-se que o tamanho e a quantidade de processos em astrócitos podem variar com o aumento da complexidade das funções cerebrais ao longo da escala evolutiva (Wang & Bordey 2008, Kimelberg & Nedergaard 2010).

1.1.3. Proteínas marcadoras

Por serem células altamente heterogêneas, torna-se difícil a identificação dos astrócitos com apenas uma proteína característica. A identidade proteica pode variar dependendo da origem, local ou mesmo as condições do microambiente onde a célula se encontra. O filamento intermediário GFAP (*glial fibrilar acid protein*) foi a primeira proteína marcadora e ainda é a mais usada como característica de astrócitos maduros, apesar de que outras células também a expressem, porém em quantidades menores, como as células ependimais (Eng 1985). Apesar da maioria dos astrócitos expressarem GFAP, astrócitos negativos para esta proteína são detectados no SNC saudável. De fato, a sua expressão é variável, dependente da região do astrócito, sendo regulada por muitas moléculas presentes nos ambientes intra e intercelulares. No entanto, sua expressão é essencial para o processo de reatividade astroglial e formação de cicatriz glial (Sofroniew & Vinters 2010).

A proteína S100B, pertencente à família de proteínas S100 “EFhand” ligantes de cálcio, também é amplamente usada como proteína marcadora de astrócitos. Apesar disso, não é uma proteína exclusiva deste tipo celular, assim como nem todos os astrócitos maduros a expressam (Vives *et al.* 2003). Além disso, outras proteínas são abundantemente expressas em astrócitos, como os transportadores de aminoácidos

excitatórios EAAT1/GLAST e EAAT2/GLT-1. EAAT1 é mais presente em astrócitos em desenvolvimento, enquanto que EAAT2 é mais expresso nas células diferenciadas (Regan *et al.* 2007). A enzima glutamina sintetase (GS) também é altamente expressa em astrócitos, com a importante função no ciclo glutamina-glutamato (Bernstein *et al.* 2014), que será abordado mais adiante. Ainda, canais de potássio internalizadores, como Kir4.1, são altamente expressos nos pés terminais e nas regiões de contato sináptico de astrócitos (Seifert *et al.* 2016). Já, a proteína transportadora de água, aquaporina-4 (AQP4), está abundantemente expressa na membrana perivascular de astrócitos protoplasmáticos (Papadopoulos & Verkman 2013). No entanto, enquanto algumas destas proteínas são expressas por todos os astrócitos (ex. EAAT2), outras são expressas apenas por alguns subtipos desta célula (ex. Kir4.1). Devido a essa heterogeneidade entre as células astrocíticas é recomendado o uso de pelo menos dois marcadores proteicos para a identificação deste tipo celular. Recentemente, a enzima ALDH1L1 (*aldehyde dehydrogenase 1 family member L1)* vem sendo usada como um novo marcador astroglial específico, também conhecida como 10-formil tetrahidrofolato desidrogenase, a qual participa do metabolismo de folato (Yang *et al.* 2011, Cahoy *et al.* 2008).

1.1.4. Funções

Como vimos anteriormente, os astrócitos são células altamente heterogêneas, não só pela diversidade morfológica, expressando diferentes identidades moleculares, mas também pelas funções especializadas que esta célula é capaz de assumir de acordo com o microambiente onde se encontra. Apesar disso, algumas funções clássicas dos astrócitos são usadas para a sua identificação, as quais serão relatadas nesta sessão.

1.1.4.1. Papel no desenvolvimento cerebral

Apesar dos astrócitos se desenvolverem após a formação inicial dos neurônios, eles tem um importante papel no desenvolvimento dos neurônios da substância branca e cinza no SNC. Estas células gliais são a principal fonte de matriz extracelular, promovendo o crescimento de neuritos pela liberação de moléculas, tais como caderina e moléculas de adesão (Tomaselli *et al.* 1988); ou então inibindo o crescimento de neuritos pela liberação de proteoglicanos (Gonzalez *et al.* 1993). Além disso, astrócitos secretam vários fatores de crescimento, como BDNF (*brain derived neurotrophic factor*) e NGF (*nerve growth factor*), os quais controlam a maturação, diferenciação ou sobrevivência neuronal (Vaca & Wendt 1992). A proteína S100B, por exemplo, auxilia o crescimento de neuritos e protege os neurônios contra a excitotoxicidade glutamatérgica (Donato 2003).

Além disso, estudos mais recentes mostram o papel dos astrócitos na sinaptogênese, liberando moléculas que auxiliam na formação das sinapses ou ainda, induzem a eliminação delas pela micróglia (Christopherson *et al.* 2005). Na substância branca, a perda da função astrocítica ou da comunicação por junção gap induz processo de desmielinização (Lutz *et al.* 2009).

1.1.4.2. Regulação do fluxo sanguíneo, barreira hematoencefálica (BHE) e angiogênese

O posicionamento estratégico dos astrócitos em contato tanto com os vasos sanguíneos (pés terminais) assim como com as sinapses, permite que estas células regulem o fluxo sanguíneo de acordo com a atividade sináptica. Moléculas liberadas pelos astrócitos tais como prostaglandinas e oxido nítrico, podem variar o diâmetro dos vasos, aumentando ou diminuindo o fluxo sanguíneo (Gordon *et al.* 2007).

Ainda, o contato físico entre células endoteliais e os pés terminais de astrócitos, permite que estas células regulem indiretamente algumas propriedades da BHE, como por exemplo, a indução de super-expressão de proteínas das junções oclusivas ou transportadores de glicose (GLUT1) nas células endoteliais (Wang & Bordey 2008). Viu-se que a interação entre estes tipos celulares deve-se a sinalização por cálcio ativado por ATP. Como resultado, as variações de cálcio nas células endoteliais interferem na permeabilidade da BHE (Paemeleire & Leybaert 2000).

Além disso, astrócitos tem a capacidade de regular a formação de vasos sanguíneos - a angiogênese. Através da liberação de moléculas, tais como laminina ou fator de crescimento vascular endotelial, promovem a crescimento dos vasos (Laterra & Goldstein 1991).

1.1.4.3. Manutenção do ambiente extracelular: fluído, íons e pH

Os astrócitos tem a importante função de controlar o balanço eletrolítico do espaço extracelular, principalmente nas regiões em contato com as sinapses. Uma das principais atuações é no tamponamento de K^+, o qual é liberado pelos neurônios durante a neurotransmissão. O K^+ em excesso causa hiperexcitabilidade e, portanto, deve ser rapidamente removido pelos astrócitos, através de canais de potássio - como Kir, ou por transportadores $Na^{2+/}K^+$ ATPase que atuam em menor extensão (Fig 1). Uma vez captado os astrócitos redistribuem o íon, através de uma rede de células formada pelas junções gap, e o liberam em regiões com concentrações mais baixas de potássio, ou mesmo na circulação sanguínea pelos pés terminais (Olsen & Sontheimer 2008) (Leis *et al.* 2005, Wang & Bordey 2008). Destaca-se a importância das junções gap não só na participação da distribuição de K^+, mas também de outros íons, como cálcio, ou até de moléculas maiores como produtos do metabolismo energético, como veremos mais

adiante. Estas junções são formadas em astrócitos principalmente pela associação de moléculas de conexina 43 (Cx43) (Fig 1) (Rouach *et al.* 2002).

Além dos transportadores de K^+, os processos astrocíticos em contato com as sinapses são ricos em AQP4, tendo importante função na homeostase de fluídos tanto nesta região, quanto nos pés terminais em contato com vasos sanguíneos (King *et al.* 2004). Ainda, a membrana de astrócitos é rica em lançadeiras de prótons, incluindo o trocador $Na^{+/}H^+$ e transportadores de bicarbonato, controlando o pH extracelular (Deitmer & Rose 2010).

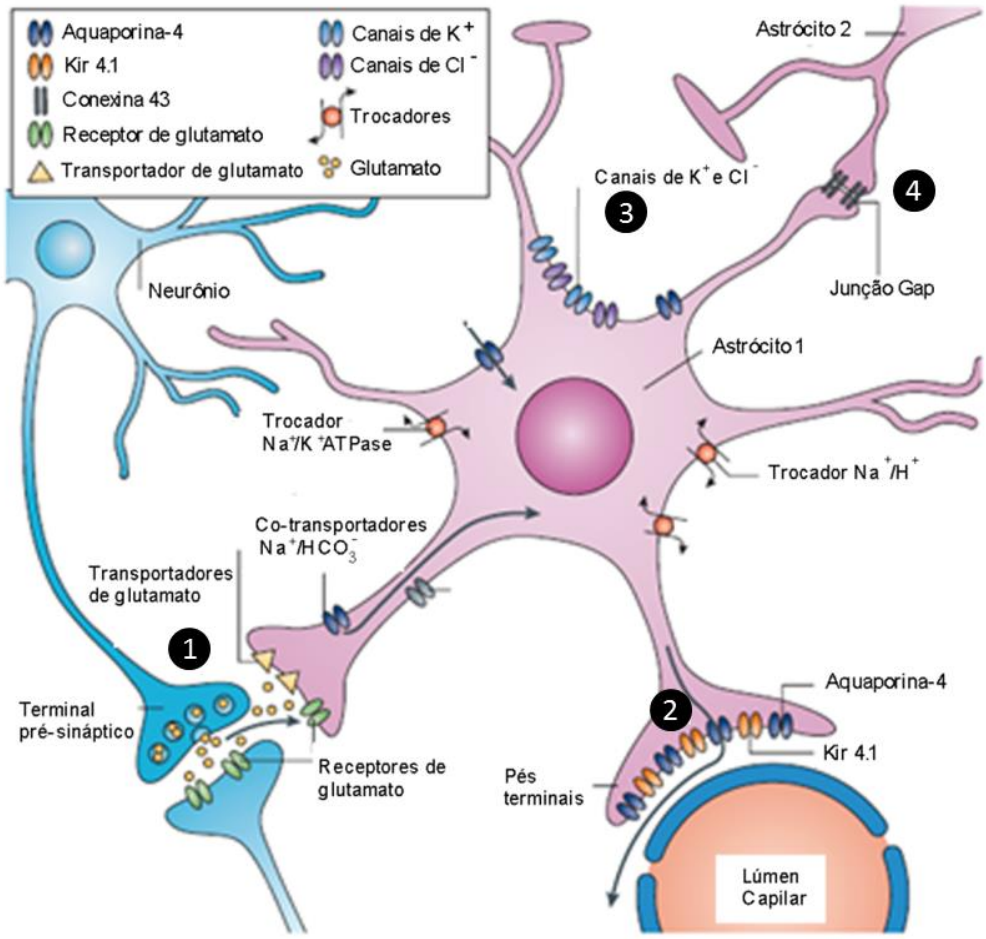

Fig 1. Representação das principais funções dos astrócitos. 1) Astrócitos atuando na sinapse tripartite; 2) Regulação do fluxo sanguíneo com a presença de aquaporina-4 e canais de potássio nos pés terminais; 3) Regulação da homeostase extracelular de íons e pH, apresentando canais de K^+, Cl^-, trocador Na^+/H^+ e co-transportadores de Na^+/HCO_3; 4) Comunicação por junção gap entre astrócitos, onde pode ocorrer a passagem de íons como o cálcio ou metabólitos energéticos, como o lactato. Figura modificada de (Seifert *et al.* 2006)

1.1.4.4. Papel dos astrócitos na função sináptica

É importante destacar que um único astrócito é capaz de cobrir centenas de milhares de sinapses em roedores e, este número pode ser de uma ordem de grandeza maior em humanos (Halassa *et al.* 2007, Oberheim *et al.* 2009). Esta ligação tão próxima entre astrócitos e neurônios permite que estas células gliais participem da homeostase de neurotransmissores, apresentando membranas ricas em transportadores de glutamato, ácido gama-aminobutírico (GABA) e glicina. A rápida captação de GABA, por exemplo, evita que o sinal inibitório se espalhe para outras regiões (Kinney & Spain 2002). Da mesma forma, os transportadores de glutamato EAAT1 e EAAT2, captam o neurotransmissor e através da atividade da GS o glutamato é convertido à glutamina (Fig 1). Uma vez produzida nos astrócito, a glutamina retorna para os neurônios para novas sinapses. Portanto, a remoção do glutamato pelos astrócitos da fenda sináptica garante o funcionamento das transmissões sinápticas, colocando os astrócitos como protagonistas, ao invés de meros coadjuvantes das sinapses. Dá-se o nome de "sinapse tripartite", onde, além do neurônio pré e pós-sináptico, o astrócito torna-se o terceiro elemento participante da sinapse (Kettenmann & Verkhratsky 2008).

Além da captação de neurotransmissores, os astrócitos participam da regulação sináptica pela liberação de moléculas ativadoras como glutamato, purinas (ATP, adenosina e guanina), GABA e D-serina, modulando assim as respostas neuronais (Bezzi & Volterra 2001). A liberação dos gliotransmissores (assim chamadas as moléculas liberadas pelos astrócitos que regulam a atividade sináptica) é ativada em resposta a mudanças da atividade neuronal. Através dos receptores presentes na membrana de astrócitos, como por exemplo, para o glutamato, acetilcolina, ATP, GABA e norepinefrina, estas células respondem com elevação transitória nas concentrações intracelulares de cálcio (De Pittà *et al.* 2016). Mais especificamente, em

resposta a estímulo sináptico os receptores ligados a proteína G na membrana dos astrócitos, ativam a fosfolipase C e a produção de IP_3, o que induz a liberação de Ca^{2+} pelo retículo endoplasmático. A variação de cálcio intracelular pode ser transmitida entre astrócitos através da passagem de IP_3 pelas junções gap e consequente aumento de cálcio na célula adjacente, produzindo as conhecidas ondas de cálcio, que garante a comunicação por longas distâncias, e é considerada uma forma de excitabilidade destas células (Perea & Araque 2005, Scemes & Giaume 2006). É importante ressaltar que esse processo de ativação dos astrócitos por ondas de cálcio é muito mais lento do que a transmissão sináptica em neurônios. Considerando isso, o quão eficiente é a liberação dos gliotransmissores em relação às respostas neurais, como ocorre a liberação e a regulação da liberação destas moléculas, e ainda, como é regulado o tempo de resposta, são temas ainda em estudo (De Pittà et al. 2016).

Além das respostas químicas, os astrócitos podem influenciar as sinapses através de mudanças morfológicas. Recentemente, relacionou-se as mudanças estruturais e funcionais na interação entre astrócitos e neurônios com a formação de memória (Zorec *et al.* 2015). Observou-se na amígdala lateral de ratos que, após o condicionamento de medo, os processos astrocíticos se retraem, ampliando a região sináptica e favorecendo a comunicação neuronal e consolidação da memória (Ostroff *et al.* 2014). Ao contrário disso, os processos astrocíticos podem servir como barreiras, limitando o sinal e a comunicação entre sinapses vizinhas e ao mesmo tempo favorecendo a especificidade da transmissão (Beenhakker & Huguenard 2010). Ainda, inibições farmacológicas ou modelos transgênicos de animais, com funções astrocíticas alteradas, como por exemplo o bloqueio da liberação de gliotransmissores, ou ainda o bloqueio do receptor de adenosina A1 nos astrócitos comprometeu a plasticidade sináptica e prejudicou a memória de longa duração. Portanto, cada vez mais estudos relacionam o papel dos

astrócitos também como participantes ativos das funções cognitivas (Oliveira *et al.* 2015).

1.1.4.5. Metabolismo energético nos astrócitos

Devido ao posicionamento estratégico dos astrócitos, em contacto com vasos sanguíneos e axônios, estas células captam glicose da circulação, através do transportador de glicose GLUT-1, e fornecem metabólitos energéticos a diferentes elementos neurais. Aproximadamente 75% de toda a glicose que entra no parênquima cerebral é fosforilada nos astrócitos (Hyder *et al.* 2006). Além disso, estas células são as principais armazenadoras de glicogênio no SNC, suprindo a demanda energética em condições de hipoglicemia. Não coincidentemente, o maior acúmulo dos grânulos de glicogênio ocorre nas áreas de alta atividade sináptica. De acordo com isso, o conteúdo de glicogênio pode ser modulado por neurotransmissores, como o glutamato. Além disso, os metabólitos da glicose podem ser transferidos pelas junções gap, e este processo também é regulado pela atividade neural (Brown & Ransom 2015, Pellerin & Magistretti 1994). A maior parte da glicose captada pelos astrócitos não será utilizada pela própria célula, mas será armazenada na forma de glicogênio ou convertida a lactato, o qual é exportado para os neurônios como substrato energético preferencial. A este processo é dado o nome de "lançadeira de lactato astrócito-neurônio" (Pellerin 2008). Isto ocorre devido às características bioquímicas da célula, apresentando altos níveis de enzimas relacionadas à glicólise e ao metabolismo do glicogênio. Ao contrário de neurônios, astrócitos apresentam altos níveis de frutose-2,6-bifosfato, molécula chave na regulação da glicólise e, baixa atividade da piruvato desidrogenase, enzima chave para a entrada no ciclo do ácido tricarboxílico. Além disso, os astrócitos

apresentam baixos níveis de proteínas relacionadas à lançadeira malato-aspartato (Bouzier-Sore & Pellerin 2013).

1.1.4.6. Astrogliose e doenças neurodegenerativas

Os astrócitos têm sido relacionados como participantes de diversas doenças neurodegerativas (Khandelwal *et al.* 2011). Nestas condições, os astrócitos podem assumir características reativas, classificadas como astrogliose. Esta definição é normalmente usada como um marcador de patologias no SNC. Conceitualmente ocorre quando os astrócitos apresentam alterações moleculares, celulares e funcionais em resposta a algum dano ou doença do SNC. As alterações sofridas pelos astrócitos reativos variam com a gravidade do insulto, sendo progressivas em relação à expressão molecular (Ex. GFAP e S100B), e hipertrofia celular. Nos casos graves, ocorre proliferação e formação de cicatrizes gliais. Estas alterações são reguladas por moléculas sinalizadoras específicas ao contexto, como citocinas inflamatórias, lipopolissacarídeo (LPS), peptídeo beta amiloide ou até neurotransmissores (Sofroniew 2009). As alterações sofridas durante a astrogliose reativa tem a capacidade de alterar as atividades da célula por ganho ou perda de função, podendo ter um impacto tanto benéfico como prejudicial nas células neurais e não neurais circundantes (Sofroniew 2015).

As disfunções astrocíticas têm sido associadas a doenças psiquiátricas, doença de Alzheimer, encefalopatia hepática, epilepsia, entre outras (Sofroniew & Vinters 2010). As alterações astrocíticas podem ocorrer simplesmente pelo aumento da idade, ou então induzidas por estímulos tóxicos. Logo, suas respostas podem modular os efeitos celulares nas patologias neurodegenerativas, contribuindo para a perda de função cerebral. Por exemplo, na encefalopatia hepática, o inchaço dos astrócitos é tido como a

principal causa do edema cerebral observado nesta doença. Além disso, estas células assumem um papel importante na detoxificação da amônia, uma vez que apresentam a enzima GS, a qual converte glutamato em glutamina captando o íon amônio. O resultado de alterações nesse processo pode gerar um desequilíbrio na homeostase do neurotransmissor glutamato, explicando alguns sintomas comportamentais desta doença (Butterworth 2014). Alterações astrocíticas também são observadas na doença de Alzheimer. Os astrócitos reativos estão intimamente associados com as placas amiloides e, são capazes de captar e degradar os depósitos extracelulares de Aβ42 (Wyss-Coray *et al.* 2003). Ainda, a intensidade da gliose reativa, determinada pelos níveis de GFAP, está aumentada com a progressão da doença, ao mesmo tempo, os transportadores de glutamato estão diminuídos, deixando os neurônios mais vulneráveis a excitotoxicidade glutamatérgica (Simpson *et al.* 2010). A proteína S100B, também está aumentada nos astrócitos reativos na doença de Alzheimer e é usada como uma proteína marcadora para esta doença. Recentemente foi relatado que a sua inibição com pentamidina, a qual inibe a sua interação com p53, é capaz de diminuir os efeitos inflamatórios no hipocampo de ratos com modelo de Alzheimer (Cirillo *et al.* 2015).

1.2. S100B

Como relatado anteriormente, a S100B é uma das principais proteínas usadas como marcadora de astrócitos. Apesar disso, a sua expressão não é exclusiva deste tipo celular, sendo encontrada também em oligodendrócitos maduros, células progenitoras neurais, ependimócitos, adipócitos, células musculares, entre outras (Donato 2001, Vives et al. 2003). Contudo, sua expressão pode ser modificada dependendo da função e do contexto celular, como por exemplo, sendo super-expressa em condições patológicas, como na doença do Alzheimer (Sorci *et al.* 2013). Esta proteína está

distribuída no citoplasma e núcleo de astrócitos de cérebro adulto, assim como nos processos astrocíticos das zonas perivasculares (Mbele *et al.* 2002). A S100B é uma proteína altamente conservada entre espécies de vertebrados e entre diferentes tecidos da mesma espécie. Ela se apresenta, na sua maioria, na forma de homodímeros de 21 kDa, e a ligação destas duas subunidades parece ser crucial para sua atividade extracelular (Berger *et al.* 2002). A S100B faz parte da família de proteínas S100, ligantes de cálcio do tipo "EF hand" (Marenholz *et al.* 2004). Esta proteína funciona como sinalizadora de Ca^{2+} e a maioria de suas funções dependem desta interação, uma vez que quando o Ca^{2+} se liga na sua estrutura muda a sua conformação expondo seu sítio de interação (Rustandi *et al.* 2000). Outros íons, como zinco e cobre, também apresentam afinidade pela S100B, podendo regular sua função (Marenholz et al. 2004).

1.2.1. Efeitos intracelulares da S100B

A S100B age tanto nos espaço intracelular quanto extracelular. No citoplasma interage com o citoesqueleto modulando a polimerização de microtúbulos e de filamentos intermediários, favorecendo a migração celular (Sorci *et al.* 1998). Além disso, a S100B está altamente expressa em células tumorais, estando, portanto, relacionada com proliferação e sobrevivência celular. Entre outras ações, esta proteína inibe a fosforilação do supressor de tumor p53, inibindo sua ativação (Wilder *et al.* 2006). Ainda, a S100B parece inibir a diferenciação celular, porém apenas nos estágios iniciais do desenvolvimento celular. Foi relatado que existe uma redução transitória da expressão de S100B durante a diferenciação de astrócitos em cultura primária, que é restaurada nos estágios de desenvolvimento posteriores (Donato *et al.* 2009). Cultura de astrócitos nocautes para S100B (células geneticamente modificadas que não expressam a proteína) demonstraram um aumento de cálcio transiente após estímulo com cafeína,

mostrando a participação desta proteína também na homeostase do cálcio (Xiong *et al.* 2000).

1.2.2. Efeitos extracelulares da S100B

Ao contrário da maioria das proteínas da família S100, a S100B pode ser encontrada no espaço extracelular, onde exerce efeitos autócrinos e parácrinos na glia, em neurônios e na microglia. O mecanismo pelo qual a S100B exerce seus efeitos extracelulares ainda está sob estudo; entretanto, grande parte desses efeitos parece ser mediado pela ligação com o RAGE (*receptor for advanced glycation end products*), apesar de alguns efeitos serem independentes deste receptor (Leclerc *et al.* 2009). Estudos sobre a estrutura de ligação revelaram que a S100B se liga ao domínio externo V do receptor e que a forma tetramérica da proteína apresenta maior afinidade do que a dimérica (Ostendorp *et al.* 2007).

Estudos em neurônios mostram que a S100B atua como uma proteína neurotrófica em concentrações baixas (pico a nanomolares), induzindo crescimento de neuritos e aumentando a sobrevivência neuronal *in vitro e vivo* (Donato et al. 2009). A extensão de neuritos induzido por S100B parece ser mediado pela ligação com RAGE, ativando Cdc42-Rac1(Huttunen *et al.* 2000). Além disso, a ligação S100B/RAGE protege neurônios contra estímulos tóxicos ativando o fator anti-apoptótico Bcl-2 e a via Ras/MEK/ERK1/2/NFκB. Em contraposição, concentrações micromolares da S100B induzem apoptose neuronal, efeito mediado também via RAGE. Esta ligação aumenta fatores da via ERK1/2, assim como a produção de espécies reativas de oxigênio (EROs) e caspase-3 (Fig 2) (Huttunen et al. 2000, Businaro *et al.* 2006, Donato 2007, Van Eldik & Wainwright 2003).

Em astrócitos, a S100B estimula a proliferação e migração celular em baixas concnetrações, além de prevenir as alterações morfológicas provocadas pela neurotoxina trimetilestanho (Reali *et al.* 2005, Selinfreund *et al.* 1991). Por outro lado, em altas doses, a S100B parece induzir a troca de resposta dos astrócitos de trófico para tóxico, promovendo a produção de fatores inflamatórios. Concentrações na ordem de micromolar de S100B induzem a ativação de oxido nítrico sintase induzível (iNOS) via NFκB, a super-expressão de interleucina-1β (IL-1b), TLR2, FGF2 e TGFβ2 e a liberação de interleucina-6 (IL-6) e fator de necrose tumoral-α (TNFα). Todos estes efeitos parecem ser mediados via RAGE (Fig 2) (Ponath *et al.* 2007, Hu *et al.* 1996, Lam *et al.* 2001, Reali *et al.* 2012, Villarreal *et al.* 2014).

Em micróglia, baixas concentrações de S100B atenuam a ativação microglial pela ativação da via STAT3 (Zhang *et al.* 2011). Já em concentrações altas, a S100B induz ativação microglial, via NFκB, estimula a secreção e liberação de citocinas AP-1 dependentes, assim como a expressão de ciclooxigenase-2, e a migração celular. Estes efeitos também parecem ser mediados por RAGE (Petrova *et al.* 2000, Reali et al. 2005). No entanto, ativação de iNOS e produção de NO em micróglia ativada por S100B mostrou-se independente de RAGE, indicando que outros receptores devem estar envolvidos na ativação desta via (Fig 2) (Adami *et al.* 2004).

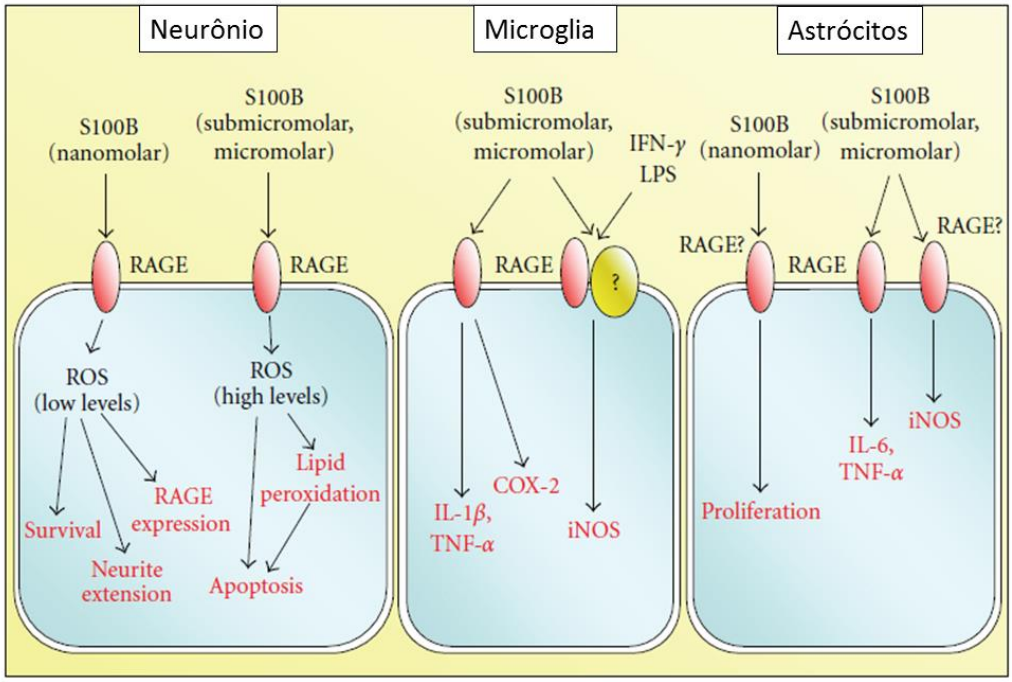

Fig 2. Representação esquemática dos efeitos da S100B extracelular sobre neurônios, micróglia e astrócito. Figura modificada de (Donato & Heizmann 2010).

Regulação da concentração de S100B no espaço extracelular

A liberação da S100B para o espaço extracelular pode ocorrer de forma regulada por um mecanismo ainda desconhecido. A sua secreção é realizada principalmente pelos astrócitos no SNC, e pelos adipócitos na periferia (Gonçalves *et al.* 2008). De fato, vários moduladores da secreção da S100B têm sido descritos, como variações na concentração intracelular de cálcio (Davey *et al.* 2001), estímulo com glutamato (Tramontina *et al.* 2006), IL-1β (de Souza *et al.* 2009), TNF-α (Edwards & Robinson 2006), amônia (Leite *et al.* 2006), fluoxetina (Tramontina *et al.* 2008), entre outros.

Por outro lado, a S100B pode ser liberada por lise celular, como no caso de um trauma cerebral. Nesta condição a ação da S100B normalmente está relacionada a efeitos tóxicos, se acumulando no espaço extracelular (Steiner *et al.* 2011). O uso da proteína S100B como marcadora de dano cerebral tem sido amplamente proposto, uma vez que esta proteína se encontra aumentada no soro ou líquor (LCR) após várias condições patológicas, como dano traumático cerebral, isquemia, doença de Alzheimer,

esclerose lateral amiotrófica, entre outras (Steiner et al. 2011, Rothermundt *et al.* 2003). No entanto, o aumento de S100B no LCR nem sempre corresponde a um aumento no soro. Da mesma forma, disfunções da BHE nem sempre correspondem a um aumento de passagem da S100B do LCR para o soro (Kleindienst *et al.* 2010, Guerra *et al.* 2011). Demonstrou-se recentemente que, após uma lesão cerebral traumática, a S100B é transportada do cérebro para o sangue através de um sistema chamado glinfático, na região perivascular entre a pia-máter e os vasos, onde ocorre a troca de substâncias entre o fluído intersticial e LCR. No entanto, uma inibição desta via bloqueia a passagem de S100B para o sangue, forçando as células cerebrais a metabolizar altas concentrações desta proteína liberadas em uma situação de dano (Plog et al., 2015).

Apesar de se saber que a maioria dos efeitos extracelulares de S100B (tróficos e tóxicos) são mediados pela sua ligação ao RAGE, pouco se sabe sobre como esta proteína é eliminada do espaço extracelular pelas células cerebrais. Em condição inflamatória, ou mesmo fisiológica algumas proteínas podem ser absorvidas do espaço extracelular, por um processo de internalização celular, na tentativa de restaurar a homeostase do ambiente extracelular, ou mesmo para fins de sinalização no caso da endocitose mediada por receptor (Megias *et al.* 2000, Gould & Lippincott-Schwartz 2009). Entretanto, se isso ocorre com a proteína S100B ainda precisa ser estudado.

1.2.3. Mecanismos de internalização

Várias vias de internalização foram descritas em células eucarióticas, entre elas o processo de fagocitose, o qual medeia à captação de partículas maiores, enquanto que a pinocitose capta partículas no fluído. Estes dois processos dependem de actina, a qual induz grandes mudanças de remodelamento na membrana plasmática, resultando em grandes vesículas intracelulares (Mayor & Pagano 2007). Partículas menores podem ser

internalizadas via endocitose mediada por clatrina e endocitose mediada por caveolina, as quais podem ser constitutivas ou desencadeadas pelo processo mediado por receptor (Gruenberg & van der Goot 2006). As duas vias dependem de uma diversidade de proteínas adaptadoras que atuam no recrutamento e seleção da carga a ser endocitada e também na formação da curvatura de membrana. A dinamina é uma proteína GTPase que atua nas duas vias tendo papel fundamental na cisão da vesícula com a membrana plasmática. Além disso, outra via de endocitose independente de clatrina e caveolina são conhecidas, como a ativada por ARF (fator de ribosilação ADP), porém são vias menos caracterizadas (Conner & Schmid 2003, El-Sayed & Harashima 2013, Mayor & Pagano 2007). Todos estes tipos de endocitose diferem na cinética de formação, maquinaria molecular associada e destino de carga.

Após a internalização, a maior parte da carga é encaminhada para a via endocítica, formando os endossomos recentes (ER), que representam o ponto chave de destino para várias proteínas (Fig 3). As moléculas captadas neste processo podem ser reconduzidas de volta a membrana, nos chamados endossomos de reciclagem; encaminhadas para a via Retículo Endoplasmático-Golgi; ou ainda conduzidas para a via de degradação em lisossomos. A mudança do endossomo recente para o endossomo tardio (ET) se dá através de mudanças de proteínas e lipídeos da membrana e a composição do lúmen da vesícula. As proteínas EEA1 (early endosomal antigen-1) e LAMP1 (lysosomal associated membrane protein-1) são classicamente usadas como marcadores de ER e ET, respectivamente. A enzima V-ATPase é responsável por manter o interior do ER e ET ácidos (pH 6,2 e 5,0 - 5,5 respectivamente). Curiosamente, essa acidificação parece controlar a função dos endossomos, como a ligação de proteínas receptoras, atividade de enzimas lisossomais e transportadoras. Ainda, nas regiões de formação dos ER, as vesículas podem fusionar-se, formando os corpos multivesiculares, os quais apresentam

estrutura mais homogênea e, ocasionalmente, podem fusionar-se com os ET, ou ainda serem reciclados de volta para a membrana plasmática, liberando os chamados exossomos os quais tem importante papel na comunicação intercelular (Basso & Bonetto 2016). Os ET também representam o ponto chave para o destino de proteínas, as quais podem ser degradadas nos lisossomos; fusionar-se com a membrana plasmática, liberando seu conteúdo interno; ou ainda interagirem com a via de autofagia, degradando componentes citosólicos e organelas (Scott *et al.* 2014, Gould & Lippincott-Schwartz 2009). Interessantemente, mostrou-se que a S100B citoplasmática está presente em vesículas endocíticas em resposta a internalização de RAGE em células de Schwann (Perrone et al., 2008). No entanto, a origem e as características das vesículas positivas a S100B ainda não foram estudadas com precisão.

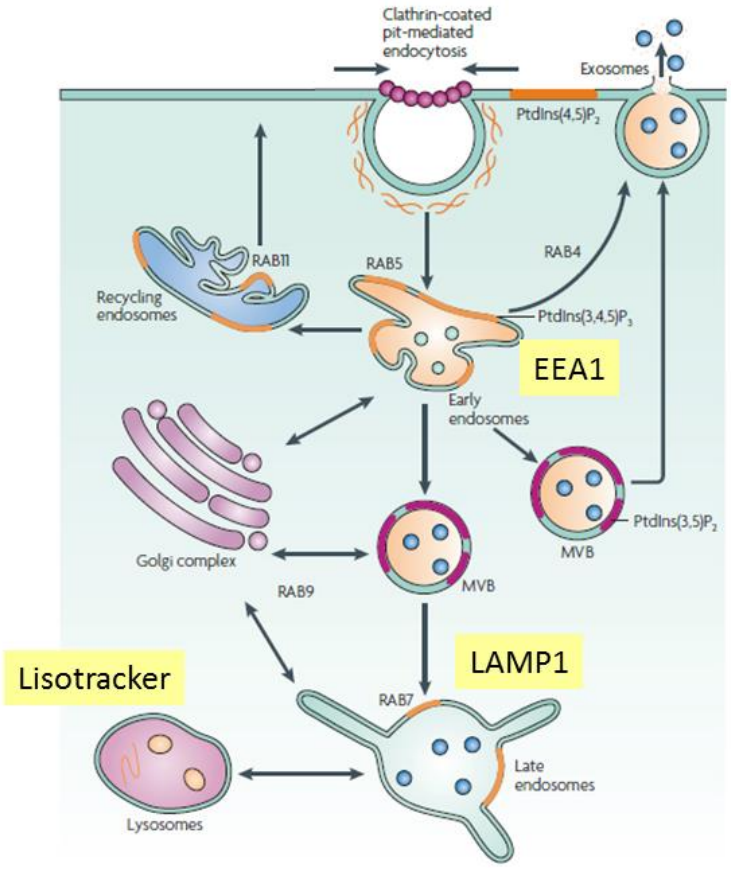

Fig 3. Representação esquemática da via endolisossomal e marcadores específicos. Modificado de (Rajendran *et al.* 2010).

1.3. Glutamina Sintetase

Além da S100B, GS é amplamente usada como marcadora de astrócitos, uma vez que está altamente expressa neste tipo celular. Apesar disso, ela não é exclusiva de astrócitos no SNC, sendo encontrada em outros tipos celulares, como neurônios e oligodendrócitos, porém em baixas quantidades (Cammer, 1990, Bernstein et al., 2014). Além de ser altamente expressa no cérebro, a GS está presente na maioria dos tecidos periféricos em mamíferos, porém em maiores quantidades no fígado, rim e músculo (Meister, 1985, Wang et al., 1996). Esta enzima possui importante função no metabolismo do nitrogênio não só em animais, mas também em plantas e bactérias, sendo evolutivamente bem conservada (Pesole *et al.* 1991, Kumada *et al.* 1993). A atividade desta enzima é a única via conhecida para a produção de glutamina a partir de glutamato e amônia. A glutamina é o aminoácido mais abundante em mamíferos e é indispensável para diversas funções do organismo, sendo precursora para a síntese de proteínas, glicose, purinas e pirimidinas. Este aminoácido também serve como doador e coletor de nitrogênio, como transportador de nitrogênio entre os órgãos, assim como na regulação da gliconeogênese hepática e renal (Chan *et al.* 2016).

No cérebro, a GS desempenha um papel essencial no ciclo glutamina-glutamato. O glutamato liberado após a neurotransmissão é rapidamente removido da fenda sináptica pelos transportadores de alta afinidade nos astrócitos (EAAT1 e EAAT2). Dentro dos astrócitos, o glutamato é convertido à glutamina pela atividade da GS, logo, a glutamina produzida será reenviada aos neurônios para uma nova sinapse. Esta reação, além de evitar a excitotoxicidade glutamatérgica, auxilia na homeostase dos níveis tóxicos de amônia, uma vez que esta reação liga o íon livre de amônia à estrutura do glutamato (Cooper 2012, McKenna 2007). Ainda, a glutamina produzida a partir da GS também é precursora da síntese de glutamato e GABA (Holten & Gundersen 2008).

A avaliação da atividade da GS é muito importante para compreender as condições fisiológicas e patológicas no tecido cerebral. Sabe-se que a redução da sua atividade em astrócitos pode limitar a depuração de glutamato pelos EAATs ou mesmo prejudicar a depuração de amônia levando ao comprometimento neurológico (Trabelsi *et al.* 2017). Por este motivo a GS tem sido proposta como um marcador de dano cerebral. De fato, a sua expressão ou atividade está comprometida em várias doenças neurodegenerativas, tais como a encefalopatia hepática, doença de Alzheimer, epilepsia e lesão cerebral traumática (Rose *et al.* 2013, Jayakumar & Norenberg 2016). Além disso, foi visto no cérebro de ratos que a atividade da GS é sensível a alterações metabólicas periféricas induzidas por restrição calórica (Ribeiro *et al.* 2009) ou exercício em esteira (Bernardi *et al.* 2013).

Fisiologicamente a GS possui a seguinte reação:

(1) glutamato + NH_4^+ + Mg^{2+} + ATP → glutamina + ADP + Pi

São conhecidos três tipos de genes para GS: GSI e III detectados principalmente em bactérias, e GSII presente em células eucarióticas e algumas bactérias. Foi descrito uma reação catalítica semelhante para os genes GSI e GSII, em que ligação do ATP à enzima favorece a ligação com o glutamato (Wang *et al.* 1996). O fosfato produzido pela clivagem do ATP permanece ligado à enzima, alterando a conformação da mesma e, portanto, formando o sítio de ligação da amônia, a qual se liga ao complexo γ-glutamil fosfato para produzir glutamina (Meister 1968, Liaw *et al.* 1995). A metionina sulfoxamina (MSO) é um inibidor irreversível da enzima, sendo fosforilado na presença de ATP e interagindo com o sítio ativo da enzima (Meister 1985).

Dois tipos de metodologias principais são utilizadas para determinar a atividade da GS: ensaios radiométricos e colorimétricos. O primeiro tipo de ensaio tem a vantagem de ser bastante sensível, porém, é de difícil manipulação, uma vez que utiliza

compostos radioativos, além de ser um ensaio mais custoso em comparação com ensaios colorimétricos (Minet *et al.* 1997). Já nos ensaios colorimétricos, são medidas duas atividades diferentes da GS: uma atividade sintetase e uma transferase, que pode ocorrer em diferentes locais ativos da enzima (Meister 1985). Ambas as reações produzem como produto final o γ-glutamil-hidroxamato, o qual quando em contato com cloreto férrico produz uma cor amarelada característica. Em ambas as reações é utilizada a hidroxilamina, ao invés do íon amônia, uma vez que é mais estável para a reação *in vitro*. A atividade sintetase utiliza glutamato como substrato, como se segue:

(2) glutamato + NH_2OH + Mg^{2+} + ATP → γ-glutamil-hidroxamato

Diferentemente, a atividade transferase utiliza glutamina como um substrato:

(3) glutamina + NH_2OH + Mg^{2+} + ADP → γ-glutamil-hidroxamato

A atividade transferase e principalmente a sintetase foram bem caracterizadas por Meister e colaboradores (Meister 1985). É importante ressaltar que as duas atividades da enzima (Eq. 2 e 3) são encontradas no mesmo isolado de proteínas de tecido cerebral altamente purificado e, respondem de forma idêntica ao mesmo tratamento. Logo, considera-se que ambas as reações refletem a atividade da mesma enzima (Meister 1985, Juurlink 1982), apesar de que alguns trabalhos contestem isso (Boksha *et al.* 2000, Herzfeld 1973). Contudo, foi relatado que a reação transferase tem menos interferentes para avaliação *in vitro* do que a reação sintetase. Isso se deve ao fato que a reação de sintetase (Eq. 2) usa ATP como substrato, sendo facilmente hidrolisado pela ATPase presente no homogeneizado de tecidos (Stadtman *et al.* 1968, Dennis *et al.* 1980). Além disso, o ADP produzido na Eq. 2 pode inibir a atividade da enzima, fazendo com que a reação da transferase seja mais eficiente do que a sintetase (Yamamoto *et al.* 1987). De fato, a reação transferase forma o produto mais rapidamente, sendo cerca de 10 vezes mais rápida, avaliado em cérebro de ovelha

(Ehrenfeld *et al.* 1963, Ronzio *et al.* 1969). Apesar de ser comumente aplicado, o ensaio para medir a reação transferase da GS foi menos padronizado do que a reação sintetase. Ensaios para atividade da glutamil-transferase mostraram-se precisos e confiáveis no tecido muscular (Minet et al. 1997) e nas bactérias (Ehrenfeld et al. 1963), porém, foi pouco padronizado para o tecido cerebral. Foi sugerido que a regulação da atividade da GS varia em músculo ou fígado, bem como em diferentes regiões cerebrais (Iqbal & Ottaway 1970, Böttcher *et al.* 2003). De acordo com a nossa pesquisa, há apenas um trabalho na literatura que mostra a padronização da atividade transferase da GS em estrutura cerebral, porém apresenta diferenças na concentração de substratos e usa método cromatográfico para a detecção do produto (Seiler *et al.* 1990). Desta forma, torna-se necessário a caracterização da atividade da glutamil-transferase da GS em diferentes tecidos cerebrais, assim como em cultura de astrócitos (Seiler et al. 1990, Yamamoto et al. 1987). Esta análise permitiria o melhor uso da atividade da enzima para avaliação em condições fisiológicas e patológicas do SNC.

1.4. Modelos de astrócitos

Ao longo dos anos de estudo foi possível provar que os astrócitos eram, ao contrário do que se pensava, células altamente ativas, envolvidas em uma diversidade de funções, participando desde a manutenção do ambiente extracelular, até na formação e regulação de sinapses. A utilização da cultura primária de astrócitos como instrumento para estudo deste tipo celular facilitou o progresso alcançado no conhecimento de propriedades e funções que esta célula adota (Lange *et al.* 2012). Graças a este modelo foi possível estudar, de forma sofisticada, características mecânicas e bioquímicas que seriam de difícil acesso *in vivo*. O estudo em um sistema isolado permitiu verificar, por exemplo, as características da sinalização por cálcio, aspectos eletrofisiológicos da célula, a

liberação e absorção de glio-moléculas, alterações morfológicas, entre outros fatores. Além disso, este sistema também contribuiu para a compreensão do papel dos astrócitos em doenças neurodegerativas como as doenças de Alzheimer e Parkinson, caracterizando assim o envolvimento dos astrócitos com a causa e/ou progressão dessas patologias, bem como a possibilidade de serem alvos de novos medicamentos (Khandelwal et al. 2011, Liu *et al.* 2012).

A técnica de cultura primária de astrócitos é amplamente utilizada como modelo para o estudo dos mecanismos celulares e, inclusive verificou-se recentemente que a expressão de genes em cultura são similares ao *in vivo* (Hertz *et al.* 2016). Esse tipo de cultura vem sendo utilizado como modelo de neuroinflamação (Guerra et al. 2011), de intoxicação por amônia (Leite et al. 2006), bem como para o estudo da secreção de diferentes compostos, como a proteína S100B (Nardin *et al.* 2007) , o ATP (Coco *et al.* 2003) e o glutamato (Bezzi & Volterra 2001). Apesar de amplamente aceito na literatura, o modelo de cultura primária de astrócitos apresenta algumas desvantagens, tais como o alto custo financeiro para a realização da técnica, a necessidade de mão de obra altamente qualificada, por ser um processo demorado e, acima de tudo, a heterogeneidade dessas células em cultura, o que aumenta a variabilidade dos resultados obtidos entre diferentes grupos de pesquisa.

Na busca de alternativas que minimizassem essas desvantagens, as linhagens celulares foram desenvolvidas. A linhagem de glioma C6 (ATCC CCL-10) foi desenvolvida a partir do isolamento de células de um glioma de rato e estão entre as linhagens mais utilizadas para o estudo de células astrogliais (Baber & Haghighat 2010, Benda *et al.* 1968). Estas células são utilizadas como linhagem celular semelhante à astrócitos em passagens elevadas (mais de cem) devido ao aumento da expressão de alguns marcadores astrócitos como GFAP, S100B, GS e transportadores de glutamato

(Parker *et al.* 1980, Raju *et al.* 1980, Tabuchi *et al.* 1982, Haghighat 2005, Baber & Haghighat 2010). Outro modelo de estudo para este tipo celular é o desenvolvimento de astrócitos imortalizados, uma técnica já estabelecida, mas pouco utilizada na literatura (Frisa & Jacobberger 2002, Geller & Dubois-Dalcq 1988). Esse tipo celular é desenvolvido a partir de uma cultura primária de astrócitos os quais, são transfectados com o plasmídeo pSV3-neo contendo o gene para o grande antígeno T do SV40, o qual afeta a atividade de supressores de tumor como, por exemplo, o retinoblastoma e a p53 (Ahuja *et al.* 2005). Esta alteração resulta, portanto, em células mais proliferativas. Após a seleção de uma única colônia essas células são isoladas e podem ser congeladas.

O uso de linhagens celulares apresenta um custo menor, quando comparado à cultura primária de células; uma maior praticidade, visto que essas células podem ser armazenadas congeladas e seu emprego não requer o uso de animais, tornando-se uma alternativa ao uso destes. Além disso, tanto a linhagem C6 quanto os astrócitos imortalizados possuem a vantagem de serem células mais homogêneas, visto que elas descendem do mesmo clone, com a diferença principal que as C6 originam-se de células tumorais e os astrócitos imortais de uma célula normal de astrócitos. Essa homogeneidade entre as células facilita a comparação de resultados entre diferentes laboratórios. Por outro lado, recentemente a literatura tem questionado o uso de linhagens celulares. Uma vez que essas células são células altamente proliferativas e apresentam algumas características diferentes das células primárias, o que pode resultar em comportamentos diferentes em resposta a estímulos (Leite *et al.* 2009, Haghighat & McCandless 1997b, Haghighat & McCandless 1997a).

Sabe-se, por exemplo, que as células da linhagem C6 possuem morfologia diferente de astrócitos primários (Zhou *et al.* 2008) e que sua taxa de proliferação é muito mais alta, o que pode ser explicado parcialmente devido à baixa expressão de conexinas,

sendo usadas como controle negativo nos ensaios de comunicação por junção gap (Leite et al. 2009). Estudos anteriores mostram que as junções gap são importantes na regulação da proliferação celular e estão envolvidas com muitas de suas funções (Tabernero *et al.* 2006). Dentre as respostas mediadas por junções comunicantes podemos citar a formação de ondas de cálcio (Bennett *et al.* 2003, Scemes & Giaume 2006); a resposta à atividade sináptica, fornecendo suporte energético aos neurônios (Rouach et al. 2002, Tabernero et al. 2006) e a regulação dos mecanismos de morte celular (Nodin *et al.* 2005). Todas essas funções podem estar alteradas nesse tipo celular e, consequentemente, ele não se torna um modelo adequado para esse tipo de estudo.

Da mesma forma, diversas pesquisas mostram que astrócitos imortalizados apresentam níveis detectáveis de proteínas características de astrócitos, como GFAP e S100B, mas na sua maioria em níveis consideravelmente menores do que astrócitos de cultura primária (Frisa & Jacobberger 2002, Furihata *et al.* 2016, Morikawa *et al.* 2001). Pouco é discutido sobre a funcionalidade das moléculas detectadas. Mostrou-se que a captação de leucina e arginina ocorre em menor escala do que em comparação com células de cultura primária (Lin *et al.* 1997) e, em alguns trabalhos mostrou-se que as células imortalizadas não foram capazes de responder a estímulos como os astrócitos de cultura primárias (Geller & Dubois-Dalcq 1988, Morikawa et al. 2001).

Portanto, apesar destas linhagens serem mais homogêneas e apresentarem algumas características similares aos astrócitos primários, existe uma carência de estudos comparativos integrando os diferentes modelos de astrócitos (cultura primária, células imortalizadas e linhagem C6), principalmente no que diz respeito as características funcionais destas células. Tendo em vista que o estudo de células astrogliais em cultura é de extrema importância para o avanço das pesquisas em sinalização celular, doenças neurodegenerativas, bem como no desenvolvimento de

novas estratégias terapêuticas, se torna fundamental a realização de um estudo comparativo entre os diferentes modelos de estudo no que se refere à caracterização morfológica e funcional dessas células. Isso possibilitará a escolha de modelos mais adequados para o objetivo de trabalhos futuros, otimizando as pesquisas nessa área do conhecimento.

2. Justificativa

Tendo em vista o crescente interesse na diversidade funcional dos astrócitos, a importância do estudo destas células em um sistema isolado para a compreensão de suas funções e ainda, a divergência de resultados encontrados na literatura nos três principais modelos experimentais de astrócitos, torna-se importante a realização de um estudo comparativo no que diz respeito a aspectos moleculares e funcionais da CP, AI e C6. Além disso, considerando o papel central dos astrócitos na regulação e manutenção do ambiente extracelular e os efeitos de sinalização e toxicidade da proteína S100B no espaço extracelular, coloca-se em questão a capacidade dos astrócitos de internalizar a proteína S100B e quais seriam os destinos intracelulares desta proteína. Por fim, a importância da avaliação da atividade da GS em condições fisiológicas e patológicas, e a carência de estudos na padronização da atividade glutamil transferase da enzima em cultura de astrócitos, assim como em outras regiões cerebrais, torna-se importante caracterizar um ensaio para GS que seja confiável, específico e de alta aplicabilidade.

Objetivos

2.1. Objetivo Geral

Comparar e caracterizar o perfil molecular e funcional da CP, AI e C6, de forma a aprofundar o estudo do papel dos astrócitos na regulação dos níveis extracelulares de S100B e os possíveis mecanismos de internalização desta proteína.

2.2. Objetivos Específicos

2.2.1. Avaliação comparativa entre CP, AI e C6 em relação às diferenças morfológicas; proteínas marcadoras; metabolismo glutamatérgico e energético e comunicação por junção gap, em condições basais e frente a estímulos específicos;

2.2.2. Avaliar a captação de S100B exógena em alta concentração por astrócitos;

2.2.3. Estudar o envolvimento da via endolisossomal no mecanismo de internalização da proteína S100B em astrócitos, caracterizando as vesículas de internalização e sua dinâmica intracelular;

2.2.4. Padronizar um ensaio para a medida da atividade da GS, utilizando sua atividade transferase em cultura de astrócitos e linhagem C6, bem como em diferentes regiões cerebrais de ratos, que seja preciso, específico e de alta aplicabilidade.

3. Resultados

3.1. Capítulo I

Molecular and functional characterization of primary culture of astrocytes, immortalized astrocytes and C6 glioma cells.

Artigo em preparação

Molecular and functional characterization of primary culture of astrocytes, immortalized astrocytes and C6 glioma cells.

Fabiana Galland[a], Marina Seady[a], Jessica Taday[a], Soraya Smaili[b], Carlos Alberto Gonçalves[a], Marina Concli Leite[a]

[a] Departamento de Bioquímica, Instituto de Ciências Básicas da Saúde, Universidade Federal do Rio Grande do Sul, Porto Alegre, Brazil.

[b] Departamento de Farmacologia, Universidade Federal de São Paulo, São Paulo, Brazil

e-mail adress:

Fabiana Galland – fabianagalland@yahoo.com.br

Marina Seady – mapseady@hotmail.com

Jéssica Taday – jessicataday@hotmail.com

Carlos-Alberto Gonçalves – casg@ufrgs.br

Marina Concli Leite - marina.leite@ufrgs.br

Corresponding author: Marina Concli Leite

Depto Bioquímica, ICBS, UFRGS

Ramiro Barcelos, 2600-anexo

Porto Alegre, RS, Brazil

90035-003

Fax: 55-51-3308 5565

E-mail: marina.leite@ufrgs.br

Abstract

Understanding the role of astrocyte functions in central nervous system is in continuous progress. Astrocyte culture is a potent instrument to study these cells in isolated system, allowing the elucidation of mechanistic features specific for this type of cell, in physiologic and pathologic state. However, the isolation of primary astrocytes culture (PC) is a laborious process, is time consuming, and costly. An alternative to this model is the use of cell lines, such as immortalized astrocyte cell line (IA) or C6 glioma cells (C6) in high passages, which present some proteins characteristic of astrocytes. These lineages have the advantage to present more homogeneous features, are easily, faster and lower cost to manipulate. Despite these facilities, cell lines present highly proliferative features and some different characteristics in compare to PC, which put into question the validity of them as an astrocyte model. The objective of this work was to show an integrative characterization and comparative analysis of PC, IA and C6 regarding molecular markers and glutamate and glucose metabolism and cell communication. Our results showed that the two cell lines (IA and C6) presented differentiated astrocytic markers (eg. GFAP, S100B, AQP4 and ALDH1L1), although expressing less quantities then PC. Similarly, the functionality of glutamatergic and energetic metabolism and cellular communication by gap junction also showed to be reduced in lineages cells. Our IA cell line did not reveal a reproducible model of classic astrocytic functions, since it did not respond to most stimuli tested, in opposite to C6 cells that presented a similar response to PC under the same stimulus. The high proliferative rate of lineage cells may explain the reduction of astrocytic differentiated characteristics discussed in this work. Here we provide an integrative and functional characterization of three astrocytic models, allowing the selection of a suitable model to the study of astrocytes, optimizing the research in the area of knowledge.

Introduction

Astrocytes represent a highly heterogeneous neuroglia cell responsible for a variety of complex and important functions in Central Nervous System (CNS). These cells have a strategic position, covering most of capillary with their endfeet, and also in contact with axon and synapses of neuronal cells (Kacem et al., 1998; Sofroniew and Vinters, 2010). Rather than supportive and passive cells, astrocyte can be activated in response to synaptic activity acting on potassium buffering or regulating fluid homeostasis through kir4.1 channel and aquaporin-4, respectively (Olsen and Sontheimer, 2008; Papadopoulos and Verkman, 2013). Furthermore, astrocytes are enriched with receptor and transporters that regulated synaptic activity. One classic and important function is the capacity of these cells to clearance neurotransmitters, such as glutamate forming the glutamine-glutamate cycle. Once taken up, glutamate is converted into glutamine through glutamine synthetase activity (GS), enzyme highly expressed in astrocytes. Then, glutamine returns to neurons, where it will be restored back to glutamate for the formation of new synapses (McKenna, 2007). The concept called "synapse tripartite" represent an integrative system between neurons and glia, giving to astrocytes a protagonist role, rather than merely supporting of synapses (Kettenmann and Verkhratsky, 2008). Furthermore, astrocytes position ensures these cells to be the main energy supplier in brain, up taking glucose from blood vessels and furnishing neurons with energy metabolism (Bouzier-Sore and Pellerin, 2013). Gap junctions have an important function in the transport of energy substrates and also in cell communication through calcium signaling (Perea and Araque, 2005; Tabernero et al., 2006).

Many important advances in the knowledge of astrocytes were facilitated thanks to the isolation of this cells in culture (Lange et al., 2012). Primary astrocytes cultures allowed the study of these cells in basal and neurotoxic condition. Although this model may represent some limitation for being an isolated system, recently, it was demonstrated that they share similar characteristic of genes when compared with freshly astrocytes brain (Hertz et al., 2017). Astrocyte culture is a potent instrument to study in a sophisticated form mechanistic features that it would be difficult to achieve *in vivo*, as electrophysiology, calcium signaling, gliosignaling release and uptake, morphologic and biochemical changes which take place specific in these cells under different insult. This model may also help in the development of new target drugs in neurodegenerative disease.

Even though these advantages, the isolation of primary astrocytes culture is a laborious process, is time consuming, present a high maintenance cost, and generate variable results as are highly heterogeneous cells, making difficult to compare results among different research groups. An alternative to this model is the use of cell lines, such as C6 (ATCC CCL-10). This glioma cell line is the most commonly used model, isolated from rat brain tumor (Benda et al., 1968). These cells are used as astrocyte-like cell line in high passages (over a hundred) due to increased expression of some astrocytes marker, as GFAP, S100B, GS and glutamate transporters (Baber and Haghighat, 2010; Haghighat, 2005; Parker et al., 1980; Raju et al., 1980; Tabuchi et al., 1982). Another model to study astrocytes in culture is immortalized astrocytes, which are genetically transformed cells with higher proliferative rate (Frisa and Jacobberger, 2002; Furihata et al., 2016; Morikawa et al., 2001). This linage has the advantage to be originated from a primary astrocyte culture and not from a tumor. This both type of cell lines provide more homogeneous features than primary astrocytes cell culture, as are originated from clones. Furthermore, are easily to manipulate once it can be stocked and thawed. The high proliferative rate of this cell lines allows faster manipulation and also are cheaper to maintain.

Despite this facilities, the use of cell lines have been questioned in the literature due to the glioma features and some different characteristics in compare to primary cells, which put into question the validity of this cell line models (Haghighat and McCandless, 1997a, b; Leite et al., 2009; Nardin et al., 2007; Tabernero et al., 2006). There is no data in literature that show a complete and integrative characterization of primary astrocytes culture (CP) in compare to linage models, such as immortalized astrocytes (IA) and C6 glioma cell line (C6). Here we show a comparative analysis of these three models regarding morphological and functional features. We show differences in cell morphology and protein expression characteristics of astrocytes, as GFAP, S100B, aldehyde dehydrogenase 1 family, member L1 (ALDH1L1), aquaporin-4 (AQP4) and potassium channel-4 (Kir4.1). Furthermore, glutamate metabolism was characterized, evaluating glutamate uptake and its transporters (EAAT1 and EAAT2), glutamine synthetase activity, and GSH content. Glucose metabolism was also assessed using H3-glucose uptake and it transport content (GLUT1). We also evaluated the communication of these cells by gap junction checking Cx43 expression and Lucifer yellow communication. In addition, we show the responsiveness of these models under

toxic stimulus evaluating astrocytic activation through GFAP content and S100B secretion, glutamate and glucose metabolism and inflammatory cytokines. This work contributes to the evaluation of astrocytes culture as an experimental model system allowing the selection of a suitable model to the study of astrocytes, optimizing the research in the area of knowledge.

Materials and Methods

Materials

Poly-L-lysine, methylthiazolyldiphenyl-tetrazolium bromide (MTT), neutral red, glutathione standard, phthaldialdehyde and lipopolysaccharides from Escherichia coli (LPS) 055:B5, L-glutamate, o-phenylenediamine (OPD), γ-glutamylhydroxamate acid, N-methyl-d-glucamine and aminoguanidine hemisulfate salt (AG) were purchased from Sigma [St. Louis, USA]. Fetal calf serum (FCS), Dulbecco's modified Eagle's medium (DMEM) and other materials for cell culture were purchased from Gibco [Carlsbad, USA]. l-[2,3-3H] glutamate was purchased from Amersham International (United Kingdom) and deoxy-d-glucose, 2-[3H(G)] (10 Ci/mmol) was purchased from American Radiolabeled Chemicals, Inc. (Saint Louis, MO, USA). Lucifer Yellow was purchase from Invitrogen, Life Technology Corporation, USA. Antibodies obtained from Sigma [St. Louis, USA] were: anti-S100B (SH-B1) and anti-GFAP. Antibodies obtained from Santa Cruz Biotechnology (SantaCruz,USA): Polyclonal anti-RAGE (N16), Anti-Glutamine Synthetase, polyclonal anti-Kir4.1, anti-BDNF, anti-GLUT1 and anti-goat IgG-R. Antibodies obtained from Chemicon (Temecula,USA): Polyclonal anti-AQP-4 antibody, and anti-Conexin-43. Monoclonal anti-Aldehyde dehydrogenase family 1 member L1 was from Neuromab. Polyclonal anti-S100B and anti-rabbit peroxidase were purchased from DAKO [São Paulo, Brazil] and GE [Little Chalfont, United Kingdom], respectively. Antibody anti-EAAT1 and EAAT2 was purchased form Abcam, and anti-actin from Merck Millipore Corporation.

Astrocytes primary cell culture (PC)

Primary astrocyte cultures from Wistar rats were prepared as previously described by (Gottfried et al., 2002). Procedures were carried out in accordance with the NIH Guide for the Care and Use of Laboratory Animals and were approved by the local authorities.

Briefly, cerebral cortices of newborn Wistar rats (1-2 days old) were removed and mechanically dissociated in Ca^{2+}- and Mg^{2+}-free balanced salt solution, pH 7.4, containing (in mM): 137 NaCl; 5.36 KCl; 0.27 Na_2HPO_4; 1.1 KH_2PO_4 and 6.1 glucose. The cortices were cleaned of meninges and mechanically dissociated by sequential passage through a Pasteur pipette. After centrifugation at 1400 RPM for 5 min the pellet was resuspended in DMEM (pH 7.6) supplemented with 8.39 mM HEPES, 23.8 mM $NaHCO_3$, 0.1% amphotericin B, 0.032% gentamicin and 10% fetal calf serum (FCS). Cells were pated into 12 or 24-well- plates pre-treated with poly-L-lysine. Cultures were maintained in DMEM containing 10% FCS in 5% CO_2/95% air at 37°C. Medium was changed every 3-4 days. Cells were allowed to grow to confluence, and used at 21 days *in vitro* (DIV).

C6 Glioma cell culture (C6)

The C6 glioma cell line was obtained from the American Type Culture Collection (Rockville, MD). Late passage cells (i.e., after at least 100 passages) were seeded in 25 cm2 flasks and cultured in DMEM 10% FCS (same medium described for astrocytes primary culture). Exponentially growing cells were detached from the culture flasks using 0.05% trypsin/ethylenediaminetetraacetic acid (EDTA) and seeded in 12 or 24-well plates. Cells were allowed to grow to confluence, and used in 3 DIV.

Culture of immortalized astrocytes (IA)

Briefly, astrocyte primary culture with 11 DIV was transfected with a mixture of 3 µg of pSV3-neo plasmid and 10 µg of lipofectAMINE (GIBCO) during 5 h. As a control, cells were also transfected with GFP plasmid (pcDNA3 vector). Four days after transfection, the antibody G418 was added for the selection of neomycin-resistant colonies. The medium was changed every 3-4 days and the concentration of G418 was gradually increased from 200 to 800 µg/mL. After 3 weeks, isolated colonies were selected and seeded in 24-well plates and gradually expended until 75cm^2 flasks. The transfected cells were maintained in DMEM with 10% FCS, 1% peniciline/streptomicine and 200 µg/mL of G418. Immortalized astrocytes of 10 to 30 passages were used for the experiments.

Immunocytochemistry

Immunocytochemistry was performed as described previously by (Lasič et al., 2016) with some modification. Briefly, cell cultures were fixed with 4% paraformaldehyde/4% sucrose for 10 min and permeabilized with 0.1% Triton X-100 in PBS for 20 min at room temperature. After blocking 1 h with 2% albumin bovine, the cells were incubated overnight with anti-GFAP, anti-S100B, anti-actin. For primary astrocytes culture antibodies were incubated at concentration of 1:1000 and for immortalized astrocytes (IA) and C6 glioma cells antibodies were incubated at 1:250. After 3 washing steps with PBS, specific secondary antibody conjugated with Alexa Fluor 488 (green staining) or 568 (red staining) was incubated for 1 h at room temperature. For all the immunostaining-negative controls, the reactions were performed by omitting the primary antibody. No reactivity was observed when the primary antibody was excluded. Cell nuclei were stained with 0.2 mg/ml of 4',6'-diamidino-2 phenylindole (DAPI). The cells were visualized with a Nikon inverted microscope and the images were transferred to a computer with a digital camera (Sound Vision Inc.).

S100B measurement

S100B was measured by ELISA, as previously described by (Leite et al., 2008). Briefly, 50 µl of sample (previously homogenized and diluted) plus 50 µl of Tris buffer 50 mM were incubated for 2 h on a microtiter plate previously coated overnight with monoclonal anti-S100B and blocked for 1 h with 2% albumin from chicken egg. Polyclonal anti-S100 was incubated for 30 min and then peroxidase-conjugated anti-rabbit antibody was added for a further 30 min. The microtiter plate was rinsed tree times between each step with a wash solution. O-phenylenediamine was added for 30 min and the colorimetric reaction was determined at 492 nm. The standard S100B curve ranged from 0.002 to 1 ng/ml.

GFAP measurement

The ELISA for GFAP was carried out, as previously described by (Tramontina et al., 2007). Homogenates of cell culture (100 µl) previously diluted in TBS or standard human GFAP (from Calbiochem) ranging from 0.1 to 5 ng were incubated in microtiter plates for 24 h at 4°C. After blocking with 5% M-TBS for 2 h at room temperature, it was incubated a rabbit polyclonal anti-GFAP (dilution in 0.5% M-TBS) for 1 h. Then, secondary antibody conjugated with peroxidase it was incubated for 1 h at room temperature. The microtiter plate was rinsed tree times between each step with a wash

solution. O-phenylenediamine was added for 30min and the colorimetric reaction was determined at 492 nm.

Glutamine Synthetase activity

The enzymatic activity of glutamine synthetase was determined using the procedures described previously by (Minet et al., 1997), with modifications. Briefly, homogenized sample diluted in 50 mM imidazole were incubated with (mM): (50 imidazole, 50 hydroxylamine, 100 L-glutamine, 25 sodium arsenate dibasic heptahydrate, 0.2 ADP, 2 manganese chloride, pH 6.2) and incubated for 15 min at 37°C. The reaction was stopped by the addition of 0.2 ml of 0.37 M $FeCl_3$, 200 mM trichloroacetic acid, and 0.67 M HCl. After centrifugation, the absorbance of the supernatant was measured at 540 nm and compared to the absorbance generated by standard quantities of γ-glutamylhydroxamate acid (Sigma) diluted in the same solution than the samples. Glutamine synthetase activity was expressed as µmol/h/mg prot.

GSH

Glutathione content was determined as previously described (Browne and Armstrong, 1998). This assay detects only the reduced glutathione content. Briefly, sample were homogenized in sodium phosphate buffer (0.1 M, pH 8.0) containing 5 mM EDTA and protein was precipitated with 1.7% meta-phosphoric acid. Supernatant was assayed with o-phthaldialdehyde (1 mg/mL methanol) at room temperature for 15 min. Fluorescence was measured using excitation and emission wavelengths of 350 and 420 nm, respectively. A calibration curve was employed using standard GSH solutions (0-500 µM).

Glutamate uptake assay

Glutamate uptake was measured, as previously described by (Gottfried et al., 2002) with some modifications (Thomazi et al., 2004). Cell culture were incubated at 37 °C in Hank's balanced salt solution (HBSS) containing (in mM): 137 NaCl, 5.36 KCl, 1.26 $CaCl_2$, 0.41 $MgSO_4$, 0.49 $MgCl_2$, 0.63 $Na_2HPO_4 \cdot 7\ H_2O$, 0.44 KH_2PO_4, 4.17 $NaHCO_3$ and 5.6 glucose, pH 7.4. The assay was started by the addition of 0.1 mM l-glutamate and 0.66 µCi/mL L-[2,3-3H] glutamate. Incubation was stopped after 7 min for PC and 10 min for IA and C6 cells, by removing the medium and rinsing the cells three times with ice cold HBSS. The slices were then lysed in a 0.5 M NaOH solution. Sodium-

independent uptake was determined using N-methyl-D-glucamine instead of NaCl. Sodium dependent glutamate uptake was obtained by subtracting the non-specific uptake from the total uptake to obtain the specific uptake. Radioactivity was measured in a scintillation counter. Results were expressed as nmol/mg protein/min.

Glucose uptake assay

Glucose uptake was measured as previously described (Pellerin and Magistretti, 1994), with modifications. Cell cultures were rinsed in with HBSS. Subsequently, cells were incubated at 35 °C in HBSS (described above). The assay was initiated by the addition of 0.1 μCi/ well deoxy-d-glucose, 2-[3H(G)]. The incubation was stopped after 15 min by removing the medium and rinsing the slices three times with ice-cold HBSS. The slices were then lysed in a solution containing 0.5 M NaOH. Glucose uptake was calculated by subtracting the non-specific uptake, obtained by the glucose transporter inhibitor, cytochalasin B (10 μM), from the total uptake in order to obtain the specific uptake. Radioactivity was measured using a scintillation counter. Results were expressed as nmol/mg protein/min.

Western blot analyses

Cell culture were homogenized in sample buffer (0.0625 M Tris–HCl, pH 6.8, 2% (w/v) SDS, 5% (w/v) b-mercaptoethanol, 10% (v/v) glycerol, 0.002% (w/v) bromphenol blue), subsequently boiled and centrifugated. Equal amounts (25 μg) of proteins were electrophoresed in a 12% (w/v) SDS–polyacrylamide gel. The separated proteins were blotted onto a nitrocellulose membrane. Membranes were incubated in TBS-T (20 mmol/L Tris–HCl, pH 7.5, 137 mmol/L NaCl, 0.05% (v/v) Tween-20) containing 2% (w/v) bovine albumine for 1 h at 4°C. Subsequently, the membranes were incubated overnight, at 4°C, with the appropriate primary antibodies at concentration (1:5000): anti-GFAP, anti-vimentin, Anti-GS, anti Kir4.1, anti-AQ-4, anti ALDH1L1, anti-Cx43, BDNF, EAAT1, EAAT2, anti-Glut-1. Membranes were then rinsed with TBS-T, and exposed to horseradish peroxidase-linked anti-IgG antibodies for 1 h at 4°C. Equivalent loading of each sample was confirmed with anti-actin. The chemiluminescence signal was detected using an ECL kit from Amersham and evaluated in the luminescence image analyzer (Image Quant LAS4000 from GE). The luminescence signal was analyzed using ImageJ software.

Lucifer Yellow

Scrape loading/dye transfer was carried out as previously described (Leite et al., 2009). After treatment, the conditioned incubation buffer was removed and saved. The cultures were quickly and carefully rinsed in Ca^{+2} -free HBSS to prevent uncoupling of the cells as a result of high Ca^{2+} levels. Two parallel scrapes were performed with a scalpel blade in the Ca^{+2} free HBSS with 0.1% (w/v) Lucifer yellow at room temperature. Disruption of the cell membrane allows the dye to permeate the cell and to diffuse to surrounding cells through GJ channels. The dye was rinsed away with HBSS after 1 min. The conditioned incubation buffer was reintroduced and cultures were left for 7 min. After that, cells were viewed with a Nikon inverted microscope and images transferred to a computer with a digital camera. All images are representative fields from at least three experiments carried out in triplicate.

Protein determination

Protein content was measured by Lowry's method, modified by Peterson, using bovine serum albumin as standard (Peterson, 1977).

Statistical analysis

Parametric data are reported as means ± standard errors and were analyzed by one-way analysis of variance (ANOVA) followed by Duncan's test, using SPSS-16.0. Tests are specified in the legends, with the level of significance set at $p < 0.05$.

Results

Differences in morphology and molecular markers of astrocytes

Astrocytes basal morphology was evaluated in PC, IA and C6 (Fig 1). To this comparison it was evaluated actin, GFAP and S100B by immunocytochemistry. As show in images, PC and IA presented similar polygonal shape with some cell process and actin label more delimited and with organized filaments. In contrast, C6 glioma cells presented elongated body and with diffuse actin fibers. Cell morphology was also evaluated after stimulated condition with forskolin, which is a classic stimulus that induces morphology changes due to variation on intracellular levels of cyclic AMP (Frizzo et al., 2004). PC and C6 showed stellated characteristic shape after forskolin

treatment noted in all labeled proteins. Nevertheless, PC was able to issue longer and thin process than C6 cells. Unexpectedly, IA did not respond to forskolin stimulus.

In order to evaluate the maturation of these cells the GFAP/Vimentin ratio was assessed. All three cell types showed greater levels of GFAP in compare to vimentin, indicating differentiated cells (Fig 2A). Characteristic proteins markers for astrocytes as GFAP and S100B ware evaluated, as well as proteins that are abundantly expressed in this glial cells as ALDH1L1, AQP4 and Kir4.1. As noted in Fig 2 (B-E) GFAP, S100B, ALDHL1 and AQP4 have reduced intracellular content in the two linage cells, compared with PC. Interestingly, Kir4.1 showed similar levels in three cells models (Fig 2 F).

Glutamate metabolism in different models of astrocytes

Astrocytes play an essential role in glutamate-glutamine metabolism. Therefore, we evaluated not only glutamate transporters content but also the functionality of these transporters by measuring glutamate uptake basal rate. As noted in Fig 3A, glutamate uptake in PC is much pronounced than IA and C6, and this reduced uptake rate may be due to low amount of EAAT1 and EAAT2 transporters (Fig 3 B and C). Once uptaked by astrocytes, glutamate is converted into glutamine, by the activity of glutamine synthetase. As expected, glutamine synthetase activity and content is reduced in IA and C6 compared to PC (Fig 3D and E). Interestingly, GSH content, which is the main antioxidant in astrocytes and its biosynthesis also depends on glutamate content, is produced in equivalent amount in the three models of astrocytes culture (Fig 3F).

Glucose metabolism in astrocyte linage and astrocytes primary culture

Astrocytes are the main energy supplier in brain, and have the important function to uptake glucose, stock or distribute to neurons. In the comparison between the three types of cells, C6 glioma cells uptake glucose in a significantly higher rate than PC and IA (Fig 4A). Despite this data, PC presented high glucose transporter (GLUT-1) content in compare to IA and C6 (Fig 4B).

Gap Junction communication

Astrocytes are interconnected by gap junction forming a syncytium between them. This is an important characteristic which may be essential for many astrocytes function (Rouach et al., 2002). This communication was evaluated by the analysis of Conexin43

content, the most abundantly expressed connexin in astrocytes culture, and by the transfer of Lucifer Yellow. Connexin 43 is lower expressed and gap junction communication is reduced in linage cells when compared to PC (Fig 5).

Astrocytes response under the same stimulus

Considering that the three models of astrocyte presented variation in basal protein profile, we wondered if they would respond different to the same stimulus. We used stimuli which are already described in the literature to interfere in astrocyte function. As shown in table 1, LPS treatment induced a decrease in S100B secretion in PC and C6. The same cells were affected under an oxidative damage induced by hydrogen peroxide, regarding GS activity and GSH content. In addition, S100B treatment affected glucose uptake in all cell models. In summary, PC and C6 present similar response under the same stimulus, in opposite to IA which showed no effect in most stimulus tested.

Discussion

With the advent of primary culture of astrocytes it was possible to explore individual characteristics of this type of cell in physiologic and toxic states which help to understand brain functionality. The purpose of this study was to compare primary astrocyte culture, genetically modify immortalized astrocytes or C6 linage cells regarding morphological and functional features in basal and stimulated conditions. Although commonly used, lineage characterizations are sparse, showing isolated features analysis, and often not compared to a normal astrocyte. A complete and integrative analysis of each cell in a single study allowed straight comparison, keeping the same culture conditions such as culture protocol and medium composition.

Morphology and plasticity evaluation

The plasticity capacity of astrocytes may be critical for studying cellular functions, since it is known that astrocyte emitting process regulate extracellular microenvironment and interfere in the synaptic activity of neurons (De Pittà et al., 2016; Ostroff et al., 2014). The capacity of the cell in culture to emit process and respond with morphological changes to some treatment is a very efficient and used tool for the evaluation of astrocytes function. In this work, morphology evaluation in basal condition showed that PC and IA have similar polygonal shape and regular filaments

then C6 cells, which presented triangular cell body and irregular network. Accordingly, a previous work observed differences in actin cytoskeleton structure between C6 and PC, associated with C6 invasiveness(Zhou et al., 2008). Although, the morphologic similarity with PC, IA did not respond to forskolin stimuli, which is a classical stimulus that mobilize intracellular levels of cAMP, indicating restriction of this cells to the study of cell plasticity. Similarly, in another work, immortalized cell lines did not change the levels of GFAP expression in response to dibutyryl cAMP, as C6 and PC did (Geller and Dubois-Dalcq, 1988). In opposite, PC and C6 cell showed high capacity to change morphology after stimuli, contracting neatly their cell body and emitting long process. Nevertheless, it was clear in our analysis that PC showed prominent thin and long process than C6 cell. Interestingly, in another work, primary cell culture loses process after subcultured, indicating that this procedure may interfere in the morphology responsiveness of the cell (Passaquin et al., 1994). A similar process may occur in C6 and IA which have many passages. Furthermore, a reduction in astrocyte cell process in C6 cells may also be explained by less quantities of GFAP, which is known to be essential to astrocyte hypertrophy (Wilhelmsson et al., 2004).

Expression profile of astrocyte markers

Astrocytes are highly heterogeneous cells and present variation of characteristic and function depending on cerebral region or specific pathologic context. Nevertheless, astrocytes share some function similarities and some molecular markers that are used to distinguish these cells from other glial cells. It is known that during development GFAP/vimentin ratio increase, which is associated with astrocytic differentiation (Menet et al., 2001). Here we show that all three models of analyzed cells presented higher levels of GFAP than vimentin.

Furthermore, in this work we evaluated conventional protein markers and abundantly expressed on astrocytes, such as GFAP and S100B (Brozzi et al., 2009; Eng, 1985; Van Eldik and Wainwright, 2003). Both proteins were detected in all three models of astrocytes cell culture, although in significantly less quantities in IA and C6 cells. Detected levels of these proteins were previously observed in other works that studied linage cells, although it was little discussed the comparative levels with PC (Furihata et al., 2016; Groves et al., 1993; Morikawa et al., 2001; Raju et al., 1980; Tabuchi et al., 1982). Besides these markers, we also evaluated ALDH1L1 protein which has been used as a new astroglial marker (Souza et al., 2013; Yang et al., 2011). Although this

protein participates in folate metabolism, interfering in cell division and growth (Krupenko, 2009), in our study we show reduced levels of ALDH1L1 in linage cells in compare to PC. The same result was seen with AQP4 levels, which is widely expressed in astrocytes membranes (Papadopoulos and Verkman, 2013). The reduced levels of important astrocytic protein markers observed in IA and C6 may be explained because of the high proliferative rate of these cells, which invest less in differentiation profile, while may express more protein related with proliferation. In opposite, Kir4.1 channel, which is also glial specific expressed (Seifert et al., 2016), was detected in equally amount in PC, IA and C6 cells. It was shown that potassium conductance is very low in gliomas in compare to differentiated cells. However, a reduction in potassium conductance it was not related with a reduction in expression but to a distinct localization of potassium channels, which were prominently expressed in nucleus instead of plasma membrane (Olsen and Sontheimer, 2008). Therefore, the equal expression observed in IA and C6 in compare PC may not represent the functionality of potassium channels.

Functional characterization of glutamate metabolism

Astrocytes play an essential role in glutamate metabolism. Any dysfunction in glutamate transporters or even GS activity may compromise brain functions. In fact, this alterations are related to the development of neurodegenerative diseases (Benarroch, 2010). Recently it was shown that astrocyte glutamate uptake depends on GS activity, which ensures an efficient clearance of glutamate by EAATs (Trabelsi et al., 2017). Our results showed reduced levels of EAAT1, EAAT2 and GS content in IA and C6 than PC, and this was related with lower glutamate metabolism as it was shown in reduced glutamate uptake and GS activity. The presence of glutamate transporters in astrocyte cell lines is unclear. Despite the detection of glutamate transporter in C6 and immortalized astrocytes were seen in earlier studies, their functionality have not been evaluated (Baber and Haghighat, 2010; Furihata et al., 2016). In opposite, other studies have not detected these transporters (Palos et al., 1996; Vanhoutte and Hermans, 2008). These differences could be explained by the number of subculturing at least in C6 cells. EAAT2-C6 negative cells were observed in low passages, in opposite to ours cells that were subcultured at least 100 times. The mechanistic reason to the switching of C6 from glioma features to astrocyte differentiated characteristics are unknown, although may be fundamental. Interestingly, EAAT2 over-expression was shown to reduce proliferative

rate of C6 cells under glutamate stimulus (Vanhoutte and Hermans, 2008), showing a negative correlation between glutamate transporters and cell proliferation.

Another important characteristic of astrocytes in CNS is the resistance to oxidative stress. This ability is thanks to high antioxidant GSH production, which uses glutamate as a precursor (Matés et al., 2002). As seen in our results, although IA and C6 uptake less glutamate, they presented similar GSH content in compare to PC. This result makes us assume that a big part of glutamate taken up by lineage cells is destined to GSH production, instead of glutamine synthesis (McKenna et al., 1996). Therefore, this pathway may be different controlled in PC and linage cells. Furthermore, the X_c^- cysteine/glutamate antiporter system has been shown to be overexpressed in glioma cells compared with normal astrocytes contributing to the growth, survival and expansion. The import of L-cystein through Sx_c^- provides the substrate do GSH synthesis (Bridges et al., 2012). Moreover, high GSH production in glioma cells may also be necessary as an antioxidant defense against the high oxidative metabolism observed in proliferative cells (Marie and Shinjo, 2011). Interestingly, GSH have been related to cell proliferation interfering in telomerase activity (Pallardó et al., 2009). Considering that linage cells presented higher proliferative rate than PC, is consistent to think that they may have GSH activated pathway.

Energetic metabolism and gap junction in astrocytes

Astrocytes represent a key element in the capture of energetic compound supplying it to active neurons. Most glucose utilized by astrocytes will be glycogen stored or/and converted to lactate for extracellular export (Bouzier-Sore and Pellerin, 2013). GLUT-1 is the main glucose transporter in astrocytes (Pellerin, 2008). In our analysis, GLUT-1 is down expressed in IA and C6 than PC. Surprisingly, the functionality of these transporters, measured by glucose uptake, is much pronounced in C6 cells than IA and PC (Fig 5). Accordingly, previews study showed that C6 glioma cells utilize more glucose and produce less lactate than normal astrocytes (Haghighat and McCandless, 1997a). The authors suggest that glucose may be used in another pathway such as the pentose phosphate shunt. These pathway produce NADPH, which could be also used by glutathione reductase for the production of GSH (Dringen et al., 2015). Furthermore, high levels of energy metabolism are common in proliferative cells (Marie and Shinjo, 2011). Taking into account that C6 originates from glioma cell lines it can be easily assumed that these cells still maintain some characteristics of tumor cells. It is

interestingly to note, that although IA have a higher proliferative rate, it did not present higher glucose metabolism as C6 cells. Immortalized astrocytes originate from a normal astrocyte and not from a malignant cell. This may imply in different features and other activated metabolic pathways.

In addition, glucose metabolism is related to gap junction communication, since metabolic substrates can cross astrocytic gap junction (Tabernero et al., 2006). Moreover, gap junction communication is related to proliferative rate. In fact, tumor cells lines are usually devoid of gap junction, and are inhibited by tumor-promoting molecules (Budunova and Williams, 1994). Astrocytes are interconnected by gap junction composed primarily of Cx43 in cell culture (Rouach et al., 2002). C6 are known to have low levels of cell communication, which is in accordance with the low levels of Cx43 seen in our results in compare to PC. Interestingly, an increase in gap junction communication decrease glucose uptake and proliferative rate in C6 cells (Tabernero et al., 2006). Thus, high levels of glucose uptake, as seen in C6 cells, may be explained by the low levels of functional communication.

Stimulus effect on astrocyte culture models

Some contradictory results are found in the literature when different models of astrocyte culture are submitted to the same treatment (Haghighat and McCandless, 1997a; Leite et al., 2009; Morikawa et al., 2001; Nardin et al., 2007). These results variation make difficult the analysis and question the validity of the model. Therefore, we tested how the three different models of astrocyte culture would respond to the same treatment. For that, we used stimuli that were already known in the literature to cause functional changes in primary culture. It is important to mention that variation in culture response may also be influenced by differences in culture procedure, such as medium composition, culture plate coating, subculture and days *in vitro* (Lange et al., 2012). These differences may interfere in gene expression and morphology variation (Passaquin et al., 1994). In fact, recently it was seen that extracellular matrix composition determines astrocyte responses to mechanical and inflammatory stimuli (Johnson et al., 2015). In this work, we maintained equal procedure to all three cultured models, ensuring that the effects observed of treatment were due to biological cell variation.

Overall, our results showed that PC and C6 cells respond similarly to the same stimulus, regarding S100B secretion, GSH oxidative metabolism, glutamine synthetase activity and glucose uptake (Table 1). Therefore, although they often presented differences in the basal amount of protein, the activated pathways appear to be similar in tested stimulus. In contrast, IA showed little reactivity in the assays tested, presenting similar response to PC only in glucose uptake analysis, indicating that it is not a good model for the study of astrocytes features, at least this clone transfected. Recently it was shown that p53 isoform expressed in different passages, regulates astrocyte-mediated neuroprotection and neurodegeneration (Turnquist et al., 2016). Therefore, IA that has p53 inhibited (due to the transfection process) may have compromised functionality.

Proliferative rate and protein expression balance

The proliferative rat it is one of the main differences between PC and linage cells. It is known, that IA and C6 growth in much higher degree than PC, which may explain some basal differences related in protein profile. These linage cells may present an incomplete differentiation phenotype while invest more in proteins related to cell proliferation. In fact, the levels of any specific protein inside cell are dynamic. Gene expression may vary dependent on cell density or cell cycle transition time. For example, a decrease in proliferative associated genes is expected in confluence cells or, an upregulation in differentiated associated genes (Frisa and Jacobberger, 2002). The attenuation in proliferative abilities may allow the cell to undergo more differentiated status. Therefore, it is important in this analysis, and in any other study that uses these cell models, to maintain a confluence pattern to reach gene expression stability.

In general, our results showed that the two models of cell lines (IA and C6) were positive for astrocytic characteristics proteins, but in much lower amount. Although IA presented a slower growth rate than C6 cells, and a similar basal morphology with PC, they did not prove to be a good reproductive model of the classic astrocytic functions. In contrast, C6 cells, which have a tumorigenic origin, were able to present differentiated characteristics, resembling more to astrocytes. In addition, the response of these cells to the same stimulus was equivalent to PC.

Conclusion

In summary, we show an integrative characterization and comparative analysis of PC, IA and C6. We analyzed in basal condition not only the expression protein profile of

each cell model, but also the functionality of this proteins regarding glutamate and glucose metabolism and cell communication. Furthermore, variation in cellular morphology or biochemistry response under the same stimulus was also assessed.

Based on our data, although PC is more time-consuming and costly technique, the use as a reproductive model for astrocyte studies is undoubtedly preferential. However, the C6 cell line, although present some limitations seems to functionally reproduce an astrocyte in a considerable way. These cells may represent a good astrocytic model for initial studies to detect in a faster way some characteristics which astrocytes are involved, although for a deep analysis PC may be rather selected. All these issues must be considered for the choice of a suitable model for the study of astrocyte. These work provided limitation and the advantages of each culture, optimizing the research in the area of knowledge.

Acknowledgements: This work was supported by Conselho Nacional de Desenvolvimento Científico e Tecnológico (CNPq), Coordenação de Aperfeiçoamento de Pessoal de Nível Superior (CAPES), Fundação de Amparo à Pesquisa do Estado do Rio Grande do Sul (FAPERGS) and Instituto Nacional de Ciência e tecnologia (INCT).

References

Baber, Z., Haghighat, N., 2010. Glutamine synthetase gene expression and glutamate transporters in C6-glioma cells. Metab Brain Dis 25(4), 413-418.

Benarroch, E.E., 2010. Glutamate transporters: diversity, function, and involvement in neurologic disease. Neurology 74(3), 259-264.

Benda, P., Lightbody, J., Sato, G., Levine, L., Sweet, W., 1968. Differentiated rat glial cell strain in tissue culture. Science 161(3839), 370-371.

Bouzier-Sore, A.K., Pellerin, L., 2013. Unraveling the complex metabolic nature of astrocytes. Front Cell Neurosci 7, 179.

Browne, R.W., Armstrong, D., 1998. Reduced glutathione and glutathione disulfide. Methods Mol Biol 108, 347-352.

Brozzi, F., Arcuri, C., Giambanco, I., Donato, R., 2009. S100B Protein Regulates Astrocyte Shape and Migration via Interaction with Src Kinase: IMPLICATIONS FOR ASTROCYTE DEVELOPMENT, ACTIVATION, AND TUMOR GROWTH. J Biol Chem 284(13), 8797-8811.

Budunova, I.V., Williams, G.M., 1994. Cell culture assays for chemicals with tumor-promoting or tumor-inhibiting activity based on the modulation of intercellular communication. Cell Biol Toxicol 10(2), 71-116.

De Pittà, M., Brunel, N., Volterra, A., 2016. Astrocytes: Orchestrating synaptic plasticity? Neuroscience 323, 43-61.

Dringen, R., Brandmann, M., Hohnholt, M.C., Blumrich, E.M., 2015. Glutathione-Dependent Detoxification Processes in Astrocytes. Neurochem Res 40(12), 2570-2582.

Dringen, R., Kussmaul, L., Gutterer, J.M., Hirrlinger, J., Hamprecht, B., 1999. The glutathione system of peroxide detoxification is less efficient in neurons than in astroglial cells. J Neurochem 72(6), 2523-2530.

Eng, L.F., 1985. Glial fibrillary acidic protein (GFAP): the major protein of glial intermediate filaments in differentiated astrocytes. J Neuroimmunol 8(4-6), 203-214.

Fernandes, S.P., Dringen, R., Lawen, A., Robinson, S.R., 2011. Inactivation of astrocytic glutamine synthetase by hydrogen peroxide requires iron. Neurosci Lett 490(1), 27-30.

Frisa, P.S., Jacobberger, J.W., 2002. Cell density related gene expression: SV40 large T antigen levels in immortalized astrocyte lines. BMC Cell Biol 3, 10.

Frizzo, J.K., Tramontina, A.C., Tramontina, F., Gottfried, C., Leal, R.B., Donato, R., Gonçalves, C.A., 2004. Involvement of the S100B in cAMP-induced cytoskeleton remodeling in astrocytes: a study using TRTK-12 in digitonin-permeabilized cells. Cell Mol Neurobiol 24(6), 833-840.

Furihata, T., Ito, R., Kamiichi, A., Saito, K., Chiba, K., 2016. Establishment and characterization of a new conditionally immortalized human astrocyte cell line. J Neurochem 136(1), 92-105.

Geller, H.M., Dubois-Dalcq, M., 1988. Antigenic and functional characterization of a rat central nervous system-derived cell line immortalized by a retroviral vector. J Cell Biol 107(5), 1977-1986.

Gottfried, C., Tramontina, F., Gonçalves, D., Gonçalves, C.A., Moriguchi, E., Dias, R.D., Wofchuk, S.T., Souza, D.O., 2002. Glutamate uptake in cultured astrocytes depends on age: a study about the effect of guanosine and the sensitivity to oxidative stress induced by H(2)O(2). Mech Ageing Dev 123(10), 1333-1340.

Groves, A.K., Entwistle, A., Jat, P.S., Noble, M., 1993. The characterization of astrocyte cell lines that display properties of glial scar tissue. Dev Biol 159(1), 87-104.

Guerra, M.C., Tortorelli, L.S., Galland, F., Da Ré, C., Negri, E., Engelke, D.S., Rodrigues, L., Leite, M.C., Gonçalves, C.A., 2011. Lipopolysaccharide modulates astrocytic S100B secretion: a study in cerebrospinal fluid and astrocyte cultures from rats. J Neuroinflammation 8, 128.

Haghighat, N., 2005. Estrogen (17beta-estradiol) enhances glutamine synthetase activity in C6-glioma cells. Neurochem Res 30(5), 661-667.

Haghighat, N., McCandless, D.W., 1997a. Effect of 6-aminonicotinamide on metabolism of astrocytes and C6-glioma cells. Metab Brain Dis 12(1), 29-45.

Haghighat, N., McCandless, D.W., 1997b. Effect of ammonium chloride on energy metabolism of astrocytes and C6-glioma cells *in vitro*. Metab Brain Dis 12(4), 287-298.

Hertz, L., Chen, Y., Song, D., 2017. Astrocyte Cultures Mimicking Brain Astrocytes in Gene Expression, Signaling, Metabolism and K(+) Uptake and Showing Astrocytic Gene Expression Overlooked by Immunohistochemistry and In Situ Hybridization. Neurochem Res 42(1), 254-271.

Johnson, K.M., Milner, R., Crocker, S.J., 2015. Extracellular matrix composition determines astrocyte responses to mechanical and inflammatory stimuli. Neurosci Lett 600, 104-109.

Kacem, K., Lacombe, P., Seylaz, J., Bonvento, G., 1998. Structural organization of the perivascular astrocyte endfeet and their relationship with the endothelial glucose transporter: a confocal microscopy study. Glia 23(1), 1-10.

Kettenmann, H., Verkhratsky, A., 2008. Neuroglia: the 150 years after. Trends Neurosci 31(12), 653-659.

Krupenko, S.A., 2009. FDH: an aldehyde dehydrogenase fusion enzyme in folate metabolism. Chem Biol Interact 178(1-3), 84-93.

Lange, S.C., Bak, L.K., Waagepetersen, H.S., Schousboe, A., Norenberg, M.D., 2012. Primary cultures of astrocytes: their value in understanding astrocytes in health and disease. Neurochem Res 37(11), 2569-2588.

Lasič, E., Galland, F., Vardjan, N., Šribar, J., Križaj, I., Leite, M.C., Zorec, R., Stenovec, M., 2016. Time-dependent uptake and trafficking of vesicles capturing extracellular S100B in cultured rat astrocytes. J Neurochem 139(2), 309-323.

Leite, M.C., Galland, F., Brolese, G., Guerra, M.C., Bortolotto, J.W., Freitas, R., Almeida, L.M., Gottfried, C., Gonçalves, C.A., 2008. A simple, sensitive and widely applicable ELISA for S100B: Methodological features of the measurement of this glial protein. J Neurosci Methods 169(1), 93-99.

Leite, M.C., Galland, F., de Souza, D.F., Guerra, M.C., Bobermin, L., Biasibetti, R., Gottfried, C., Gonçalves, C.A., 2009. Gap junction inhibitors modulate S100B secretion in astrocyte cultures and acute hippocampal slices. J Neurosci Res 87(11), 2439-2446.

Marie, S.K., Shinjo, S.M., 2011. Metabolism and brain cancer. Clinics (Sao Paulo) 66 Suppl 1, 33-43.

Matés, J.M., Pérez-Gómez, C., Núñez de Castro, I., Asenjo, M., Márquez, J., 2002. Glutamine and its relationship with intracellular redox status, oxidative stress and cell proliferation/death. Int J Biochem Cell Biol 34(5), 439-458.

McKenna, M.C., 2007. The glutamate-glutamine cycle is not stoichiometric: fates of glutamate in brain. J Neurosci Res 85(15), 3347-3358.

McKenna, M.C., Sonnewald, U., Huang, X., Stevenson, J., Zielke, H.R., 1996. Exogenous glutamate concentration regulates the metabolic fate of glutamate in astrocytes. J Neurochem 66(1), 386-393.

Menet, V., Giménez y Ribotta, M., Chauvet, N., Drian, M.J., Lannoy, J., Colucci-Guyon, E., Privat, A., 2001. Inactivation of the glial fibrillary acidic protein gene, but not that of vimentin, improves neuronal survival and neurite growth by modifying adhesion molecule expression. J Neurosci 21(16), 6147-6158.

Minet, R., Villie, F., Marcollet, M., Meynial-Denis, D., Cynober, L., 1997. Measurement of glutamine synthetase activity in rat muscle by a colorimetric assay. Clin Chim Acta 268(1-2), 121-132.

Morikawa, M., Asai, K., Kokubo, M., Fujita, K., Yoneda, K., Yamamoto, N., Inoue, Y., Iida, J., Kishimoto, T., Kato, T., 2001. Isolation and characterization of a new immortal rat astrocyte with a high expression of NGF mRNA. Neurosci Res 39(2), 205-212.

Nardin, P., Tramontina, F., Leite, M.C., Tramontina, A.C., Quincozes-Santos, A., de Almeida, L.M., Battastini, A.M., Gottfried, C., Gonçalves, C.A., 2007. S100B content and secretion decrease in astrocytes cultured in high-glucose medium. Neurochem Int 50(5), 774-782.

Olsen, M.L., Sontheimer, H., 2008. Functional implications for Kir4.1 channels in glial biology: from K+ buffering to cell differentiation. J Neurochem 107(3), 589-601.

Ostroff, L.E., Manzur, M.K., Cain, C.K., Ledoux, J.E., 2014. Synapses lacking astrocyte appear in the amygdala during consolidation of Pavlovian threat conditioning. J Comp Neurol 522(9), 2152-2163.

Pallardó, F.V., Markovic, J., García, J.L., Viña, J., 2009. Role of nuclear glutathione as a key regulator of cell proliferation. Mol Aspects Med 30(1-2), 77-85.

Palos, T.P., Ramachandran, B., Boado, R., Howard, B.D., 1996. Rat C6 and human astrocytic tumor cells express a neuronal type of glutamate transporter. Brain Res Mol Brain Res 37(1-2), 297-303.

Papadopoulos, M.C., Verkman, A.S., 2013. Aquaporin water channels in the nervous system. Nat Rev Neurosci 14(4), 265-277.

Parker, K.K., Norenberg, M.D., Vernadakis, A., 1980. "Transdifferentiation" of C6 glial cells in culture. Science 208(4440), 179-181.

Passaquin, A.C., Schreier, W.A., de Vellis, J., 1994. Gene expression in astrocytes is affected by subculture. Int J Dev Neurosci 12(4), 363-372.

Pellerin, L., 2008. Brain energetics (thought needs food). Curr Opin Clin Nutr Metab Care 11(6), 701-705.

Pellerin, L., Magistretti, P.J., 1994. Glutamate uptake into astrocytes stimulates aerobic glycolysis: a mechanism coupling neuronal activity to glucose utilization. Proc Natl Acad Sci U S A 91(22), 10625-10629.

Perea, G., Araque, A., 2005. Glial calcium signaling and neuron-glia communication. Cell Calcium 38(3-4), 375-382.

Peterson, G.L., 1977. A simplification of the protein assay method of Lowry et al. which is more generally applicable. Anal Biochem 83(2), 346-356.

Raju, T.R., Bignami, A., Dahl, D., 1980. Glial fibrillary acidic protein in monolayer cultures of C-6 glioma cells: effect of aging and dibutyryl cyclic AMP. Brain Res 200(1), 225-230.

Rouach, N., Avignone, E., Même, W., Koulakoff, A., Venance, L., Blomstrand, F., Giaume, C., 2002. Gap junctions and connexin expression in the normal and pathological central nervous system. Biol Cell 94(7-8), 457-475.

Seifert, G., Henneberger, C., Steinhäuser, C., 2016. Diversity of astrocyte potassium channels: An update. Brain Res Bull.

Sofroniew, M.V., Vinters, H.V., 2010. Astrocytes: biology and pathology. Acta Neuropathol 119(1), 7-35.

Souza, D.G., Bellaver, B., Souza, D.O., Quincozes-Santos, A., 2013. Characterization of adult rat astrocyte cultures. PLoS One 8(3), e60282.

Tabernero, A., Medina, J.M., Giaume, C., 2006. Glucose metabolism and proliferation in glia: role of astrocytic gap junctions. J Neurochem 99(4), 1049-1061.

Tabuchi, K., Imada, M., Nishimoto, A., 1982. Effects of cyclic AMP on S-100 protein level in C-6 glioma cells. J Neurol Sci 56(1), 57-63.

Thomazi, A.P., Godinho, G.F., Rodrigues, J.M., Schwalm, F.D., Frizzo, M.E., Moriguchi, E., Souza, D.O., Wofchuk, S.T., 2004. Ontogenetic profile of glutamate uptake in brain structures slices from rats: sensitivity to guanosine. Mech Ageing Dev 125(7), 475-481.

Trabelsi, Y., Amri, M., Becq, H., Molinari, F., Aniksztejn, L., 2017. The conversion of glutamate by glutamine synthase in neocortical astrocytes from juvenile rat is important to limit glutamate spillover and peri/extrasynaptic activation of NMDA receptors. Glia 65(2), 401-415.

Tramontina, F., Leite, M.C., Cereser, K., de Souza, D.F., Tramontina, A.C., Nardin, P., Andreazza, A.C., Gottfried, C., Kapczinski, F., Gonçalves, C.A., 2007. Immunoassay for glial fibrillary acidic protein: antigen recognition is affected by its phosphorylation state. J Neurosci Methods 162(1-2), 282-286.

Turnquist, C., Horikawa, I., Foran, E., Major, E.O., Vojtesek, B., Lane, D.P., Lu, X., Harris, B.T., Harris, C.C., 2016. p53 isoforms regulate astrocyte-mediated neuroprotection and neurodegeneration. Cell Death Differ 23(9), 1515-1528.

Van Eldik, L.J., Wainwright, M.S., 2003. The Janus face of glial-derived S100B: beneficial and detrimental functions in the brain. Restor Neurol Neurosci 21(3-4), 97-108.

Vanhoutte, N., Hermans, E., 2008. Glutamate-induced glioma cell proliferation is prevented by functional expression of the glutamate transporter GLT-1. FEBS Lett 582(13), 1847-1852.

Wartchow, K.M., Tramontina, A.C., de Souza, D.F., Biasibetti, R., Bobermin, L.D., Gonçalves, C.A., 2016. Insulin Stimulates S100B Secretion and These Proteins Antagonistically Modulate Brain Glucose Metabolism. Neurochem Res 41(6), 1420-1429.

Wilhelmsson, U., Li, L., Pekna, M., Berthold, C.H., Blom, S., Eliasson, C., Renner, O., Bushong, E., Ellisman, M., Morgan, T.E., Pekny, M., 2004. Absence of glial fibrillary acidic protein and vimentin prevents hypertrophy of astrocytic processes and improves post-traumatic regeneration. J Neurosci 24(21), 5016-5021.

Yang, Y., Vidensky, S., Jin, L., Jie, C., Lorenzini, I., Frankl, M., Rothstein, J.D., 2011. Molecular comparison of GLT1+ and ALDH1L1+ astrocytes *in vivo* in astroglial reporter mice. Glia 59(2), 200-207.

Zhou, D., Jiang, X., Xu, R., Cai, Y., Hu, J., Xu, G., Zou, Y., Zeng, Y., 2008. Assessing the cytoskeletal system and its elements in C6 glioma cells and astrocytes by atomic force microscopy. Cell Mol Neurobiol 28(6), 895-905.

Table 1 Astrocytes culture response under stimulus

Assay	Stimulus	PC	IA	C6
GFAP	LPS 1 µg/mL 24h [1]	↑ 178.1* ± 20 %	-- 81 ± 10.2 %	-- 122 ± 27 %
S100B	LPS 1 µg/mL 24h [2]	↓ 77.6* ± 6.2 %	-- 121.5 ± 30 %	↓ 37.5* ± 4.8 %
GS activity	H_2O_2 50 µM 3h [3]	↓ 84.6* ± 3.4 %	-- 125 ± 11 %	↓ 75.6* ± 8.9 %
Glucose uptake	S100B 0.1ng/mL 30 min [4]	↓ 67.6* ± 4.8 %	↓ 78.6* ± 7.8 %	↓ 66.8* ± 11.7 %
GSH content	H_2O_2 50 µM 3h [5]	↓ 70.2* ± 8.0 %	-- 91.4* ± 6.3 %	↓ 66.9* ± 9.2 %

Table 1. Astrocytes were treated with the indicated stimulus and times and assays were preceded. Stimuli were chosen in accordance with previews works which showed alteration in PC parameters: 1 and 2 (Guerra et al., 2011); 3 (Fernandes et al., 2011), 4 (Dringen et al., 1999) 5 (Wartchow et al., 2016). Numbers indicate the percentage in relation to controls. Arrows up indicate an increase, arrows down indicate a reduction in compare to controls and trace indicates no effect. Statistical analysis was performed T-test, with a significance level of $p < 0.05$.

Legends of Figures

Fig 1. Morphology and plasticity evaluation in PC, C6 and IA.
Immunocytochemistry for actin, GFAP and S100B was done in basal and forskolin stimulated condition (15 min) in primary culture, immortalized astrocytes and C6 cells.

Fig 2. Astrocytes markers protein profile in PC, IA and C6. The content of characteristic proteins of astrocytes were analysed in basal condition in PC, IA and C6. Imunoblot for GFAP and vimentin ratio (A); GFAP (B) and S100B (C) content was measured by ELISA; ALDH1L1 (D); AQP4 (E) and Kir4.1 (F) content was measured by immunoblot. Representative immunoblot are shown in inserts. Each value is the mean (± standard error) from at least 5 experiments. Statistical analysis was performed one way ANOVA followed by Tukey's test, with a significance level of $p < 0.05$.

Fig 3. Characterization of glutamate metabolism in PC, IA and C6 cells. Glutamate uptake was examined in cells in basal condition by radiometric assay (A). The immunocontent of EAAT1 (B) and EAAT2 (C) was measured by immunoblot. Glutamine synthetase activity was measured by a colorimetric assay (D) and GS immunocontent by immunoblot analysis (E). GSH content was measured by fluorimetric assay (F). Representative immunoblot are shown in inserts. Each value is the mean (± standard error) from at least 5 experiments. Statistical analysis was performed one way ANOVA followed by Tukey's test, with a significance level of $p < 0.05$.

Fig 4. Characterization of glucose metabolism in PC, IA and C6 cells. Glucose uptake was examined in cells in basal condition by radiometric assay (A). The immunocontent of GLUT-1 was measured by immunoblot (B). Representative immunoblot is shown in insert. Each value is the mean (± standard error) from at least 5 experiments. Statistical analysis was performed one way ANOVA followed by Tukey's test, with a significance level of $p < 0.05$.

Fig 5. Gap junction comunication in PC, IA and C6. Conexin-43 immunocontent it was evaluated in basal condition (A). Astrocytes were submitted to scrape loading with Lucifer yellow for 10 min, as detailed in Materials and Methods. Cells in basal state are shown in green fluorescent staining (B). Values of gross density luminescence unit (mean ± SE) from three independent experiments performed in triplicate are indicated.

Figure 1

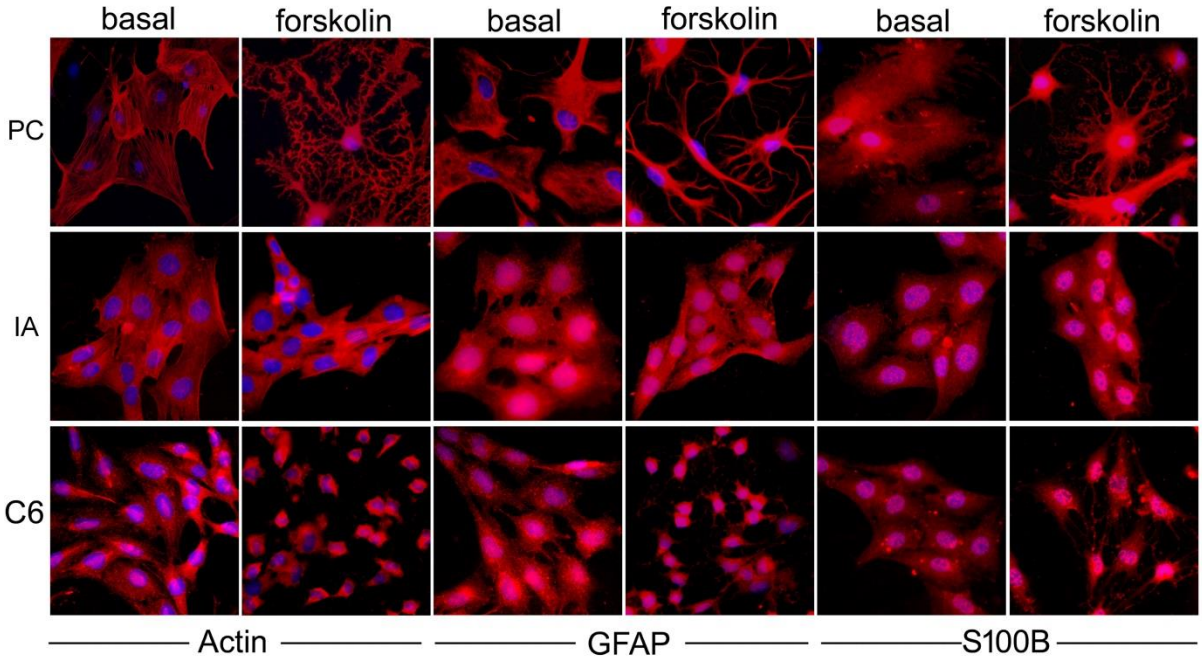
basal
forskolin
basal
forskolin
basal
forskolin
PC
IA
C6
Actin
GFAP
S100B

Figure 2

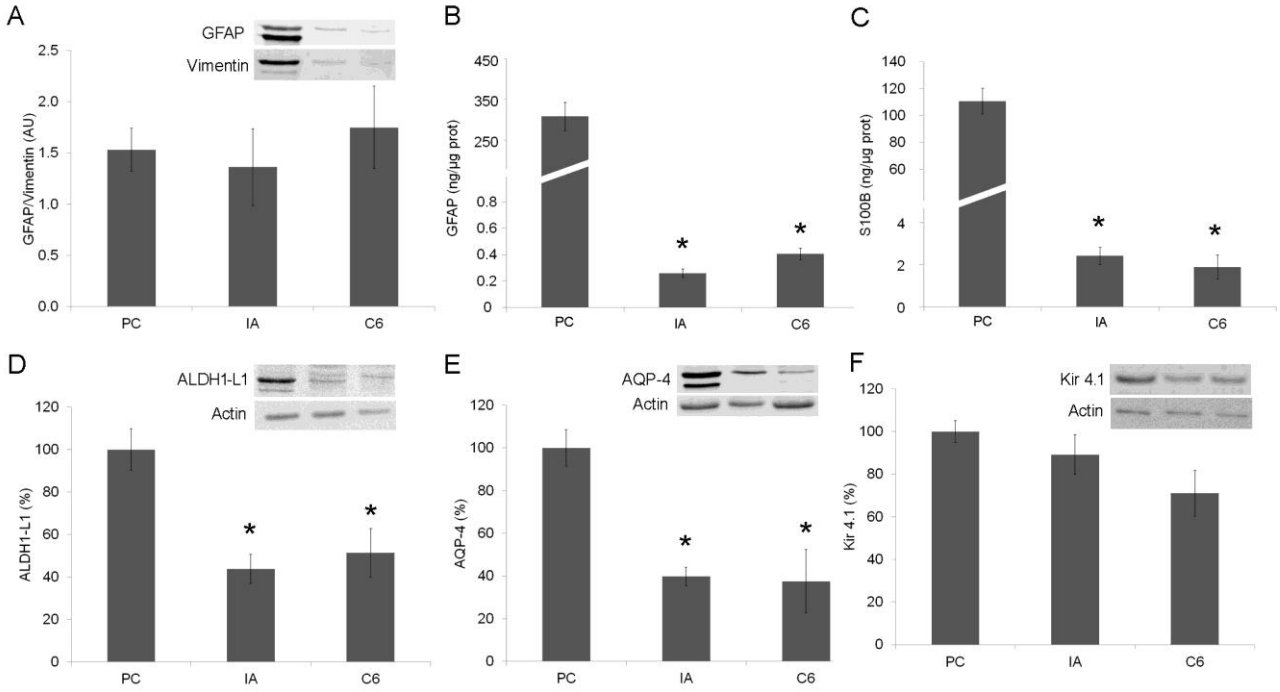
A
GFAP
Vimentin
GFAP/Vimentin (AU)
2.5
2.0
1.5
1.0
0.5
0.0
PC
IA
C6
B
GFAP (ng/µg prot)
450
350
250
0.8
0.6
0.4
0.2
0
*
*
PC
IA
C6
C
S100B (ng/µg prot)
140
120
100
80
60
4
2
0
*
*
PC
IA
C6
D
ALDH1-L1
Actin
ALDH1-L1 (%)
120
100
80
60
40
20
0
*
*
PC
IA
C6
E
AQP-4
Actin
AQP-4 (%)
120
100
80
60
40
20
0
*
*
PC
IA
C6
F
Kir 4.1
Actin
Kir 4.1 (%)
120
100
80
60
40
20
0
PC
IA
C6

Figure 3

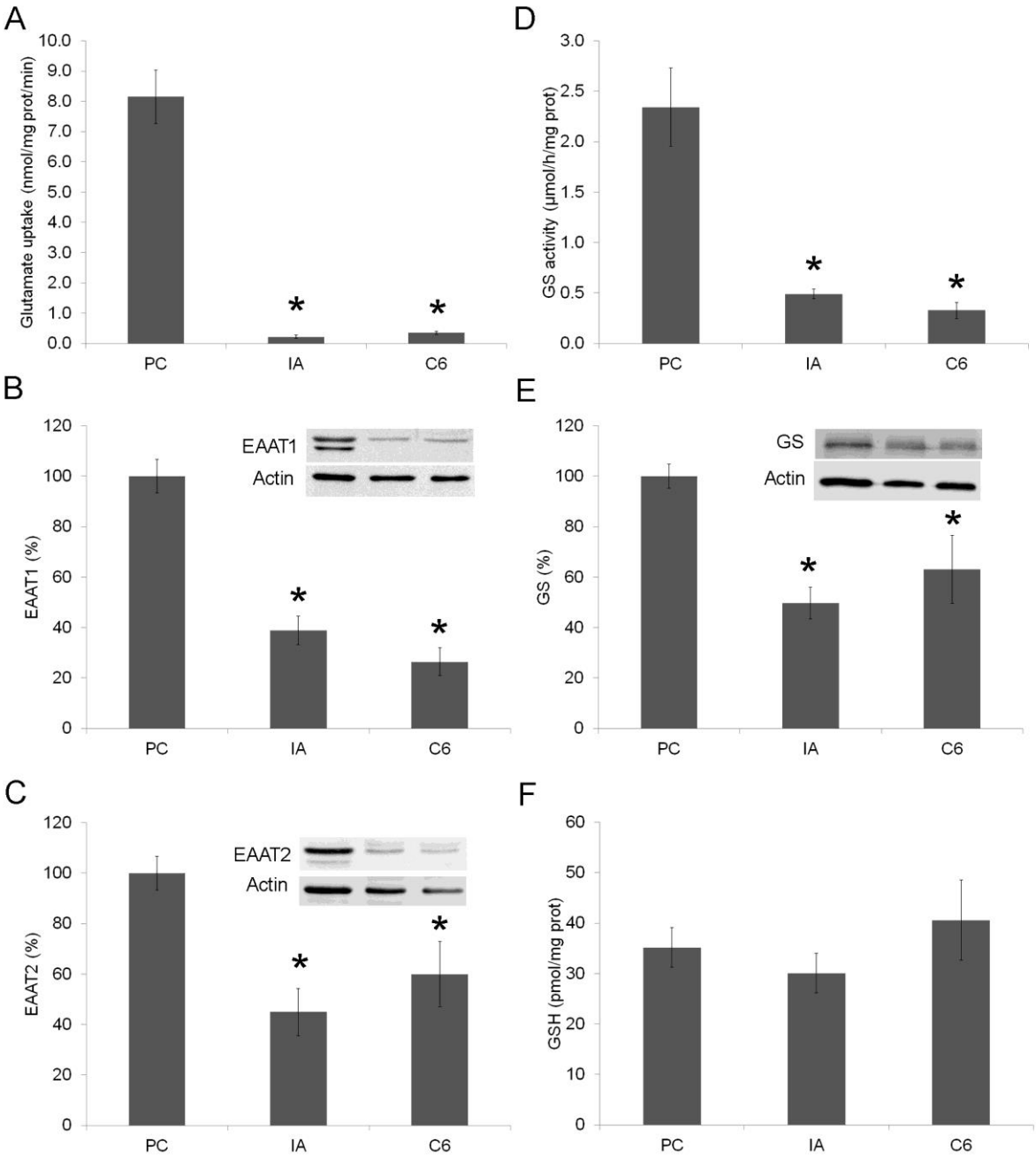
A
Glutamate uptake (nmol/mg prot/min)
10.0
9.0
8.0
7.0
6.0
5.0
4.0
3.0
2.0
1.0
0.0
PC
IA
C6
D
GS activity (µmol/h/mg prot)
3.0
2.5
2.0
1.5
1.0
0.5
0.0
B
EAAT1 (%)
EAAT1
Actin
E
GS (%)
GS
Actin
C
EAAT2 (%)
EAAT2
Actin
F
GSH (pmol/mg prot)
60
50
40
30
20
10
0

Figure 4

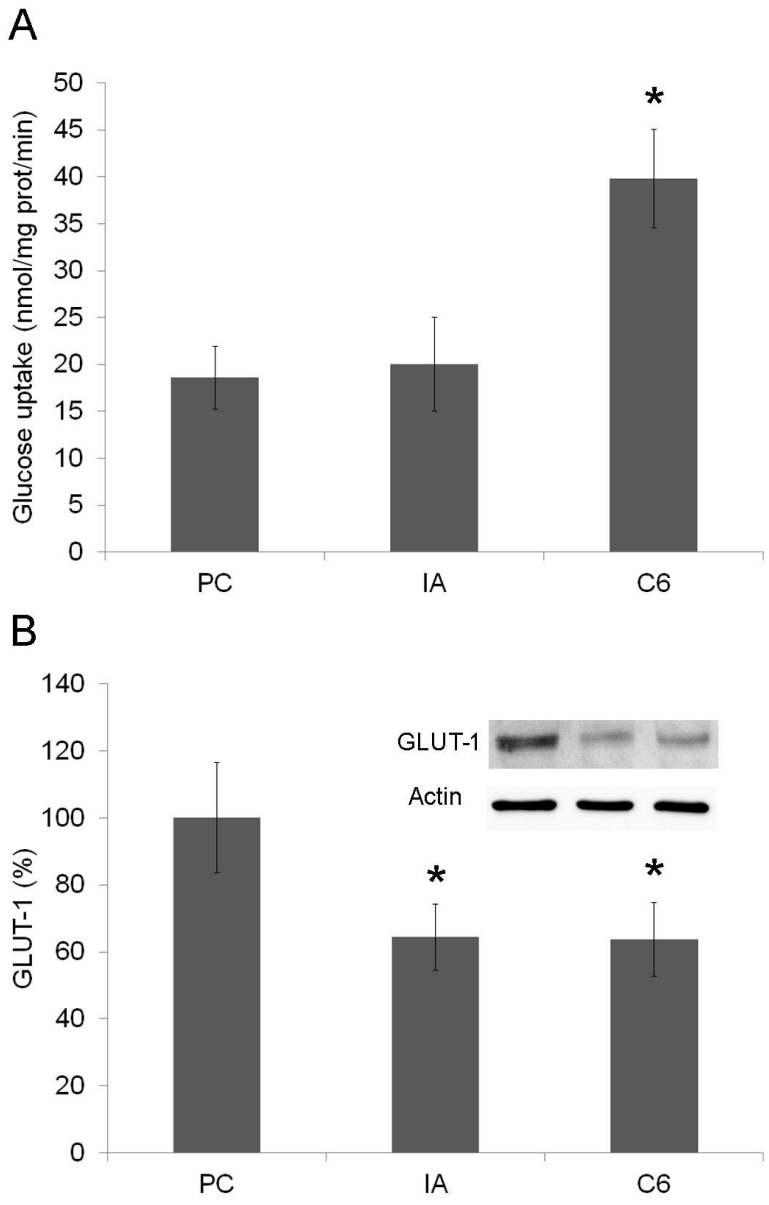
A
Glucose uptake (nmol/mg prot/min)
50
45
40
35
30
25
20
15
10
5
0
*
PC
IA
C6
B
GLUT-1 (%)
140
120
100
80
60
40
20
0
GLUT-1
Actin
*
*
PC
IA
C6

Figure 5

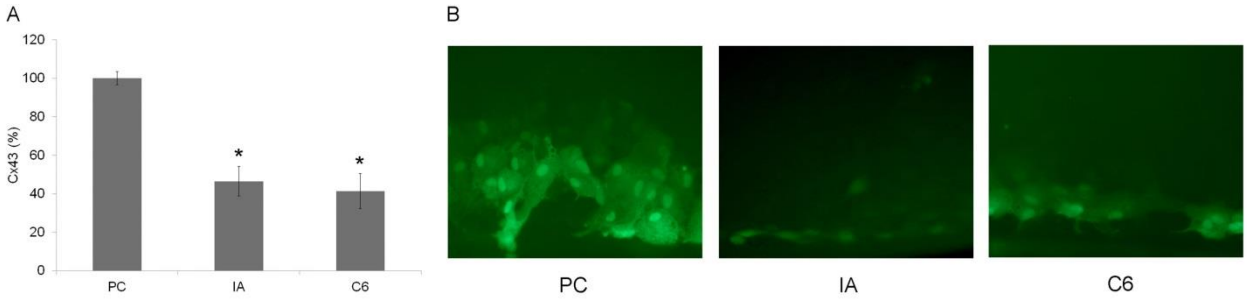

3.2. Capítulo II

Time-dependent uptake and trafficking of vesicles capturing extracellular S100B in cultured rat astrocytes

Artigo publicado no periódico *Journal of Neurochemistry*

Journal of Neurochemistry

JOURNAL OF NEUROCHEMISTRY | 2016 | 139 | 309–323 doi: 10.1111/jnc.13754

ORIGINAL ARTICLE

Time-dependent uptake and trafficking of vesicles capturing extracellular S100B in cultured rat astrocytes

Eva Lasič,*,[1] Fabiana Galland,*,†,[1] Nina Vardjan,*,‡ Jernej Šribar,§ Igor Križaj,§¶ Marina Concli Leite,† Robert Zorec*,‡ and Matjaž Stenovec*,‡,[1]

*Laboratory of Neuroendocrinology – Molecular Cell Physiology, Institute of Pathophysiology, Faculty of Medicine, University of Ljubljana, Ljubljana, Slovenia

†Departamento de Bioquímica, Instituto de Ciências Básicas da Saúde, Universidade Federal do Rio Grande do Sul, Porto Alegre, Brazil

‡Celica Biomedical, Ljubljana, Slovenia

§Department of Molecular and Biomedical Sciences, Jožef Stefan Institute, Ljubljana, Slovenia

¶Faculty of Chemistry and Chemical Technology, University of Ljubljana, Ljubljana, Slovenia

Abstract

Astrocytes, the most heterogeneous glial cells in the central nervous system, contribute to brain homeostasis, by regulating a myriad of functions, including the clearance of extracellular debris. When cells are damaged, cytoplasmic proteins may exit into the extracellular space. One such protein is S100B, which may exert toxic effects on neighboring cells unless it is removed from the extracellular space, but the mechanisms of this clearance are poorly understood. By using time-lapse confocal microscopy and fluorescently labeled S100B (S100B-Alexa^{488}) and fluorescent dextran (Dextran^{546}), a fluid phase uptake marker, we examined the uptake of fluorescently labeled S100B-Alexa^{488} from extracellular space and monitored trafficking of vesicles that internalized S100B-Alexa^{488}. Initially, S100B-Alexa^{488} and Dextran^{546} internalized with distinct rates into different endocytotic vesicles; S100B-Alexa^{488} internalized into smaller vesicles than Dextran^{546}. At a later stage, S100B-Alexa^{488}-positive vesicles substantially co-localized with Dextran^{546}-positive endolysosomes and with acidic LysoTracker-positive vesicles. Cell treatment with anti-receptor for advanced glycation end products (RAGE) antibody, which binds to RAGE, a 'scavenger receptor', partially inhibited uptake of S100B-Alexa^{488}, but not of Dextran^{546}. The dynamin inhibitor dynole 34-2 inhibited internalization of both fluorescent probes. Directional mobility of S100B-Alexa^{488}-positive vesicles increased over time and was inhibited by ATP stimulation, an agent that increases cytosolic free calcium concentration ($[Ca^{2+}]_i$). We conclude that astrocytes exhibit RAGE- and dynamin-dependent vesicular mechanism to efficiently remove S100B from the extracellular space. If a similar process occurs *in vivo*, astroglia may mitigate the toxic effects of extracellular S100B by this process under pathophysiologic conditions.

Keywords: astrocyte, intracellular trafficking, lysosome, S100 proteins, vesicles, waste removal.

J. Neurochem. (2016) **139**, 309–323.

The human cortex represents most of the brain mass; in this structure, non-neuronal cells, which include astrocytes, outnumber neurones (Azevedo *et al.* 2009). Astrocytes are placed between neuronal elements and the vasculature, which

Received February 29, 2016; revised manuscript received July 21, 2016; accepted July 26, 2016.

Address correspondence and reprint requests to Robert Zorec or Matjaž Stenovec, Laboratory of Neuroendocrinology – Molecular Cell Physiology, Institute of Pathophysiology, University of Ljubljana, Faculty of Medicine, Zaloška 4, 1000 Ljubljana, Slovenia. E-mails: robert.zorec@mf.uni-lj.si; matjaz.stenovec@mf.uni-lj.si

[1]These authors contributed equally to this work.

Abbreviations used: $[Ca^{2+}]_i$, cytosolic free calcium concentration; A.U., arbitrary units; ANP, atrial natriuretic peptide; BBB, blood–brain barrier; BSA, bovine serum albumin; CD36, cluster of differentiation 36; CD47, cluster of differentiation 47; CNS, central nervous system; EEA1, early endosome antigen 1; LAMP1, lysosomal-associated membrane protein 1; NFκB, nuclear factor kappa B; PBS, phosphate-buffered saline; proBDNF, pro brain-derived neurotrophic factor; Rab11, RAS-related GTP-binding protein 11; Rab7, RAS-related GTP-binding protein 7; RAGE, receptor for advanced glycation endproducts; rNadA, Neisseria meningitidis adhesin A; SDS–PAGE, sodium dodecyl sulfate–polyacrylamide gel electrophoresis; SIM, structured illumination microscopy; TI-VAMP, tetanus neurotoxin-insensitive vesicle-associated membrane protein; VGLUT1, vesicular glutamate transporter 1.

indicates that these cells have a myriad of homeostatic functions in the brain (Nedergaard *et al.* 2003; Pekny and Pekna 2014). A single human astrocyte may be associated with up to two million synapses (Oberheim *et al.* 2006) and may enwrap several neuronal somata (Halassa *et al.* 2007). Astrocytes are also connected to the blood–brain barrier (Alvarez *et al.* 2013), a tightly regulated interface in the central nervous system (CNS) that controls the exchange of molecules in and out of the brain.

The central morphological position of astrocytes makes these cells ideal hubs to communicate with endothelial cells and neurones. The comprehensive glial communication system, which is much slower than the neuronal networks (milliseconds to seconds, in some processes minutes to hours), was termed the gliocrine system by analogy to the endocrine system (Vardjan and Zorec 2015). Similar to the endocrine system, in which hormones and chemical signals are released into the blood and transported by convection/circulation to their targets, gliosignaling molecules released by gliocrine cells, including astroglia, into the extracellular milieu of the brain parenchyma can be transported by the convective glymphatic system (Thrane *et al.* 2014). Simultaneously, the glymphatic system is considered to remove extracellular debris and protein wastage from the interstitial fluid (Plog *et al.* 2015). This is particularly pertinent to pathologic conditions, including chronic cerebral ischemia, brain trauma, cell edema, epilepsy, Alzheimer disease, and Parkinson disease, in which the blood–brain barrier is disrupted (Pangrsic *et al.* 2006; Alvarez *et al.* 2013; Vardjan *et al.* 2016), allowing the entry of 'peripheral' molecules into the CNS. As a defense mechanism, the glymphatic system, consisting of astroglia, can remove waste molecules and particles from the extracellular milieu. However, the capacity for removal of extracellular debris is poorly understood.

S100B is a cytoplasmic protein of astrocytes (Donato *et al.* 2009). This rather small protein (10.5 kDa) is typically present in the homodimer form consisting of two beta subunits and is among the best characterized members of the S100 family constituting Ca^{2+} binding proteins of the 'EF hand' type (Van Eldik and Wainwright 2003; Gilquin *et al.* 2010). Inside cells, S100B affects diverse physiologic functions including Ca^{2+} homeostasis, regulates cell morphology by interacting with the cytoskeleton, and inhibits differentiation of glia (Donato *et al.* 2009). In the extracellular space, S100B can act as a signaling molecule, but at high concentration is considered to be a marker of brain damage, because its level in serum is increased in several pathophysiologic conditions, including brain aging and traumatic brain injury, and in psychiatric disorders (Rothermundt *et al.* 2003; Steiner *et al.* 2011). After brain trauma and ischemia, S100B is found in the extracellular space (Rothermundt *et al.* 2003; Donato *et al.* 2009; Goncalves *et al.* 2010; Steiner *et al.* 2011). Currently little is known about the regulation of this protein concentration in the extracellular fluid. Although the glymphatic system may help to clear it from there, an inhibition of this pathway, e.g. by sleep deprivation, suppress traumatic brain injury induced increases in serum S100B (Plog *et al.* 2015). Moreover, increased concentrations of S100B in the cerebrospinal fluid do not always correlate with an increase in serum protein concentration (Guerra *et al.* 2011). Whether astrocytes, the most versatile homeostatic cells in the brain, can remove released S100B from the extracellular space is still unclear.

Here, we examined *in vitro* whether and how extracellular S100B is taken up by rat astroglial cells in primary culture. We also followed the trafficking of these molecules once they were internalized and determined their accumulation in subcellular organelles. For this, we used fluorescently labeled protein S100B-Alexa^{488} in combination with fluorescent organelle markers and confocal microscopy. The results revealed that extracellularly added S100B-Alexa^{488} and Dextran^{546}, an endolysosomal fluorescent marker, initially internalized to distinct vesicle types, but were routed to a common endolysosomal compartment over time. Directional mobility of S100B-Alexa^{488}-positive vesicles increased in a time-dependent manner on exposure of cells to S100B-Alexa^{488} and was inhibited by an ATP-evoked increase in cytosolic free calcium concentration ($[Ca^{2+}]_i$).

Methods

Cell cultures

Astrocyte cultures were prepared from cortices of 3-day-old female Wistar rats (obtained from Medical Experimental Centre at the Institute of Pathology, University of Ljubljana, Slovenia) as described (Schwartz and Wilson 1992). For the experiments, the cells were then subcultured onto 22-mm diameter poly-L-lysine-coated coverslips and used within 4 days after plating. They were maintained in high glucose Dulbecco's modified Eagle's medium (Thermo Fisher Scientific, Waltham, MA, USA) containing 10% fetal bovine serum, 1 mM pyruvate, 2 mM glutamine, and 25 mg/mL penicillin/streptomycin at 37°C in a 95% air/5% CO_2 atmosphere. The experimental animals were cared for in accordance with the European and Slovenian legislation (Official Gazette of the RS 38/13; UVHVVR, No.U34401-47/2014/7).

Unless stated otherwise all chemicals used to maintain the cell cultures and in the experimental procedures were obtained from Sigma-Aldrich (Munich, Germany) and were of highest purity grade available.

S100B-Alexa^{488} labeling and electrophoretic analysis

S100B from bovine brain was dissolved in deionized water to 1 mg/mL and stored in aliquots at −20°C until use. Fluorescently labeled S100B (S100B-Alexa^{488}) was obtained by labeling S100B with an Alexa Fluor^{488} Microscale Protein Labelling Kit (Thermo Fisher Scientific) according to the manufacturer's instructions.

S100B-Alexa^{488} (2 μg) was analyzed by sodium dodecyl sulfate–polyacrylamide gel electrophoresis (SDS–PAGE) (15% acrylamide gel) (Laemmli 1970) under reducing conditions (0.5% (m/v) SDS, 10% (v/v) glycerol and 30 mM Tris–HCl, pH 6.8), fixed for 30 min

in 30% (v/v) ethanol, 10% (v/v) acetic acid and finally washed in dH_2O. The gel was imaged on a ChemiDoc MP System (Bio-Rad, Hercules, CA, USA) gel imager. The fluorescence of Alexa Fluor^{488} was detected using a Blue Epi illuminator and a 530/28 emission filter using the ChemiDoc MP Alexa^{488} application.

Real-time confocal imaging

Cultured astrocytes were incubated with 1 μM S100B-Alexa^{488} for 0.25, 1, 3, and 24 h at 37°C in serum-free medium and thereafter vesicle mobility was imaged in live cells using confocal microscopy. In some experiments, cells were co-incubated with S100B-Alexa^{488} (1 μM) and 10 kDa Alexa Fluor^{546}-Dextran (Dextran^{546}; 0.1 or 0.01 mg/mL; Thermo Fisher Scientific). The labeling of S100B-Alexa^{488} pre-labeled cells (1 μM) with LysoTracker Red DND-99 (200 nM; Thermo Fisher Scientific), an acidic endosomal/lysosomal vesicle marker, was performed in living cells at 22–24°C for 5 min.

To examine whether S100B-Alexa^{488} is internalized into astrocytes in a receptor for advanced glycation endproducts (RAGE)-dependent manner, the RAGE receptor-S100B interaction was first manipulated by a 2 h cell incubation with a goat blocking antibody raised against rat RAGE (25 mg/mL) (R&D System, Minneapolis, MN, USA). Then, cells were co-incubated with S100B-Alexa^{488} and Dextran^{546} (1 μM) in serum-free medium at 37°C. In control experiments, cells were treated with a control goat antibody (25 mg/mL) (R&D Systems) and then labeled with both fluorescent probes as stated above. To examine whether S100B-Alexa^{488} and Dextran^{546} internalize via dynamin-dependent endocytosis, cells were pre-incubated for 30 min with 5 μM dynole 34-2 (Tocris Bioscience, Bristol, UK), a potent dynamin inhibitor (Hill *et al.* 2009), and then co-incubated with S100B-Alexa^{488} and Dextran^{546} (1 μM) for 1 h in serum-free medium at 37°C.

After labeling, the cells were washed with standard saline solution (in mM: 131.8 NaCl, 1.8 $CaCl_2$, 2 $MgCl_2$, 5 KCl, 10 D-glucose, 10 HEPES/NaOH, pH 7.2), mounted onto the recoding chamber, supplied with standard saline solution preheated to 37°C and transferred to the microscope for real-time observation.

Fluorescently labeled cells were imaged with an inverted confocal microscope LSM 780 (Zeiss, Jena, Germany) equipped with an oil immersion objective 63×/NA 1.4. Time-lapse fluorescence images (512 × 512 pixels) were recorded in live cells every 0.9 s for 1 min before and 3 min after the addition of 1 mM ATP to the cells. S100B-Alexa^{488} was excited by an argon laser line (488 nm) and emission fluorescence was filtered with a bandpass filter 500–550 nm. The Dextran^{546} and LysoTracker Red DND-99 were excited by a 561-nm diode-pumped solid-state (DPSS) laser line and emission fluorescence was filtered with a bandpass filter 565–615 nm. To eliminate possible bleed through, the green and red emission fluorescence were acquired sequentially.

Structured illumination microscopy

The diameter of vesicles capturing S100B-Alexa^{488} and Dextran^{546} after 15 min cell incubation with both probes was determined in fixed cells by the super-resolution structured illumination microscopy (SIM; ELYRA PS.1; Zeiss). Double-labeled cells were imaged by an oil-immersion plan apochromatic differential interference contrast (DIC) objective (63×/NA 1.4) and 3D-SIM images (taken sequentially every 0.5 μm in the z-axis) were acquired with an EMCCD camera (Andor iXon 885; Belfast, UK) with an exposure time of 500–600 ms. S100B-Alexa^{488} was excited by a 488 nm argon laser line and emission fluorescence was filtered with a bandpass filter 495–575 nm. Dextran^{546} was excited by a 561 nm DPSS laser line and emission fluorescence was filtered with a bandpass filter 570–650 nm. The diameter of vesicles was estimated in SIM micrographs that were exported as TIFF's to ImageJ software (National Institutes of Health, Bethesda, MD, USA; available at http://rsbweb.nih.gov/ij/).

Immunocytochemistry experiments

Cells were incubated simultaneously with S100B-Alexa^{488} (1 μM) and the combination of S100B-Alexa^{488} and Dextran^{546} (0.1 mg/mL) at 37°C for different times. After treatment, the cells were washed with phosphate-buffered saline (PBS) and fixed in 2% (m/v) paraformaldehyde for 5–7 min at 22–24°C. Non-specific background staining was reduced by incubating the cells in blocking buffer with 3% (m/v) bovine serum albumin (BSA) and 10% (v/v) goat serum in PBS at 37°C for 1 h. Cells were then rinsed in PBS and exposed to primary antibodies, diluted in 3% (m/v) BSA/PBS and incubated at 37°C for 2 h or at 4°C overnight. Afterwards, the cells were rinsed in PBS and stained with fluorescent secondary antibodies at 37°C for 45 min. At the end of the staining procedure, the cells were mounted onto glass slides using Slow Fade Gold Antifade reagent (Thermo Fisher Scientific). The following primary antibodies were used: mouse monoclonal to S100B (1 : 500; Sigma, St Louis, MO, USA), mouse monoclonal to early endosomal antigen 1 (EEA1, 1 : 100; BD Biosciences, Oxford, UK), rabbit polyclonal to lysosomal associated membrane protein (LAMP1, 1 : 200; Abcam, Cambridge, UK), mouse monoclonal to tetanus neurotoxin-insensitive vesicle-associated membrane protein (1 : 500; Covalab, Cambridge, UK), rabbit polyclonal to atrial natriuretic peptide (ANP, 1 : 2000; Abcam), and rabbit polyclonal to vesicular glutamate transporter 1 (VGLUT1, 1 : 2000; Synaptic Systems, Goettingen, Germany). Anti-rabbit or anti-mouse secondary antibodies conjugated to fluorescent dyes (Alexa Fluor^{546}, 1 : 500 or Alexa Fluor^{488}, 1 : 500; Thermo Fisher Scientific) were used in accordance with the primary antibodies.

Z-stacked images were acquired in either live or fixed double-labeled cells for analysis of fluorescence co-localization. S100B-Alexa^{488} was excited by an argon laser line (488 nm) and emission fluorescence was filtered with a bandpass filter 500–550 nm. Dextran^{546} was excited by a 561-nm DPSS laser line and emission fluorescence was filtered with a bandpass filter 565–615 nm.

In a subset of experiments, 20 μL of PBS, non-fluorescent S100B (1 μM in PBS) or fluorescent S100B-Alexa^{488} (1 μM in PBS) were pipetted onto the poly-L-lysine-coated coverslips, respectively and proteins were allowed to attach to the glass surface for 20 min. Thereafter, coverslips were washed with PBS and fixed in 2% (m/v) paraformaldehyde for 7 min at 22–24°C. Non-specific background staining was reduced by applying blocking buffer with 3% (m/v) BSA and 10% (v/v) goat serum in PBS at 37°C for 1 h. Then, coverslips were rinsed in PBS and exposed to primary mouse monoclonal antibody against S100B (1 : 500; Sigma), diluted in 3% (m/v) BSA/PBS and incubated at 37°C for 2 h. Afterwards, coverslips were rinsed in PBS and stained with fluorescent Alexa Fluor^{546}-conjugated anti-mouse secondary antibody (1 : 500; Thermo Fisher Scientific) at 37°C for 45 min. At the end of the staining procedure, the coverslips were mounted onto

glass slides using Slow Fade Gold Antifade reagent (Thermo Fisher Scientific).

Analysis of vesicle mobility and vesicle size

Vesicle trafficking was analyzed using ParticleTR software (Celica Biomedical, Ljubljana, Slovenia) in exported TIFF files as described previously (Potokar *et al.* 2005). Briefly, individual S100B-Alexa^{488}-positive vesicles were randomly selected in the first image by the cursor option. In all subsequent images, the software fitted a two-dimensional Gaussian curve to the vesicle intensity profile using a simplex algorithm with a least square estimator to obtain the coordinates (x,y) of the peak of the Gaussian 2D curve. The tracking mostly proceeded automatically and was closely inspected visually. Whenever two vesicles moved into close proximity, the automatic tracking was paused and the position of the selected vesicle was determined manually until vesicles separated enough to resume the automated tracking. The coordinates of the curve peaks pinpointed the precise 2D vesicle position (x,y) within the image (Potokar *et al.* 2005). These coordinates were used to calculate several mobility parameters: TL (total length of the travelled pathway), MD (maximal displacement, a measure of net vesicle translocation), and speed. The mobility parameters estimated on the basis of 2D vesicle coordinates were unlikely affected much by vesicle z-motions because of thin vertical profile of cultured astrocytes (Potokar *et al.* 2005).Vesicle mobility was analyzed in at least six cells per treatment.

To estimate the apparent vesicle size (vesicle image area), confocal images were analyzed with ImageJ software. The minimum particle size taken to identify an individual vesicle was three adjacent pixels (0.132 × 0.132 μm) and the minimum surface area covered by a fluorescent spot was 0.052 μm^2. The number of internalized vesicles per cell was analyzed with 3D Object Counter plugin for ImageJ in z-stacked images by considering that a minimum vesicle consisted of three adjacent voxels; thus, a broad span of vesicles with different apparent sizes and intensities imaged at different z position was covered by the analysis. In SIM micrographs, the minimum fluorescent spot size taken to identify an individual vesicle consisted of five adjacent pixels (0.040 × 0.040 μm) and the minimum surface area (S) covered by the fluorescent spot was 0.008 μm^2. The vesicle diameter ($2r$) was calculated from the formula $r = (S/\pi)^{0.5}$ by considering the circular shape of imaged vesicles.

Fluorescence co-localization analysis

In double-fluorescent confocal images, co-localization of S100B-Alexa^{488} with various fluorescent markers was quantified in exported 8-bit TIFF files using ColocAna software (Celica Biomedical) (Kreft *et al.* 2004). The threshold for the co-localized pixel count was set to 20% of the maximal fluorescence to minimize fluorescence overlap originating from closely positioned fluorescent structures, structures above and below the focal plane that may contribute some out of focus scatter because of the point spread function, and from background fluorescence. The threshold was experimentally verified as the optimal one to quantitate the degree of co-localization in related (co-localized) and non-related (non-co-localized) fluorescent markers (Kreft *et al.* 2004). The program summed up all pixels above the threshold in each channel (green, red) and pixels above the threshold in both channels (green and red). Co-localization (%) between fluorescently labeled S100B-Alexa^{488} and Dextran^{546}, LysoTracker, anti-EEA1, anti-LAMP1, anti-tetanus neurotoxin-insensitive vesicle-associated membrane protein, anti-ANP, and anti-VGLUT1 (red) was expressed with respect to pixels of other (non-S100B-Alexa^{488}) markers (red).

Calcium imaging

Astrocyte-loaded coverslips were incubated for 30 min at 22–24°C in culture medium supplemented with 5 μM Fluo-4-AM (Thermo Fisher Scientific). After loading of fluorescent calcium indicator, cells were washed with extracellular solution, incubated for further 30 min to allow de-esterification of acetoxymethyl (AM) ester, and mounted to the recording chamber on a confocal microscope (LSM 780; Zeiss) equipped with a Plan-Apochromat air objective 20×/NA 0.8. Fluo-4 was excited by a 488 nm argon laser line and emission fluorescence was filtered with a 495–565 nm bandpass filter. Time-lapse images were acquired every second for 4 min before and 4 min after bolus addition of control solution or extracellular solution containing ATP that reached a final concentration of 100 μM. The changes in Fluo-4 fluorescence were obtained in regions of interest that encompassed individual cells by Zen 2010 software (Zeiss). Time-resolved fluorescence changes from 50 cells were analyzed by a custom-written MATLAB software (MathWorks, Natick, MA, USA) that was used to measure the peak calcium amplitude ($\Delta F/F_0$) and to calculate the surface under the curve [corresponding to the calcium amplitudes integrated over time ($\Delta F/F_0 \times t$)] evoked by control or ATP-containing solution. The baseline fluorescence (F_0) was determined at the beginning of each record as the average intensity (in A.U.) during the first 60 frames.

Statistical analysis

The co-localization of different fluorescent probes, parameters of vesicle mobility (TL, MD and speed), the number, the area, and the normalized fluorescence of vesicles were expressed as average ± SEM. Statistical significance was estimated by one-way analysis of variance (ANOVA) and the Tukey *post hoc* test or by the Student t-test or by the Mann–Whitney U-test as stated in the legends to the figures.

Results

Time-dependent internalization of S100B-Alexa^{488} and Dextran^{546} into astrocytes

In order to investigate the uptake of exogenous S100B into astrocytes, we pre-labeled the protein with Alexa^{488} (see the Methods) and used confocal microscopy to monitor the internalization of the S100B-Alexa^{488}. The protein labeling procedure resulted in the preparation of a fluorescent probe that consisted mainly, if not entirely of the fluorescently conjugated S100B protein (S100B-Alexa^{488}) containing no free Alexa^{488} dye as determined by SDS–PAGE (Fig. 1a). To experimentally determine whether S100B-Alexa^{488} is recognized by the anti-S100B antibody, a small quantity (20 μL) of non-fluorescent or fluorescent S100B-Alexa^{488} was pipetted to the poly-L-lysine-coated coverslips (Fig. 1b) and protein molecules were allowed to attach to the glass

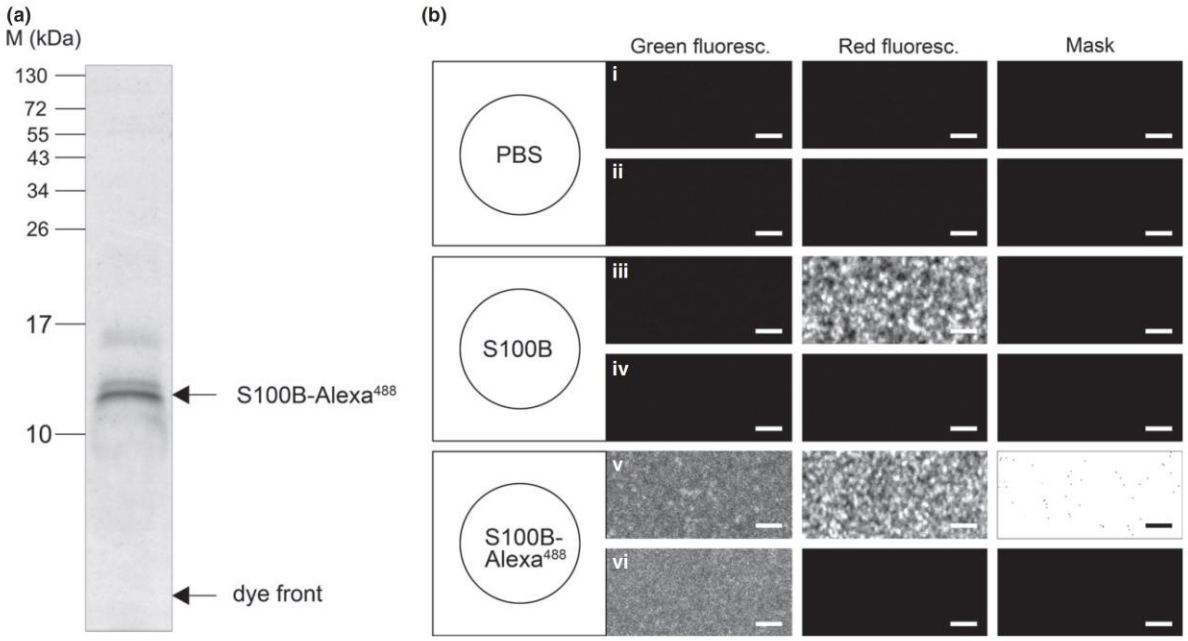

Fig. 1 The analysis of S100B-Alexa^{488} by sodium dodecyl sulfate–polyacrylamide gel electrophoresis (SDS–PAGE) and confocal microscopy. (a) The purified S100B-Alexa^{488} conjugate was analyzed by SDS–PAGE under reducing conditions and the gel was imaged using a fluorescence gel imager. The position of the S100B-Alexa^{488} band is indicated by an arrow. Molecular mass standards are indicated on the left. No free Alexa Fluor^{488} was detected in the sample of the fluorescent S100B. (b) The schematic representation of poly-L-lysine-coated glass coverslips that were covered with phosphate-buffered saline (PBS) (top left), S100B (middle left) or S100B-Alexa^{488} (bottom left) and subjected to immunolabeling by the primary mouse anti-S100B and Alexa-Fluor^{546}-conjugated secondary antibody (i, iii and v) or to Alexa-Fluor^{546}-conjugated secondary antibody alone (ii, iv and vi). Confocal images display green fluorescence (left), red fluorescence (middle), and the corresponding fluorescence mask images (right) observed in particular coverslips. Fluorescence from Alexa-Fluor^{546}-conjugated antibody (middle) was observed only in S100B and S100B-Alexa^{488}-covered coverslips that were exposed to primary and secondary antibodies (iii and v). In the S100B-Alexa^{488}-covered coverslip, green fluorescence (left) in addition to red fluorescence (middle) was detected, and both fluorescent signals displayed a high degree of co-localization as revealed by the white fluorescent mask image (right). Scale bars: 2 μm.

surface for 20 min. Thereafter, protein-covered coverslips were immunolabeled by the exposure to primary anti-S100B and secondary Alexa-Fluor^{546}-conjugated anti-mouse antibody (Fig. 1b i, iii and v) or to secondary antibody alone (ii, iv and vi). As revealed by the confocal images, red fluorescence originating from the secondary antibody was observed only in S100B and S100B-Alexa^{488}-covered coverslips that were stained with primary and secondary antibodies (iii and v). No red fluorescence was observed in control coverslips (loaded with PBS alone; i and ii), or in coverslips loaded with non-fluorescent S100B (iv) or fluorescent S100B-Alexa^{488} (vi) exposed only to the fluorescent secondary antibody. In S100B-Alexa^{488}-covered coverslips exposed to both antibodies (v), massive co-localization of green and red fluorescence was observed as revealed by the fluorescent mask image (white). These results indicate that anti-S100B antibody recognizes fluorescent S100B-Alexa^{488} in addition to non-fluorescent S100B.

S100B-Alexa^{488} extracellularly applied to astrocytes localized to vesicle-like structures, visible as numerous green fluorescent puncta in the cell cytoplasm (Fig. 2). To determine the nature of the compartment into which S100B-Alexa^{488} is taken up, we examined whether S100B-Alexa^{488} enters the same compartment as extracellular Dextran^{546}, a polysaccharide commonly used to study the endocytotic pathway, which on longer term (several hours) accumulates in astrocytic endolysosomes (Lim and Gleeson 2011; Vardjan *et al.* 2012). Astrocytes were exposed to both fluorescent probes simultaneously in order to evaluate the putative differences in the dynamics of internalization of the respective probes. To monitor the time dependence of S100B-Alexa^{488} and Dextran^{546} internalization in detail, we evaluated the number of fluorescent vesicles (as seen in Fig. 2) internalized per cell in a given time period of incubation (p.i.). The left and middle panels in Fig. 2(a) show the cells exposed to S100B-Alexa^{488} and Dextran^{546}, respectively, recorded after different p.i. The right panels show overlay images in which the yellow pixels represent the co-localization of the two fluorescent markers. Figure 2(b) shows that the number of fluorescent vesicles per cell,

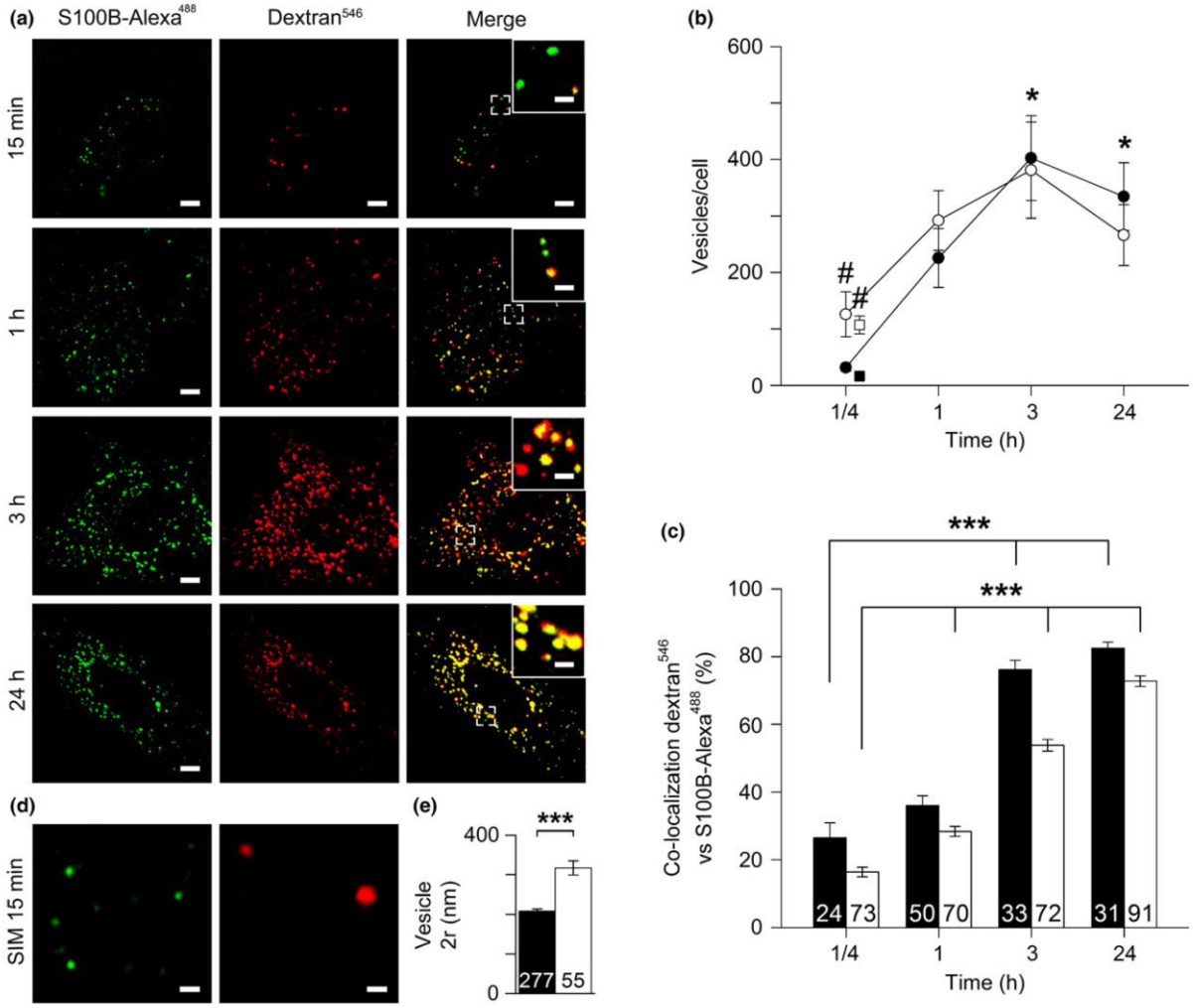

Fig. 2 Time-dependent internalization of S100B-Alexa^{488} and the increase in fluorescence co-localization between S100B-Alexa^{488} and Dextran^{546}. (a) Representative confocal images of astrocytes co-incubated with S100B-Alexa^{488} (green) and Dextran^{546} (red) at 37°C for 15 min, 1, 3, and 24 h. Merged images (in yellow) display co-localization between S100B-Alexa^{488} and Dextran^{546}; insets display magnified view on the selected vesicles (white open frames). Scale bars: 4 μm (large images) and 1 μm (insets). (b) Time-dependent increase in the number of S100B-Alexa^{488}- (black circles and black square; 1 μM) and Dextran^{546}-positive vesicles per cell (white circles; 10 μM and white square; 1 μM). *Denotes the difference ($p < 0.05$, ANOVA, Tukey *post hoc* test) in internalized vesicles per cell between successive incubation times; #Denotes the difference ($p < 0.05$, Student *t*-test) between S100B-Alexa^{488} and Dextran^{546} internalized vesicles within the same incubation time. At least seven cells from three different cultures were analyzed per given incubation time. (c) Time-dependent increase in fluorescence co-localization between S100B-Alexa^{488} and Dextran^{546} (black bars, 1 μM S100B-Alexa^{488} and 10 μM Dextran^{546} and white bars, 1 μM S100B-Alexa^{488} and 1 μM Dextran^{546}) ***$p < 0.001$. Note the time-dependent increase in fluorescence co-localization between both fluorescent probes in cells that were exposed either to high (10 μM) or to low (1 μM) concentration of Dextran^{546} co-applied with 1 μM S100B-Alexa^{488}. Numbers at the bar bases indicate the number of cell planes analyzed. (d) Structured illumination microscopy (SIM) images of an astrocyte co-incubated with S100B-Alexa^{488} and Dextran^{546} (1 μM each) for 15 min at 37°C. Note the difference in size of S100B-Alexa^{488}- and Dextran^{546}-positive vesicles. Scale bar: 0.5 μm. (e) The diameter of S100B-Alexa^{488}- (black bar) and Dextran^{546}-positive vesicles (white bar) estimated from SIM images. Numbers at the bar bases indicate the number of vesicles analyzed in nine cells.

representing S100B-Alexa^{488} (black circles) and Dextran^{546} (white circles), increased as a function of p.i. Note that the exposure of cells to S100B-Alexa^{488} revealed an increased number of internalized vesicles per cell even after 15 min and the number of vesicles increased by 10-fold within 3 h p.i. (*$p < 0.05$; Fig 2b, black circles). Interestingly, the

initial efficiency of Dextran^{546} uptake into astrocytes appeared higher than that of S100B-Alexa^{488} because after 15 min, the average number of internalized vesicles was at least 2-fold higher in comparison with the ones that were labeled with S100B-Alexa^{488} ($^{\#}p < 0.05$; Fig. 2b, circular symbols). Similar number of internalized S100B-Alexa^{488}- and Dextran^{546}-positive vesicles was observed also in cells that were exposed to equimolar concentration (1 μM) of both fluorescent probes for 15 min ($^{\#}p < 0.05$; Fig. 2b; squared symbols). However, after a longer p.i., the number of internalized vesicles per cell was similar for the respective fluorescent probes. These results indicate that, under the experimental conditions used, the rate of Dextran^{546} uptake into astrocytes is initially more rapid and that, at least initially, these two fluorescent probes are internalized into distinct compartments.

To verify the latter hypothesis, we studied the level of co-localization between the two fluorescent probes. Figure 2(c) (black bars) shows that the level of co-localization between the two probes after 15 min (27 ± 4%, $n = 24$) and 1 h p.i. (36 ± 3%, $n = 50$) was relatively low. However, after prolonged exposure, S100B-Alexa^{488} and Dextran^{546} appeared to end up in a similar compartment because the degree of co-localization was substantially higher after 3 h (76 ± 3%, $n = 33$) and 24 h p.i. (82 ± 2%, $n = 31$). A similar time-dependent increase in fluorescence co-localization was observed in cells that were simultaneously loaded with both probes applied at equimolar concentration (1 μM). In these cells, the fluorescence co-localization increased from 16 ± 1% ($n = 73$) after 15 min to 28 ± 1% ($n = 70$) at 1 h p.i., 54 ± 2% ($n = 72$) at 3 h and finally to 73 ± 2% ($n = 91$) at 24 h p.i. (Fig. 2c, white bars). To independently confirm that S100B-Alexa^{488} and Dextran^{546} initially internalize to distinct vesicles, cells were loaded with both fluorescent probes (1 μM) for 15 min, fixed and examined by the super-resolution microscopic technique SIM to estimate the diameter of individual S100B-Alexa^{488}- and Dextran^{546}-positive vesicles (Fig. 2d). After 15 min incubation, S100B-Alexa^{488} localized to vesicles with an apparent diameter of 208 ± 5 nm, while Dextran^{546} localized to vesicles with a considerably larger apparent diameter of 317 ± 18 nm (Fig. 2e). These results further indicate that S100B-Alexa^{488} and Dextran^{546} initially internalize to distinct compartments, probably by a different mechanism. After prolonged exposure, however, they are routed to a common subcellular compartment.

Internalization of S100B-Alexa^{488} is mediated by RAGE- and dynamin-dependent endocytosis and is distinct from Dextran^{546} internalization

To further elucidate the mechanism by which S100B-Alexa^{488} and Dextran^{546} internalize into astrocytes, we conducted experiments with an aim to interfere with the putative binding of S100B-Alexa^{488} to RAGE (Perrone *et al.* 2008) or to inhibit dynamin, a large GTPase, that is crucial for vesicle membrane fission (Hinshaw 2000) during receptor-mediated endocytosis (Hill *et al.* 2009). In control conditions, astrocytes (Fig. 3a, left) were exposed to both

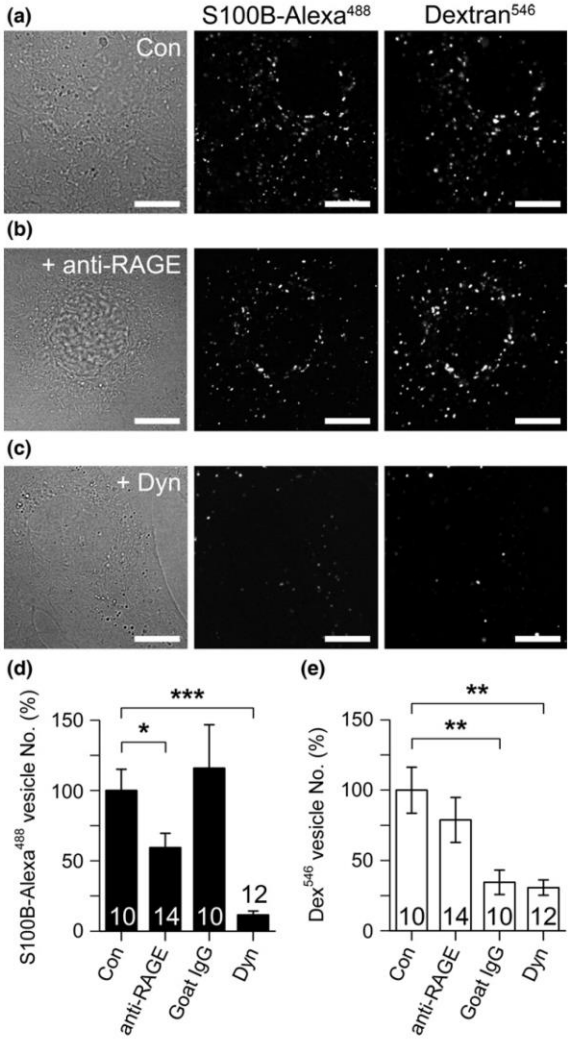

Fig. 3 Receptor for advanced glycation endproducts (RAGE)- and dynamin-dependent internalization of S100B-Alexa^{488} into cultured rat astrocytes. (a–c) Representative differential interference contrast images (left) and confocal images of S100B-Alexa^{488}- (middle) and Dextran^{546}-positive vesicles (right) in non-treated control astrocyte (Con), astrocyte pretreated with anti-RAGE antibody for 2 h at 37°C (+ anti-RAGE), and astrocyte pretreated with 5 μM dynole 34-2 for 30 min at 37°C (+ Dyn). (d, e) Relative number (average ± SE) of S100B-Alexa^{488}-positive (d) and Dextran^{546}-positive vesicles (e) in non-treated controls (Con), cells pretreated with anti-RAGE antibody, control goat antibody (Goat IgG), and cells pretreated with 5 μM dynole 34-2 (Dyn). Numbers at the bar bases indicate the number of analyzed cells obtained from two different cell cultures ($^{*}p < 0.05$, $^{**}p < 0.02$, $^{***}p < 0.001$).

fluorescent probes for 1 h. Thereafter, numerous S100B-Alexa^{488}- and Dextran^{546}-positive vesicles were observed that were localized to the periphery and to the perinuclear cytoplasmic regions (Fig. 3a middle and right). In astrocytes (Fig. 3b left) pretreated with the anti-RAGE antibody, a reduced number of S100B-Alexa^{488}-positive vesicles was observed (Fig. 3b middle) than in non-treated controls, while the number of Dextran^{546}-positive vesicles appeared similar as in controls (Fig. 3b right). In cells pretreated with 5 μM dynole 34-2 (Fig. 3c left), a significantly reduced number of S100B-Alexa^{488}- and Dextran^{546}-positive vesicles were observed (Fig. 3c middle and right) than in controls. To quantitatively asses the impairment of fluorescent probe uptake because of particular cell treatment, the number of fluorescent-positive internalized vesicles per cell was normalized versus the average number of vesicles in controls. Blocking of RAGE function by an antibody against the RAGE receptor diminished the uptake of extracellular S100B-Alexa^{488} as indicated by the reduced percent of internalized vesicles of 59 ± 3% (n = 14) versus control values of 100 ± 15% (n = 10). Cell treatment with a control antibody obtained from naive (non-immunized) goats did not affect the uptake process. In contrast, cell treatment with 5 μM dynole 34-2 strongly inhibited the uptake of extracellular S100B-Alexa^{488}; the number of S100B-Alexa^{488}-positive vesicles decreased to 11 ± 3% (n = 12) of control values (Fig. 3d). In contrast to impaired uptake of S100B-Alexa^{488}, cell treatment with the anti-RAGE antibody did not affect the internalization of Dextran^{546}, while treatment with control goat antibody and with 5 μM dynole 34-2 diminished internalization of Dextran^{546} into astrocytes; the relative vesicle number decreased to 34 ± 9% (n = 14) and to 31 ± 5% (n = 10), respectively (Fig. 3e). These data indicate that S100B-Alexa^{488} internalizes into astrocytes in part via RAGE-mediated dynamin-dependent endocytosis that differs from the internalization of Dextran^{546}.

Late S100B-Alexa^{488}-positive vesicles in astrocytes represent mainly acidified endolysosomes

To further characterize the compartments that captured extracellular S100B-Alexa^{488}, cells preloaded with S100B-Alexa^{488} for 3 h were immnuolabeled with antibodies against several proteins of the endosomal pathway and against specific proteins of peptidergic and glutamatergic secretory vesicles. The co-localization of S100B-Alexa^{488} fluorescence with fluorescent dextran and LysoTracker, a dye accumulating inside heterogeneous acidic compartments (Potokar *et al.* 2010), was analyzed in live cells (Fig. 4a and b), and the presence of other proteins, such as EEA1 and LAMP1, was evaluated in fixed cells (Fig. 4c and d). Many S100B-Alexa^{488}-positive vesicles were found to be acidified as indicated by their co-localization with LysoTracker dye (56 ± 2%; Fig. 4e). This is consistent with the high co-localization of S100B-Alexa^{488} with Dextran^{546} (51 ± 3%; Fig. 4e), as dextrans have been reported inside acidic compartments (Carme Coll Ferrer *et al.* 2013). In addition, some of the S100B-Alexa^{488}-positive vesicles co-localized (10 ± 1%; Fig. 4e) with the lysosomal membrane marker LAMP1 (Blott and Griffiths 2002) and with the early endosomal marker (EEA1; 9 ± 0%; Fig. 4e) (Dumas *et al.* 2001). Our results indicate that S100B-Alexa^{488} mostly internalized into endocytotic vesicles that contained Dextran^{546} and to vesicles loaded with the LysoTracker dye. This is consistent with the relatively poor co-localization of S100B-Alexa^{488} fluorescence with ANP (2 ± 0%), a peptidergic vesicle marker (Potokar *et al.* 2008) and with VGLUT1 (1 ± 0%), a protein of glutamatergic vesicles (Stenovec 2007; Potokar *et al.* 2010) (Fig. 4e).

To further characterize endocytotic compartments that internalized extracellular S100B-Alexa^{488} after variable p.i. times (15 min 1, 3 and 24 h) with S100B-Alexa^{488}, astrocytes were immnuofluorescently labeled with antibodies against EEA1 or LAMP1, and with the corresponding fluorescent secondary antibodies. The fluorescence co-localization between S100B-Alexa^{488} and EEA1 decreased from 23 ± 3%, to 16 ± 1%, 9 ± 0%, and 6 ± 0% after 15 min, 1, 3, and 24 h p.i., respectively (Fig. 4f). In contrast, the fluorescence co-localization between S100B-Alexa^{488} and LAMP1 increased from 4 ± 1%, to 7 ± 0%, 9 ± 1%, and 13 ± 1% after 15 min, 1, 3 and 24 h p.i., respectively (Fig. 4g). The apparent Pearson's correlation coefficient (R) of 0.978 (p = 0.022) suggested a negative correlation between the increase in fluorescence co-localization of S100B-Alexa^{488} with LAMP1 and the decrease in co-localization of S100B-Alexa^{488} with EEA1 (data not shown). These data indicate that internalized S100B-Alexa^{488} transits through early endosomes and accumulates in late endolysosomes over prolonged periods of time.

Directional mobility of S100B-Alexa^{488}-positive vesicles increases with incubation time

To evaluate the mobility of S100B-Alexa^{488}-positive vesicles, cells were imaged every 0.9 s for 60 s and the MD (maximal displacement) and the vesicle TL (total length of the travelled pathway) were calculated as described previously (Potokar *et al.* 2005). S100B-Alexa^{488}-positive vesicles exhibited two types of mobility: directional (vesicles with MD > 1 μm, elongated trajectories) and non-directional (MD < 1 μm, contorted trajectories) (Potokar *et al.* 2005; Vardjan *et al.* 2012). The fraction of S100B-Alexa^{488}-positive vesicles exhibiting directional mobility increased in cells with longer incubation times (15 min, 2.2%; 1 h, 2.6%; 3 h, 8.1%; and 24 h, 13%) (Fig. 5a). A statistically significant difference in the increase in MD and TL of directional vesicles between cells with different incubation times is shown in Fig. 5b and c. This suggests that the directional mobility of S100B-Alexa^{488}-positive vesicles increases with incubation time, likely because of time-

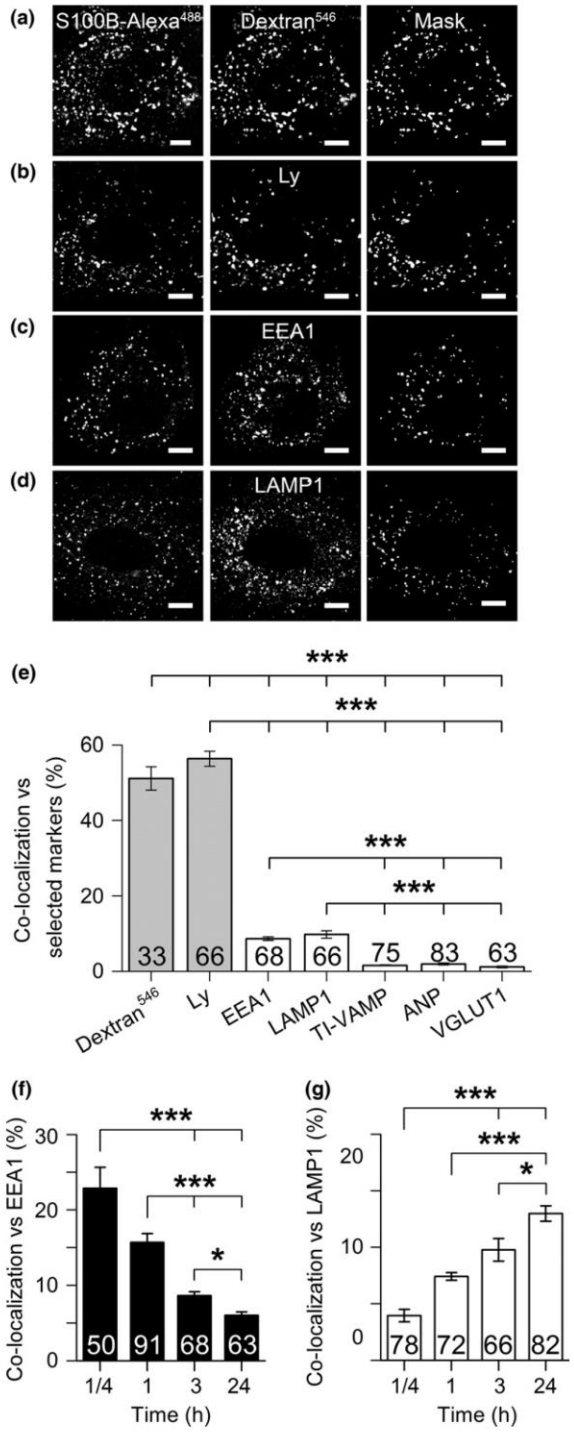

Fig. 4 Immunocytochemical characterization of S100B-Alexa^{488}-positive vesicles in cultured rat astrocytes. Representative confocal images of astrocytes incubated with S100B-Alexa^{488} for 3 h at 37°C and co-labeled with the following fluorescent probes: (a) Dextran^{546}, a marker of late endolysosomes; (b) LysoTracker (Ly), a dye staining acidic subcellular compartments; (c) antibody against early endosome antigen 1 (EEA1), a marker of early endosomes; (d) antibody against lysosomal-associated membrane protein 1 (LAMP1), a marker of late endolysosomes. Co-localized pixels are represented by 'Mask' images (right panels) in white. Scale bars: 5 μm. (e) The average (± SE) fluorescence co-localization between S100B-Alexa^{488} and the selected vesicle markers, expressed as the percentage of co-localized pixels versus pixels of the selected markers. Fluorescence co-localization against tetanus toxin insensitive vesicle-associated membrane protein (TI-VAMP), a marker of late endolysosomes; atrial natriuretic peptide (ANP), a marker of peptidergic vesicles and vesicular glutamate transporter 1 (VGLUT1), a marker of glutamatergic vesicles was also examined. Gray bars denote live cells, white bars denote fixed cells. The numbers at the bar bases indicate the number of cell images analyzed. ***$p < 0.001$ (ANOVA, Tukey *post hoc* test). (f) Time-dependent decrease in fluorescence co-localization between S100B-Alexa^{488} and immunolabeled EEA1-positive vesicles (black bars), and (g) time-dependent increase in fluorescence co-localization between S100B-Alexa^{488} and immunolabeled LAMP1-positive vesicles (white bars). Numbers at the bar bases indicate the numbers of cell images analyzed. *$p < 0.05$, **$p < 0.01$, ***$p < 0.001$ (Mann–Whitney *U*-test).

dependent accumulation of S100B-Alexa^{488} in compartments with different mobility characteristics.

Next, we examined if the dimension of S100B-Alexa^{488}-positive vesicles changes with the time of incubation. An increase in the fluorescent vesicle area, indicating an apparent larger vesicle size, was observed after prolonged (p.i. > 3 h) cell treatment with S100B-Alexa^{488} (Fig. 5d). Interestingly, the fluorescence intensity per vesicle also increased with the time of incubation (Fig. 5e). The latter result supports the view that there is an accumulation of cargo inside the vesicles, which increases fluorescence and the apparent size of the vesicles (Potokar *et al.* 2014). It is important to mention that we did not observe any relationship between vesicle size (area) and total TL (data not shown), as noticed previously (Potokar *et al.* 2014), meaning that the mobility of S100B-Alexa^{488}-positive vesicles is probably not affected by their apparent size but rather depends on the molecular characteristics of the vesicles that determine their interaction with the cytoskeleton and intracellular signaling pathways (Potokar *et al.* 2010). The area of S100B-Alexa^{488}-positive vesicles increased from an average of 0.140 μm^2 at 15 min exposure to an average of 0.279 μm^2 at 24 h of incubation (Fig. 5d), respectively.

Astrocyte stimulation with ATP diminishes the mobility of S100B-Alexa^{488}-positive vesicles

To demonstrate that ATP application evokes increases in intracellular calcium activity, cells were loaded with fluorescent Ca^{2+} indicator Fluo-4 and changes in $[Ca^{2+}]_i$ were measured after application of control or ATP-containing extracellular solution (Fig. 6a). Application of ATP to cells evoked robust biphasic and long-lasting responses (a rapid

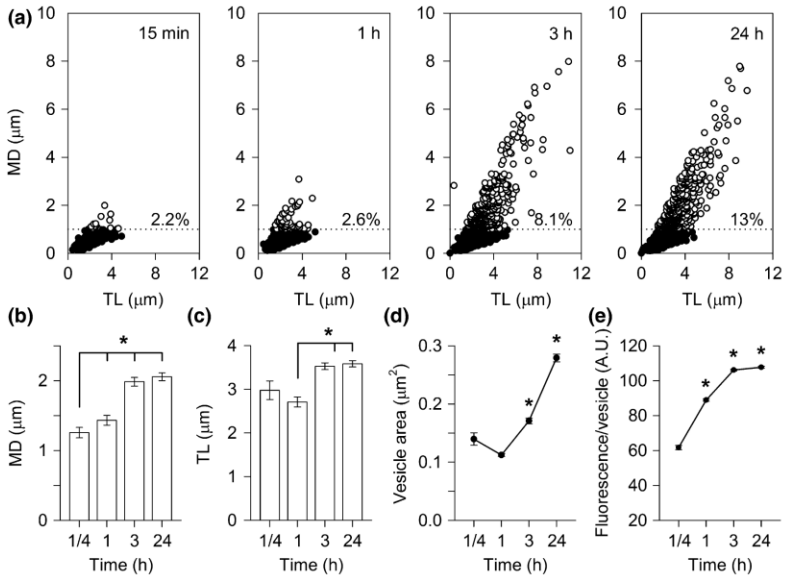

Fig. 5 Time-dependent increase in directional mobility of S100B-Alexa^{488}-positive vesicles. (a) The relationship between the maximal displacement (MD) and the track length (TL) in S100B-Alexa^{488}-positive vesicles monitored over time. Vesicles with MD > 1 μm (dashed line) were characterized as directional vesicles (white circles). Other vesicles were characterized as non-directional vesicles (black circles). The percentage of directional vesicles is displayed above the dashed horizontal line. (b) Average MD and (c) average TL of directional vesicles measured after 15 min, 1, 3, and 24 h incubation of cells with S100B-Alexa^{488}. (d) The area of S100B-Alexa^{488}-positive vesicles measured as a function of incubation time with S100B-Alexa^{488}. (e) The fluorescence per vesicle in S100B-Alexa^{488}-positive vesicles. Note the time-dependent increase in S100B-Alexa^{488}-positive vesicle area. *$p < 0.05$ (ANOVA, Tukey *post hoc* test).

increase in fluorescence was followed by a decline toward a plateau; Fig. 6b). Increases in $[Ca^{2+}]_i$ were quantified by measuring the peak amplitudes (p) in $[Ca^{2+}]_i$ and the time integrals (S) of increased calcium activity (Fig. 6b). In controls ($n = 50$), p and S values in $[Ca^{2+}]_i$ were negligible (Fig. 6c and d), while in ATP-stimulated cells ($n = 50$), significant increases in $[Ca^{2+}]_i$ were recorded ($p < 0.001$; Fig. 6c and d). Next, we examined the effect of ATP stimulation on the mobility of S100B-Alexa^{488}-positive vesicles.

The mobility of different types of vesicles (recycling glutamatergic, peptidergic, and endolysosomal vesicles) have been shown to be differently affected by ATP stimulation (Potokar *et al.* 2010), which increases $[Ca^{2+}]_i$ (Bennett *et al.* 2005; Stenovec 2007; Stenovec *et al.* 2015). Because cytosolic S100B translocation was shown to be affected by an increase in $[Ca^{2+}]_i$, (Davey *et al.* 2001), we examined the effect of $[Ca^{2+}]_i$ on the mobility of S100B-Alexa^{488}-positive vesicles by the addition of ATP to cells. ATP stimulation diminished the directional mobility of S100B-Alexa^{488}-positive vesicles; the fraction of directionally moving vesicles dropped from 5% before the stimulus to 2.4% after the stimulus (Fig. 6e and f). The remaining parameters of mobility were also significantly reduced ($p < 0.05$) after ATP stimulation; TL, MD, and speed were diminished by 5%, 17%, and 5%, respectively (Figs. 6g–i).

Discussion

To better understand how astrocytes are engaged in the maintenance of brain homeostasis, especially in the detoxification of S100B, we studied the internalization of fluorescently labeled S100B. This cytoplasmic protein is mainly present in astrocytes (Donato *et al.* 2009), but its levels in extracellular space can increase in neuropathological conditions (Rothermundt *et al.* 2003; Steiner *et al.* 2011). The results in this study revealed that cultured astrocytes efficiently remove fluorescently labeled extracellular S100B in a time-dependent manner by vesicle endocytosis. In time, vesicles capturing S100B-Alexa^{488} exhibit directional mobility, meaning that vesicles get functionally attached to the cytoskeleton (Potokar *et al.* 2007). Moreover, the mobility of vesicles capturing S100B-Alexa^{488} appears to be regulated by changes in $[Ca^{2+}]_i$ evoked by ATP stimulation, as was previously determined for endolysosomes, peptidergic, and glutamatergic secretory vesicles in astrocytes (Stenovec 2007; Potokar *et al.* 2008, 2010).

The fluorescent tagging of purified S100B protein (Fig. 1) enabled us to examine the process of extracellular S100B uptake into cultured astrocytes (Fig. 2). For the first time, the results show that astrocytes effectively internalize extracellular S100B, manifested as early as 15 min after the exposure of cells to S100B-Alexa^{488} (Fig. 2). Only the initial uptake of

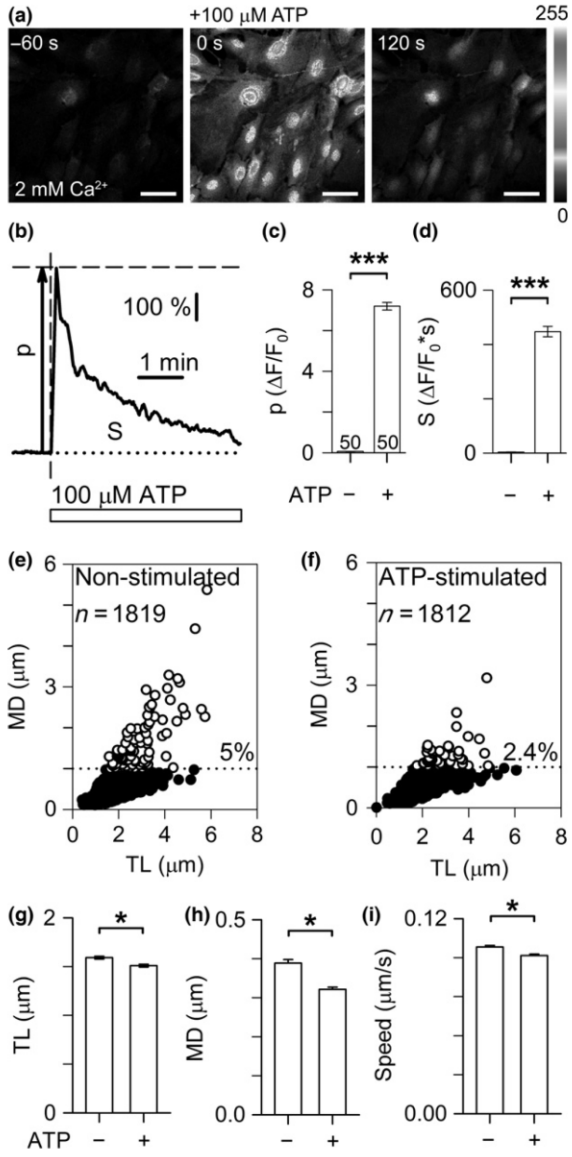

Fig. 6 Cell stimulation with ATP elevates $[Ca^{2+}]_i$ and attenuates the mobility of S100B-Alexa^{488}-positive vesicles in live cultured rat astrocytes. (a) Confocal images of fluorescent Ca^{2+} indicator loaded into astrocytes before stimulation (−60 s before ATP application) and during stimulation with 100 μM ATP that increased $[Ca^{2+}]_i$ (0 s at peak of calcium response and 120 s after the peak calcium response). Increases in $[Ca^{2+}]_i$ are indicated by the grayscale intensity levels (right, 0–255 intensity levels). Scale bars: 50 μm. (b) The ATP-evoked increases in $[Ca^{2+}]_i$ were quantified by measuring the peak (*p*, average ± SE) calcium response relative to the baseline fluorescence (dotted line, F_0) and the time-integrated calcium response (*S*) evoked by ATP. Note the transient increase in $[Ca^{2+}]_i$ evoked by ATP in astrocytes. (c, d) The ATP-evoked peak (*p*) calcium responses and the time-integrated calcium responses (*S*) measured within 4 min in controls and in ATP-stimulated astrocytes. The numbers at the bar bases indicate the number of cells analyzed. ***$p < 0.001$ (Mann–Whitney *U*-test). (e, f) Graphs displaying the relationship between vesicle MD and TL in cells (after 3 h incubation) before (e) and after (f) stimulation with 100 μM ATP. Directional vesicles (white circles) with MD > 1 μm (dashed line) and the corresponding percentage, and non-directional vesicles with MD < 1 μm (black circles) are displayed. Note that the percentage of directional vesicles halved after cell stimulation with ATP. *n*, number of vesicles. Average (± SE) vesicle TL (g), MD (h) and speed (i) in non-stimulated and ATP-stimulated cells. *$p < 0.05$ (Student *t*-test).

S100B-Alexa^{488} appeared distinct from that of Dextran^{546}; after a prolonged incubation time, both fluorescent probes ended up in the common subcellular compartment(s) (Fig. 2c). Over time, the apparent size of these structures increased as monitored by the increased area of the fluorescent puncta (Fig. 5d). A similar observation was reported for internalization of relatively large particles, such as viruses (Potokar *et al.* 2014). Although the size of the smallest vesicles was inevitably underestimated by the confocal microscopy because of the point spread function (Stenovec 2007), it seems that S100B-Alexa^{488} molecules initially internalized into smaller vesicles and were then routed to the larger ones. The latter result indicates dynamic handling of S100B-Alexa^{488} by endocytic vesicles and their fusion pores, which appear to be determined by vesicle size and molecular machinery (Jorgacevski *et al.* 2010, 2011).

Dynamic handling of S100B-Alexa^{488} by endocytotic vesicles in astrocytes

Although localization of endogenous S100B in vesicle-like compartments was considered previously (Davey *et al.* 2001; Perrone *et al.* 2008), the nature of S100B-positive vesicles in living cells remained poorly characterized. In our study, S100B-Alexa^{488} internalized to endolysosome-like compartments (Fig. 4). After prolonged incubation, S100B-Alexa^{488} strongly co-localized with Dextran^{546}-laden compartments (51% after 3 h p.i.), which bear endocytotic pathway markers, such as LAMP1 and RAS-related GTP-binding protein 7 (Rab7) proteins (Humphries *et al.* 2011; Vardjan *et al.* 2012). In live astrocytes, S100B-Alexa^{488}-positive compartments co-localized substantially with LysoTracker (56%, Fig. 4b and e), which also labels LAMP1- and EEA1-positive endocytotic vesicles (Potokar *et al.* 2010). A fraction of S100B-Alexa^{488}-positive vesicles was labeled with antibodies directed against early (anti-EEA1, 9%) and late endolysosomes (anti-LAMP1, 10%; Fig. 4c–e). The endolysosomal pathway consists of distinct subpopulations of vesicles characterized by different membrane markers, such as Rab7-, LAMP1-, or Rab7/LAMP1-positive vesicles that display different dynamics (Humphries *et al.* 2011; Szymanski *et al.* 2011). Similarly, two different subpopulations of recycled endocytotic vesicles, bearing RAS-related GTP-binding protein 11 (Rab11) were found in human epithelial cells: the Rab11/transferrin-positive and the Rab11/

Neisseria meningitidis adhesin A-positive vesicle (Bozza *et al.* 2014). In our study, most of the S100B-Alexa^{488}-positive vesicles co-localized with Dextran^{546} and with LysoTracker, but less with EEA1 and LAMP1 vesicle markers. At a first glance, the difference in the fluorescence co-localization between S100B-Alexa^{488} and LysoTracker, and S100B-Alexa^{488} and LAMP1 is high, however, it could be simply explained by the modality used to estimate the fluorescence co-localization; namely, in respect to the LysoTracker or LAMP1 fluorescence, respectively. These data thus primarily indicate that only a minute fraction of all available LAMP1-positive vesicles internalized S100B-Alexa^{488}, and not that S100B-Alexa^{488} predominantly localized to non-LAMP1-positive vesicles after given p.i. In fact, if S100B-Alexa^{488} fluorescence was used as a reference signal, high co-localization between anti-LAMP1 and S100B-Alexa^{488} fluorescence was obtained already after 1 h p.i., 39.35 ± 1.54% (n = 72), and this further increased to 78.65 ± 1.26% (n = 82) after 24 h p.i. (data not shown). These data indicate that numerous vesicles accumulating S100B-Alexa^{488} at a later stage were LAMP1-positive (endolysosomes). Notably, other vesicles with acidified lumen could also pick up and internalize extracellular S100B-Alexa^{488}, such as brain-derived neurotrophic factor-laden astrocytic vesicles (Stenovec *et al.* 2015; Guček *et al.* 2016), consisted with the previous work (Potokar *et al.* 2010) reporting that astrocytic LysoTracker-positive vesicles co-localize modestly (39.20 ± 5.80%), but not exclusively with anti-LAMP1-positive fluorescent vesicles. The molecular composition of endocytotic vesicles is dynamic and may change every time vesicles fuse with one another (Gould and Lippincott-Schwartz 2009; Scott *et al.* 2014), thus it is expected that the co-localization of S100B-Alexa^{488}-positive vesicles with endocytotic markers will not remain constant over time, as is also evident from Fig. 2a and c.

Why is the initial internalization of S100B and dextran distinct?

A relatively slow rate of S100B-Alexa^{488} internalization and a relatively low initial fluorescence co-localization with Dextran^{546} in astrocytes (Fig. 2) indicate that the probes are internalized via distinct mechanisms. Moreover, SIM estimates of diameters of vesicles that internalized S100B-Alexa^{488} and Dextran^{546} (Fig. 2e) indicate that both probes were initially localized to apparently distinct endocytotic pathways. Both molecules have a similar molecular mass, therefore it is unlikely that the molecular mass determines the kinetics of the uptake process (Li *et al.* 2015). More likely, the reason for distinct internalization kinetics arises from the nature of the interaction of the two probes with the plasma membrane. Dextrans have been used extensively as molecules that undergo fluid phase uptake, rather than receptor-mediated endocytotic uptake (Thilo *et al.* 1995; Commisso *et al.* 2013; Gimenez *et al.* 2015), whereas S100B may be more prone to be taken up into cells by receptor-mediated mechanisms, including cluster of differentiation 47, cluster of differentiation 36, and RAGE receptors (Jones *et al.* 2013). It has been demonstrated that S100B may interact via RAGE ligation (Donato *et al.* 2009). S100B promoted phosphorylation and activation of caveolin-1 followed by RAGE internalization in Schwann cells (Perrone *et al.* 2008). Hence, in comparison with the internalization of Dextran^{546}, S100B-Alexa^{488} uptake is dominated by RAGE-mediated endocytosis (Fig. 3). Although different kinetics of uptake of the two fluorescent probes is potentially explained also by S100B-elicited changes in Ca^{2+} signaling during probe internalization (Porras *et al.* 2008), this appears unlikely because astrocyte treatment with 1 μM S100B did not evoke changes in $[Ca^{2+}]_i$ (data not shown).

The mobility of S100B-Alexa^{488} vesicles is perturbed by ATP stimulation

S100B-Alexa^{488}-positive vesicles displayed a time-dependent increase in directional mobility (Fig. 5a and b). A similar observation was made when the internalization of tick-borne encephalitis virus into cultured rat astrocytes was studied (Potokar *et al.* 2014). The time-dependent increase in directional vesicle mobility is best explained by the progressive coupling of vesicles to the cytoskeleton, which generally serves as a vesicle trafficking substrate (Potokar *et al.* 2007, 2010, 2013; Vardjan *et al.* 2012). ATP stimulation of astrocytes, which transiently increase $[Ca^{2+}]_i$, diminished the mobility of S100B-Alexa^{488}-positive vesicles (Fig 6). This is a characteristic of endolysosomes in astrocytes as previously observed in LysoTracker- (Potokar *et al.* 2010) and in Dextran^{546}-labeled compartments (Vardjan *et al.* 2012). An increase in $[Ca^{2+}]_i$ may affect structural integrity of the cytoskeleton, in particular of microtubules and/or actin filaments along which motor proteins propel vesicles (Soldati and Schliwa 2006). Partial disassembly of astrocytic microtubules was observed after prolonged increase in $[Ca^{2+}]_i$ (Stenovec *et al.* 2012). Since microtubule disassembly typically occurs at $[Ca^{2+}]_i$ > 1–4 μM (Schliwa *et al.* 1981), whereas 100 μM ATP typically evokes transient increases in $[Ca^{2+}]_i$ that peak at 780 ± 120 nM (Salter and Hicks 1994), different mechanisms are more likely to account for the diminished vesicle mobility. In response to 100 μM ATP, lysotracker-labeled endolysosomes display greater reduction in directional mobility than secretory peptidergic vesicles (Stenovec *et al.* 2016). It is thus possible that some types of mobile vesicles more readily disconnect from the cytoskeletal tracks than others and are thereafter displaced in the cytosol by Brownian motion.

Removal of extracellular S100B may prevent the toxic effects exerted by this protein

In vitro studies demonstrated contrasting effects of extracellular S100B application to cells, with the outcome largely

depending on its local concentration. At nanomolar concentrations, S100B can induce astrocyte proliferation, neurite outgrowth, and survival of neurons in response to a toxic stimulus (Van Eldik and Wainwright 2003; Kleindienst *et al.* 2007). At micromolar concentrations, however, it can induce apoptosis (Hu *et al.* 1997) and an increase in the expression of amyloid precursor protein in neurons (Businaro *et al.* 2006). Moreover, in glia, the addition of S100B induced the release of nitric oxide and inflammatory cytokines through activation of the NF-κB pathway (Lam *et al.* 2001; Bianchi *et al.* 2011). Thus, an increased extracellular S100B concentration is considered to be associated with increased cell toxicity engaging a pro-inflammatory response (Van Eldik and Wainwright 2003; Villarreal *et al.* 2014), and promoting neurodegenerative diseases (Rothermundt *et al.* 2003). Therefore, removal of this molecule (Dang *et al.* 2014) is essential to minimize the effects that may compromise neuronal function (Hu *et al.* 1997; Lam *et al.* 2001; Businaro *et al.* 2006; Bianchi *et al.* 2010). The glymphatic system is thought to play an essential function in this respect (Plog *et al.* 2015). After traumatic brain injury (Kruse *et al.* 1991; Berger *et al.* 2002) and in inflammatory responses (Guerra *et al.* 2011), a peak of S100B in the cerebrospinal fluid is followed by a subsequent reduction of the protein concentration. Astrocyte exposure to cytokines (de Souza *et al.* 2013) and fluoxetine (Tramontina *et al.* 2008) *in vitro* also results in an acute increase in extracellular S100B concentration followed by a reduction over longer periods. The decrease in extracellular S100B concentration is likely due to reduced S100B secretion and/or enhanced uptake into astrocytes. In part, waste removal by internalization of S100B to the endocytotic compartments of astrocytes contributes to the lowering of the extracellular levels of S100B. Moreover, this may represent a form of signaling termination and an attempt to recover the molecular composition of the extracellular environment. Astrocytes *in vivo* may thus play a role in mitigating the cytotoxic effects of S100B exerted by micromolar protein concentrations (Hu *et al.* 1997; Businaro *et al.* 2006) and protein uptake into endocytotic organelles may be a key process in this respect. Notably, microglia, in addition to astrocytes (Lee *et al.* 2008; Mandrekar *et al.* 2009; Alonso *et al.* 2011), exhibit highly effective clearance of extracellular debris (Lee *et al.* 2008; Mandrekar *et al.* 2009). Microglia express RAGE (Yan *et al.* 1996) that is involved in clearance function (Wilkinson and El Khoury 2012; Yu and Ye 2015) and in S100B-mediated activation of microglia (Donato 2007). Microglia engage in constant endocytotic clearance of debris, which is enhanced during injury, via phagocytosis (Neumann *et al.* 2009), fluid phase macropinocytosis (Mandrekar *et al.* 2009), and receptor-mediated endocytosis (Lee *et al.* 2008).

In summary, the capacity of astrocytes to remove extracellular S100B may prevent the potentially toxic effects that this molecule exerts on neural cells. Moreover, it may also be involved in the modification of extracellular signaling that this molecule may mediate (Leclerc *et al.* 2009; Sorci *et al.* 2013), as is the case in pro-brain-derived neurotrophic factor internalization (Bergami *et al.* 2008). Thus, the mechanism of protein removal revealed in this study has a wider significance because astrocytes are engaged in the clearance of a diverse array of extracellular molecules (Sofroniew 2015).

Acknowledgments and conflict of interest disclosure

This work was supported by the Slovenian Research Agency grant Nos. P3-310, J3-3632, J3-4051, J3-6790, P1-0207 and the travel grant by Brazilian Conselho Nacional de Desenvolvimento Científico e Tecnológico (CNPq). The authors declare that they have no conflicts of interest with the contents of this article.

All experiments were conducted in compliance with the ARRIVE guidelines.

References

Alonso A., Reinz E., Fatar M., Hennerici M. G. and Meairs S. (2011) Clearance of albumin following ultrasound-induced blood-brain barrier opening is mediated by glial but not neuronal cells. *Brain Res.* **1411**, 9–16.

Alvarez J. I., Katayama T. and Prat A. (2013) Glial influence on the blood brain barrier. *Glia* **61**, 1939–1958.

Azevedo F. A., Carvalho L. R., Grinberg L. T., Farfel J. M., Ferretti R. E., Leite R. E., Jacob Filho W., Lent R. and Herculano-Houzel S. (2009) Equal numbers of neuronal and nonneuronal cells make the human brain an isometrically scaled-up primate brain. *J. Comp. Neurol.* **513**, 532–541.

Bennett M. R., Farnell L. and Gibson W. G. (2005) A quantitative model of purinergic junctional transmission of calcium waves in astrocyte networks. *Biophys. J .* **89**, 2235–2250.

Bergami M., Santi S., Formaggio E., Cagnoli C., Verderio C., Blum R., Berninger B., Matteoli M. and Canossa M. (2008) Uptake and recycling of pro-BDNF for transmitter-induced secretion by cortical astrocytes. *J. Cell Biol.* **183**, 213–221.

Berger R. P., Pierce M. C., Wisniewski S. R., Adelson P. D., Clark R. S., Ruppel R. A. and Kochanek P. M. (2002) Neuron-specific enolase and S100B in cerebrospinal fluid after severe traumatic brain injury in infants and children. *Pediatrics* **109**, E31.

Bianchi R., Giambanco I. and Donato R. (2010) S100B/RAGE-dependent activation of microglia via NF-kappaB and AP-1 Co-regulation of COX-2 expression by S100B, IL-1beta and TNF-alpha. *Neurobiol. Aging* **31**, 665–677.

Bianchi R., Kastrisianaki E., Giambanco I. and Donato R. (2011) S100B protein stimulates microglia migration via RAGE-dependent up-regulation of chemokine expression and release. *J. Biol. Chem.* **286**, 7214–7226.

Blott E. J. and Griffiths G. M. (2002) Secretory lysosomes. *Nat. Rev. Mol. Cell Biol.* **3**, 122–131.

Bozza G., Capitani M., Montanari P. *et al.* (2014) Role of ARF6, Rab11 and external Hsp90 in the trafficking and recycling of recombinant-soluble Neisseria meningitidis adhesin A (rNadA) in human epithelial cells. *PLoS ONE* **9**, e110047.

Businaro R., Leone S., Fabrizi C., Sorci G., Donato R., Lauro G. M. and Fumagalli L. (2006) S100B protects LAN-5 neuroblastoma cells

against Abeta amyloid-induced neurotoxicity via RAGE engagement at low doses but increases Abeta amyloid neurotoxicity at high doses. *J. Neurosci. Res.* **83**, 897–906.

Carme Coll Ferrer M., Sobolewski P., Composto R. J. and Eckmann D. M. (2013) Cellular uptake and intracellular cargo release from dextran based nanogel drug carriers. *J. Nanotechnol. Eng. Med.*, **4**, 110021–110028.

Commisso C., Davidson S. M., Soydaner-Azeloglu R. G. *et al.* (2013) Macropinocytosis of protein is an amino acid supply route in Ras-transformed cells. *Nature* **497**, 633–637.

Dang X., Guan L., Hu W., Du G. and Li J. (2014) S100B ranks as a new marker of multiple traumas in patients and may accelerate its development by regulating endothelial cell dysfunction. *Int. J. Clin. Exp. Pathol.* **7**, 3818–3826.

Davey G. E., Murmann P. and Heizmann C. W. (2001) Intracellular Ca^{2+} and Zn^{2+} levels regulate the alternative cell density-dependent secretion of S100B in human glioblastoma cells. *J. Biol. Chem.* **276**, 30819–30826.

Donato R. (2007) RAGE: a single receptor for several ligands and different cellular responses: the case of certain S100 proteins. *Curr. Mol. Med.* **7**, 711–724.

Donato R., Sorci G., Riuzzi F., Arcuri C., Bianchi R., Brozzi F., Tubaro C. and Giambanco I. (2009) S100B's double life: intracellular regulator and extracellular signal. *Biochim. Biophys. Acta* **1793**, 1008–1022.

Dumas J. J., Merithew E., Sudharshan E., Rajamani D., Hayes S., Lawe D., Corvera S. and Lambright D. G. (2001) Multivalent endosome targeting by homodimeric EEA1. *Mol. Cell* **8**, 947–958.

Gilquin B., Cannon B. R., Hubstenberger A. *et al.* (2010) The calcium-dependent interaction between S100B and the mitochondrial AAA ATPase ATAD3A and the role of this complex in the cytoplasmic processing of ATAD3A. *Mol. Cell. Biol.* **30**, 2724–2736.

Gimenez M. C., Rodríguez Aguirre J. F., Colombo M. I. and Delgui L. R. (2015) Infectious bursal disease virus uptake involves macropinocytosis and trafficking to early endosomes in a Rab5-dependent manner. *Cell. Microbiol.* **17**, 988–1007.

Goncalves C. A., Leite M. C. and Guerra M. C. (2010) Adipocytes as an important source of serum S100B and possible roles of this protein in adipose tissue. *Cardiovasc. Psychiatry Neurol.* **2010**, 790431.

Gould G. W. and Lippincott-Schwartz J. (2009) New roles for endosomes: from vesicular carriers to multi-purpose platforms. *Nat. Rev. Mol. Cell Biol.* **10**, 287–292.

Guček A., Jorgacevski J., Singh P., Geisler C., Lisjak M., Vardjan N., Kreft M., Egner A. and Zorec R. (2016) Dominant negative SNARE peptides stabilize the fusion pore in a narrow, release-unproductive state. *Cell. Mol. Life Sci.* doi:10.1007/s00018-016-2213-2.

Guerra M. C., Tortorelli L. S., Galland F., Da Ré C., Negri E., Engelke D. S., Rodrigues L., Leite M. C. and Gonçalves C. A. (2011) Lipopolysaccharide modulates astrocytic S100B secretion: a study in cerebrospinal fluid and astrocyte cultures from rats. *J. Neuroinflammation* **8**, 128.

Halassa M. M., Fellin T., Takano H., Dong J. H. and Haydon P. G. (2007) Synaptic islands defined by the territory of a single astrocyte. *J. Neurosci.* **27**, 6473–6477.

Hill T. A., Gordon C. P., McGeachie A. B. *et al.* (2009) Inhibition of dynamin mediated endocytosis by the dynoles–synthesis and functional activity of a family of indoles. *J. Med. Chem.* **52**, 3762–3773.

Hinshaw J. E. (2000) Dynamin and its role in membrane fission. *Annu. Rev. Cell Dev. Biol.* **16**, 483–519.

Hu J., Ferreira A. and Van Eldik L. J. (1997) S100beta induces neuronal cell death through nitric oxide release from astrocytes. *J. Neurochem.* **69**, 2294–2301.

Humphries W. H., Szymanski C. J. and Payne C. K. (2011) Endo-lysosomal vesicles positive for Rab7 and LAMP1 are terminal vesicles for the transport of dextran. *PLoS ONE* **6**, e26626.

Jones R. S., Minogue A. M., Connor T. J. and Lynch M. A. (2013) Amyloid-β-induced astrocytic phagocytosis is mediated by CD36, CD47 and RAGE. *J. Neuroimmune Pharmacol.* **8**, 301–311.

Jorgacevski J., Fosnaric M., Vardjan N., Stenovec M., Potokar M., Kreft M., Kralj-Iglic V., Iglic A. and Zorec R. (2010) Fusion pore stability of peptidergic vesicles. *Mol. Membr. Biol.* **27**, 65–80.

Jorgacevski J., Potokar M., Grilc S. *et al.* (2011) Munc18-1 tuning of vesicle merger and fusion pore properties. *J. Neurosci.* **31**, 9055–9066.

Kleindienst A., Hesse F., Bullock M. R. and Buchfelder M. (2007) The neurotrophic protein S100B: value as a marker of brain damage and possible therapeutic implications. *Prog. Brain Res.* **161**, 317–325.

Kreft M., Milisav I., Potokar M. and Zorec R. (2004) Automated high through-put colocalization analysis of multichannel confocal images. *Comput. Methods Programs Biomed.* **74**, 63–67.

Kruse A., Cesarini K. G., Bach F. W. and Persson L. (1991) Increases of neuron-specific enolase, S-100 protein, creatine kinase and creatine kinase BB isoenzyme in CSF following intraventricular catheter implantation. *Acta Neurochir (Wien)* **110**, 106–109.

Laemmli U. K. (1970) Cleavage of structural proteins during the assembly of the head of bacteriophage T4. *Nature* **227**, 680–685.

Lam A. G., Koppal T., Akama K. T., Guo L., Craft J. M., Samy B., Schavocky J. P., Watterson D. M. and Van Eldik L. J. (2001) Mechanism of glial activation by S100B: involvement of the transcription factor NFkappaB. *Neurobiol. Aging* **22**, 765–772.

Leclerc E., Fritz G., Vetter S. W. and Heizmann C. W. (2009) Binding of S100 proteins to RAGE: an update. *Biochim. Biophys. Acta* **1793**, 993–1007.

Lee H. J., Suk J. E., Bae E. J. and Lee S. J. (2008) Clearance and deposition of extracellular alpha-synuclein aggregates in microglia. *Biochem. Biophys. Res. Commun.* **372**, 423–428.

Li L., Wan T., Wan M., Liu B., Cheng R. and Zhang R. (2015) The effect of the size of fluorescent dextran on its endocytic pathway. *Cell Biol. Int.* **39**, 531–539.

Lim J. P. and Gleeson P. A. (2011) Macropinocytosis: an endocytic pathway for internalising large gulps. *Immunol. Cell Biol.* **89**, 836–843.

Mandrekar S., Jiang Q., Lee C. Y., Koenigsknecht-Talboo J., Holtzman D. M. and Landreth G. E. (2009) Microglia mediate the clearance of soluble Abeta through fluid phase macropinocytosis. *J. Neurosci.* **29**, 4252–4262.

Nedergaard M., Ransom B. and Goldman S. A. (2003) New roles for astrocytes: redefining the functional architecture of the brain. *Trends Neurosci.* **26**, 523–530.

Neumann H., Kotter M. R. and Franklin R. J. (2009) Debris clearance by microglia: an essential link between degeneration and regeneration. *Brain* **132**, 288–295.

Oberheim N. A., Wang X., Goldman S. and Nedergaard M. (2006) Astrocytic complexity distinguishes the human brain. *Trends Neurosci.* **29**, 547–553.

Pangrsic T., Potokar M., Haydon P. G., Zorec R. and Kreft M. (2006) Astrocyte swelling leads to membrane unfolding, not membrane insertion. *J. Neurochem.* **99**, 514–523.

Pekny M. and Pekna M. (2014) Astrocyte reactivity and reactive astrogliosis: costs and benefits. *Physiol. Rev.* **94**, 1077–1098.

Perrone L., Peluso G. and Melone M. A. (2008) RAGE recycles at the plasma membrane in S100B secretory vesicles and promotes Schwann cells morphological changes. *J. Cell. Physiol.* **217**, 60–71.

Plog B. A., Dashnaw M. L., Hitomi E., Peng W., Liao Y., Lou N., Deane R. and Nedergaard M. (2015) Biomarkers of traumatic injury are

transported from brain to blood via the glymphatic system. *J. Neurosci.* **35**, 518–526.

Porras O. H., Ruminot I., Loaiza A. and Barros L. F. (2008) Na(+)-Ca (2+) cosignaling in the stimulation of the glucose transporter GLUT1 in cultured astrocytes. *Glia* **56**, 59–68.

Potokar M., Kreft M., Pangrsic T. and Zorec R. (2005) Vesicle mobility studied in cultured astrocytes. *Biochem. Biophys. Res. Commun.* **329**, 678–683.

Potokar M., Kreft M., Li L., Daniel Andersson J., Pangrsic T., Chowdhury H. H., Pekny M. and Zorec R. (2007) Cytoskeleton and vesicle mobility in astrocytes. *Traffic* **8**, 12–20.

Potokar M., Stenovec M., Kreft M., Kreft M. E. and Zorec R. (2008) Stimulation inhibits the mobility of recycling peptidergic vesicles in astrocytes. *Glia* **56**, 135–144.

Potokar M., Stenovec M., Gabrijel M., Li L., Kreft M., Grilc S., Pekny M. and Zorec R. (2010) Intermediate filaments attenuate stimulation-dependent mobility of endosomes/lysosomes in astrocytes. *Glia* **58**, 1208–1219.

Potokar M., Vardjan N., Stenovec M., Gabrijel M., Trkov S., Jorgačevski J., Kreft M. and Zorec R. (2013) Astrocytic vesicle mobility in health and disease. *Int. J. Mol. Sci.* **14**, 11238–11258.

Potokar M., Korva M., Jorgacevski J., Avsic-Zupanc T. and Zorec R. (2014) Tick-borne encephalitis virus infects rat astrocytes but does not affect their viability. *PLoS ONE* **9**, e86219.

Rothermundt M., Peters M., Prehn J. H. and Arolt V. (2003) S100B in brain damage and neurodegeneration. *Microsc. Res. Tech.* **60**, 614–632.

Salter M. W. and Hicks J. L. (1994) ATP-evoked increases in intracellular calcium in neurons and glia from the dorsal spinal cord. *J. Neurosci.* **14**, 1563–1575.

Schliwa M., Euteneuer U., Bulinski J. C. and Izant J. G. (1981) Calcium lability of cytoplasmic microtubules and its modulation by microtubule-associated proteins. *Proc. Natl Acad. Sci. USA* **78**, 1037–1041.

Schwartz J. P. and Wilson D. J. (1992) Preparation and characterization of type 1 astrocytes cultured from adult rat cortex, cerebellum, and striatum. *Glia* **5**, 75–80.

Scott C. C., Vacca F. and Gruenberg J. (2014) Endosome maturation, transport and functions. *Semin. Cell Dev. Biol.* **31**, 2–10.

Sofroniew M. V. (2015) Astrocyte barriers to neurotoxic inflammation. *Nat. Rev. Neurosci.* **16**, 249–263.

Soldati T. and Schliwa M. (2006) Powering membrane traffic in endocytosis and recycling. *Nat. Rev. Mol. Cell Biol.* **7**, 897–908.

Sorci G., Riuzzi F., Arcuri C., Tubaro C., Bianchi R., Giambanco I. and Donato R. (2013) S100B protein in tissue development, repair and regeneration. *World J. Biol. Chem.* **4**, 1–12.

de Souza D. F., Wartchow K., Hansen F., Lunardi P., Guerra M. C., Nardin P. and Gonçalves C. A. (2013) Interleukin-6-induced S100B secretion is inhibited by haloperidol and risperidone. *Prog. Neuropsychopharmacol. Biol. Psychiatry* **43**, 14–22.

Steiner J., Bogerts B., Schroeter M. L. and Bernstein H. G. (2011) S100B protein in neurodegenerative disorders. *Clin. Chem. Lab. Med.* **49**, 409–424.

Stenovec M. (2007) Ca2 + -dependent mobility of vesicles capturing anti-VGLUT1 antibodies. *Exp. Cell Res.* **313**, 3809–3818.

Stenovec M., Trkov S., Kreft M. and Zorec R. (2012) Alterations of calcium homoeostasis in cultured rat astrocytes evoked by bioactive sphingolipids. *Acta Physiol. (Oxf)* **212**, 49–61.

Stenovec M., Lasic E., Bozic M., Bobnar S. T., Stout R. F., Jr, Grubisic V., Parpura V. and Zorec R. (2015) Ketamine inhibits ATP-evoked exocytotic release of brain-derived neurotrophic factor from vesicles in cultured rat astrocytes. *Mol. Neurobiol.* doi:10.1007/s12035-015-9562-y.

Stenovec M., Trkov S., Lasic E., Terzieva S., Kreft M., Rodriguez Arellano J. J., Parpura V., Verkhratsky A. and Zorec R. (2016) Expression of familial Alzheimer disease presenilin 1 gene attenuates vesicle traffic and reduces peptide secretion in cultured astrocytes devoid of pathologic tissue environment. *Glia* **64**, 317–329.

Szymanski C. J., Humphries W. H. and Payne C. K. (2011) Single particle tracking as a method to resolve differences in highly colocalized proteins. *Analyst* **136**, 3527–3533.

Thilo L., Stroud E. and Haylett T. (1995) Maturation of early endosomes and vesicular traffic to lysosomes in relation to membrane recycling. *J. Cell Sci.* **108**(Pt 4), 1791–1803.

Thrane A. S., Rangroo Thrane V. and Nedergaard M. (2014) Drowning stars: reassessing the role of astrocytes in brain edema. *Trends Neurosci.* **37**, 620–628.

Tramontina A. C., Tramontina F., Bobermin L. D., Zanotto C., Souza D. F., Leite M. C., Nardin P., Gottfried C. and Gonçalves C. A. (2008) Secretion of S100B, an astrocyte-derived neurotrophic protein, is stimulated by fluoxetine via a mechanism independent of serotonin. *Prog. Neuropsychopharmacol. Biol. Psychiatry* **32**, 1580–1583.

Van Eldik L. J. and Wainwright M. S. (2003) The Janus face of glial-derived S100B: beneficial and detrimental functions in the brain. *Restor. Neurol. Neurosci.* **21**, 97–108.

Vardjan N. and Zorec R. (2015) Excitable astrocytes: Ca(2+)- and cAMP-regulated exocytosis. *Neurochem. Res.* **40**, 2414–2414.

Vardjan N., Gabrijel M., Potokar M. *et al.* (2012) IFN-γ-induced increase in the mobility of MHC class II compartments in astrocytes depends on intermediate filaments. *J. Neuroinflammation* **9**, 144.

Vardjan N., Horvat A., Anderson J. E. *et al.* (2016) Adrenergic activation attenuates astrocyte swelling induced by hypotonicity and neurotrauma. *Glia*. doi:10.1002/glia.22981.

Villarreal A., Seoane R., González Torres A., Rosciszewski G., Angelo M. F., Rossi A., Barker P. A. and Ramos A. J. (2014) S100B protein activates a RAGE-dependent autocrine loop in astrocytes: implications for its role in the propagation of reactive gliosis. *J. Neurochem.* **131**, 190–205.

Wilkinson K. and El Khoury J. (2012) Microglial scavenger receptors and their roles in the pathogenesis of Alzheimer's disease. *Int. J. Alzheimers Dis.* **2012**, 489456.

Yan S. D., Chen X., Fu J. *et al.* (1996) RAGE and amyloid-beta peptide neurotoxicity in Alzheimer's disease. *Nature* **382**, 685–691.

Yu Y. and Ye R. D. (2015) Microglial Abeta receptors in Alzheimer's disease. *Cell. Mol. Neurobiol.* **35**, 71–83.

3.3. Capítulo III

Standardization of a routine protocol for glutamine synthetase activity in astrocytes and cerebral tissue, using glutamyl-transferase activity

Artigo submetido ao periódico *Analytical Biochemistry*

Standardization of a routine protocol for glutamine synthetase activity in astrocytes and cerebral tissue, using glutamyl-transferase activity

Fabiana Galland, Marina Seady, Jessica Taday, Carlos Alberto Gonçalves, Marina Concli Leite

Departamento de Bioquímica, Instituto de Ciências Básicas da Saúde, Universidade Federal do Rio Grande do Sul, Porto Alegre, Brazil.

e-mail adress:

Fabiana Galland – fabianagalland@yahoo.com.br

Marina Seady – mapseady@hotmail.com

Jéssica Taday – jessicataday@hotmail.com

Carlos-Alberto Gonçalves – casg@ufrgs.br

Marina Concli Leite - marina.leite@ufrgs.br

Corresponding author: Marina Concli Leite

Depto Bioquímica, ICBS, UFRGS

Ramiro Barcelos, 2600-anexo

Porto Alegre, RS, Brazil

90035-003

Fax: 55-51-3308 5565

E-mail: marina.leite@ufrgs.br

Abstract

Classically glutamine synthetase (GS) converts glutamate and NH4+ into glutamine, playing an important role in glutamine-glutamate cycle in brain tissue and alterations of this enzyme have been described in neurodegenerative diseases, including Alzheimer´s disease. Beyond synthetase activity, GS has also the transferase activity, which converts glutamine and hydroxylamine into γ-glutamyl-hydroxamate. This reaction also reflects GS activity but the assay was little standardized for brain tissue and would be very useful for clinical and experimental studies. The aim of this study was to evaluate an assay for the measurement of glutamyl-transferase activity of GS in a colorimetric method for the applicability in different brain tissues, in astrocytes culture and C6 lineage cells. The assay was accurate, sensible and linear. It had a good reproducibility having good intra and inter assays coefficients. It was applicable in many brain structures and in glial cultures. The assay is specific for GS activity, as a selective inhibitor of GS (MSO) reduces its activity, but not the quantity of enzyme. This assay has the advantage of being less subjective to interference than synthetase reaction, fast and samples were stable after thawing. Increase in GS activity may reflect on glia maturation, furthermore, this assay is useful for the investigation of this enzyme in physiological and pathological situations.

Keywords: Glutamine synthetase activity assay, astrocyte culture, brain.

1. Introduction

Glutamine synthetase (GS) is a well evolutionarily conserved enzyme which has important function in nitrogen metabolism in different organisms like bacteria, plants and animals [1, 2]. GS is present in most mammalian tissues, however abundantly expressed in liver, kidney, muscle and brain [3, 4]. The activity of this enzyme is the only known route for the synthesis of glutamine from glutamate and ammonia. Glutamine production is important as a nitrogen donor and collector, being essential for the transport of nitrogen between organs, hepatic and renal gluconeogenesis and protein turnover in the muscle [5].

In brain, GS activity plays an important role in glutamine-glutamate cycle, converting glutamate into glutamine inside astrocytes, which prevents excitotoxicity of glutamate in the synaptic cleft [6]. GS is also responsible for the main detoxification of ammonia in the central nervous system (CNS) once add free ion ammonium in to skeleton of glutamate, protecting against neurotoxicity [7]. Glutamine produced from GS is also precursor for glutamate and GABA production [8]. This enzyme is abundantly present in astrocytes in CNS, although some cells, as neurons and oligodendrocytes, were reported to express low quantities of GS in human and rats' brain [9, 10].

The measurement of GS activity is very important to understand physiologic and pathological conditions in brain tissue. A reduction in GS activity in astrocytes may limit glutamate clearance by the EAATs and ammonia detoxification, leading to neurologic impairment [11]. Therefore, GS has been proposed as a marker of brain damage [6, 12]. In fact, variations in the activity or expression of GS have been reported in several neurodegenerative diseases, such as in hepatic encephalopathy (HE), Alzheimer's disease (AD), epilepsy and traumatic brain injury [13, 14]. Furthermore, brain GS activity is sensitive to peripheral metabolic changes induced by caloric restriction [15] or treadmill exercise [16].

GS in physiologic state has the following reaction:

(1) glutamate $+NH_4^+ + Mg^{2+} + ATP \rightarrow$ glutamine + ADP + Pi

Three types of GS genes are known: GSI and III mainly detected in bacteria, and GSII present in eukaryotic cells [3]. Similar catalytic reaction has been reported for GSI and GSII genes in which ATP bond to the enzyme favored glutamate binding. The

phosphate produced by the cleavage of ATP to ADP remain attached to the enzyme, changing the complex enzyme conformation forming the binding site for ammonia, which attacks the intermediate γ-glutamyl phosphate to yield glutamine [17, 18]. Methionine sulfoxamine (MSO) is an irreversible inhibitor of the enzyme, which is phosphorylated in the presence of ATP and interacts with the active site of the enzyme.

Two main methods are used to determine GS activity: radioactive and colorimetric assays. The first method has the advantage of being highly sensible; however, it is costly and of difficult employment since the use of radioactive compounds request extra care of manipulation from the researcher [19]. In colorimetric assays two different activities of GS are measured: a synthetase and a transferase reaction, which may occur in different active sites of the enzyme [4]. Both reactions produce as final product γ-glutamyl-hydroxamate, which react with ferric chloride producing a characteristic yellowish color. Hydroxylamine, which is more stable for *in vitro* reaction, is used instead of ammonia. The synthetase reaction use glutamate as a substrate, as follow:

(2) $\text{glutamate} + NH_2OH + Mg^{2+} + \text{ATP} \rightarrow \gamma\text{-glutamyl-hydroxamate}$

Differentially to the synthetase reaction, the transferase reaction uses glutamine as a substrate:

(3) $\text{glutamine} + NH_2OH + Mn^{2+} + \text{ADP} \rightarrow \gamma\text{-glutamyl-hydroxamate}$

The transferase and specially the synthetase activity were very well characterized by Meister and co-workers [4, 18, 20]. Both activities (Eq. 2 and 3) are present in the same highly purified pellet and respond identical to the same treatment. Thus, both reactions may reflect the levels of the same protein [4, 21]. The transferase reaction has the advantage to have less interference for *in vitro* measurements than the synthetase reaction, since synthetase reaction (Eq. 2) uses ATP as a substrate and it could be easily hydrolyzed by the ATPase present in homogenate tissues [22, 23]. Furthermore, ADP produced in equation 2 was shown to inhibit the enzyme [24]. Still, transferase reaction was shown to be 10 times faster than synthetase in sheep brain [25, 26]. Despite being commonly applied, GS transferase assay was less standardized than synthetase method. Glutamyl-transferase activity assay was shown to be accurate and reliable in muscle tissue [19] and in bacteria [26], however, was little standardized for brain tissue. In fact, in the best of our knowledge, there is only one paper that standardized this method in cerebral tissue, although with some differences in substrate composition, the use of

chromatographic method to identify γ-glutamyl-hydroxamate product and without discriminate different cerebral regions [27]. It was suggested that GS enzyme from muscle and kidney, or even in different regions from the brain are differently regulated, therefore it is important standardize a method that is suitable for cerebral tissue [28, 29]. For this purpose, in this work we characterized an assay for glutamyl-transferase activity of GS for the applicability in different brain tissues and in astrocytes culture. We evaluated the sensibility and the linearity of the assay in time and quantity of protein. We tested precision of the method evaluating intra and inter assays coefficients. Stability of the enzyme after freezing and inhibition of activity comparing with its expression was also assessed.

2. Materials and Methods

2.1. Rat sample

Thirty-day old female Wistar rats were obtained from the Central Animal House of the Department of Biochemistry, ICBS, Universidade Federal do Rio Grande do Sul, Porto Alegre, RS – Brazil. The animals were maintained on a 12:12 h light/dark cycle (lights on 07.00–19.00 h) in an air conditioned constant temperature (22°C ± 1°C) colony room, with free access to water and a 20% (w/w) protein commercial chow (SUPRA, Porto Alegre, RS, Brazil). The experimental protocol was approved by the Ethics Committee for animal research of the Federal University of Rio Grande do Sul, Porto Alegre, Brazil and followed the "Principles of Laboratory Animal Care (NIH publication 85-23, revised 1996). All efforts were made to minimize the number of animals used and their suffering.

Rats were killed by decapitation, without any previously treatment, and cerebral structures (cerebral cortex, hippocampus, cerebellum, striatum and hypothalamus) were quickly dissected out and sliced. The tissue samples were immediately homogenized to glutamine synthetase activity measurement or frozen for sample stability test.

2.2. Astrocytes Cell culture

Primary astrocyte cultures from Wistar rats were prepared as previous described [30]. Procedures were carried out in accordance with the NIH Guide for the Care and Use of Laboratory Animals and were approved by the local authorities. Briefly, cerebral cortices of newborn Wistar rats (1-2 days old) were removed and mechanically dissociated in Ca^{2+}- and Mg^{2+}-free balanced salt solution, pH 7.4, containing (in mM): 137 NaCl; 5.36 KCl; 0.27 Na_2HPO_4; 1.1 KH_2PO_4 and 6.1 glucose. The cortices were cleaned of meninges and mechanically dissociated by sequential passage through a Pasteur pipette. After centrifugation at 1400 RPM for 5 min the pellet was resuspended in DMEM (pH 7.6) supplemented with 8.39 mM HEPES, 23.8 mM $NaHCO_3$, 0.1% amphotericin B, 0.032% gentamicin and 10% fetal calf serum (FCS). Cultures were maintained in DMEM containing 10% FCS in 5% CO_2/95% air at 37°C, allowed to grow to confluence, and used at 21 days *in vitro*.

2.3. C6 Glioma cell culture

The C6 glioma cell line was obtained from the American Type Culture Collection (Rockville, MD). Late passage cells (i.e., after at least 100 passages) were seeded in 25 cm^3 flasks and cultured in DMEM 10% FCS (same medium described for astrocytes primary culture). Exponentially growing cells were detached from the culture flasks using 0.05% trypsin/ethylenediaminetetraacetic acid (EDTA) and seeded in 12 or 24-well plates. Cells were allowed to grow to confluence, and used at 3 days *in vitro*.

2.4. Chemicals and enzymes

Fetal calf serum (FCS), Dulbecco's modified Eagle's medium (DMEM) and other materials for cell culture were purchased from Gibco [Carlsbad, USA]. Poly-L-lysine, hydroxylamine, L-glutamine, adenosine 5′-diphosphate sodium salt, L-Glutamic acid γ-monohydroxamate and L-methionine sulfoximine were purchased from Sigma [St. Louis, USA].

2.5. Preparation of solutions

All solutions were prepared with distilled water. Imidazole and hydroxylamine were adjusted to pH 6.8 with hydrochloric acid. Solutions were stored at 4°C except for glutamine, ADP, hydroxylamine and L-Glutamic acid γ-monohydroxamate which were stored at -20°C.

2.6. Protein determination

Protein content was measured by Lowry's method modified by Peterson using bovine serum albumin as standard [31].

2.7. GS activity assay

The enzymatic activity of glutamine synthetase was determined using the procedures described previously [19] with modifications. Confluent astrocytes culture or rat tissue sample were homogenized in 50 mM imidazole and lysed on ice with syringe. Homogenates (100 µL) were incubated with 100 µL of the solution (mM): (50 imidazole, 50 hydroxylamine, 100 L-glutamine, 25 sodium arsenate dibasic heptahydrate, 0.2 ADP, 2 manganese chloride, pH 6.8) 15 min at 37°C. To avoid the non-enzymatic formation of γ-glutamylhydroxamate, this solution was prepared immediately before its use. The reaction was stopped by the addition of 200 µL of 0.37 M $FeCl_3$, 200 mM trichloroacetic acid, and 0.67 M HCl. Insoluble material was removed by centrifugation at 1000 g for 15 min. The absorbance of 200 µL supernatant was measured at 540 nm on a microtiter plate (SpectraMax I3, Molecular Devices). Blank (the same volume of water instead of sample) or standard quantities of γ-glutamylhydroxamate acid (Sigma) ranged from 0,156 mM to 10 mM, containing the total incubation mixture, were compared with the absorbance of the samples. Glutamine synthetase activity was expressed as µmol/h/mg prot.

2.8. Substrate curve

Confluent astrocytes culture from 24 well plates or a slice of 300 µm of brain tissue sample were homogenized in 50 µL of imidazole (50 mM) and lysed on ice with syringe. Several dilutions were made from the first homogenized and GS activity was measured as previously described.

2.9. Time curve

Confluent astrocytes culture from 24 well plates or a slice of 300 µm of tissue sample were homogenized in 200 µL of imidazole (50 mM) and lysed on ice with syringe. GS activity was measured and the reaction was stopped at 5, 10, 15, 20, 25 or 30 minutes.

2.10. GS activity inhibition

MSO 5 mM or H_2O_2 5 mM were added in cell culture homogenates during 1 h at 37°C. After, GS activity was measured as previously described. In another set of experiments, the extracellular medium of confluent astrocyte culture was replaced by DMEM without serum and MSO 1 mM or H_2O_2 50 µM was added. Enzymatic activity was measured after 3 h of treatment.

2.11. Sample stability test

In order to determine the stability of the enzyme after freezing, the enzymatic reaction was measured fresh, 1 or 7 days after frozen in -20 or -80°C. Cell culture samples were homogenized in (mM): 50 imidazole, 100 EGTA and 100 EDTA and frozen in solution. Cerebral tissue samples were frozen dry.

2.12. GS immunocontent determination

Cerebral tissues of rats or cell culture were homogenized in sample buffer (0.0625 M Tris–HCl, pH 6.8, 2% (w/v) SDS, 5% (w/v) b-mercaptoethanol, 10% (v/v) glycerol, 0.002% (w/v) bromphenol blue), boiled and centrifuged 5 min at 10000g. Equal amounts (30 µg) of proteins from each sample were electrophoresed in a 12% (w/v) SDS–polyacrylamide gel. The separated proteins were blotted onto a nitrocellulose membrane. Anti-Glutamine Synthetase was used at a dilution of 1:10000. After incubating with the primary antibody for 24 h at 4°C, filters were washed and incubated for 1h at 4°C with peroxidase-conjugated anti-goat immunoglobulin (IgG) at a dilution of 1:5000. Equivalent loading of each sample was confirmed with anti-actin, except from the culture sample, as different cells contains different amounts of actin. The chemiluminescence signal was detected using an ECL kit from Amersham and evaluated in the luminescence image analyzer (Image Quant LAS4000 from GE). The luminescence signal differences were analyzed using ImageJ software.

2.13. Statistical analysis

Parametric data are reported as means ± standard error and were analyzed by T-test or one-way analysis of variance (ANOVA) followed by Duncan's test, in the SPSS-16.0. Tests are specified in the legends, with the level of significance set at $p < 0.05$.

3. Results

3.1. Sensibility, linearity and reproducibility of the assay

The dilution of standard quantities of γ-glutamylhydroxamate acid was sensible from 0.156 mM and linear until 20 mM. The standard curve shows high linearity presenting equation y=0.0736x + 0.0399 and R= 0.99 (Fig 1).

In order to verify the reproducibility of the method intra-assay and inter-assay coefficients of variance (CV) were obtained from culture samples. For intra-assay analysis the enzymatic activity of five aliquots from the same sample were measured in the same experiment. This was repeated eight times with different samples. For inter-assays analysis GS activity of the same sample was measured in different experiments. The mean of eleven experiments were obtained. The coefficient of variation was obtained by the ratio of standard deviation to the mean. This analysis showed good intra-assay (5.58% N=8) and inter-assay (8.33% N=11) CV.

3.2. Time of incubation and amount of protein linearity

In order to verify the reliability of the technique the linearity of the assay was tested with time of incubation and with quantity of protein in different samples (Fig 2). Astrocytes culture and hippocampal slices show high linearity between 5 and 30 minutes of incubation with R=0.9879 and R=0.9804, respectively (Fig, 2A and B). The quantity of product formed was also correspondent with the amount of protein either in culture cells (Fig 2C) or hippocampal slices (Fig 2D), showing linearity of R=0.9898 and R=0.9871, respectively. All subsequent experiments were performed using an incubation time of 15 min.

3.3. Frozen stability test

Freezing samples for subsequent determination of enzyme activity is a common procedure. To verify the stability of the enzyme after thawed we tested the same sample fresh and after thawed. Homogenates of astrocytes culture in solution with addition of protease inhibitors and dry slice of hippocampal tissue were immediately frozen in -20°C or -80°C. After 24 h or 1 week samples were thawed and enzymatic activity was compared to fresh sample. Table 1 shows that hippocampal slices and homogenized cell cultures samples are stable for GS activity measurement for a week in both tested

conditions (-20 or -80°C). It is important to mention that the stability of the enzyme was not preserved after a moth frozen (data not shown).

3.4. Assay applicability

GS activity was detectable in astrocyte culture, C6 glioma cell line and different areas of the brain (Fig 3). C6 glioma cell line showed significantly less enzyme activity than astrocytes cell culture (Fig 3A). Immunocontent of enzyme was also measured (Fig 3A, insert). In tissue sample, cerebellum showed an increased enzyme activity compared to other cerebral regions (Fig 3B). GS content was also measured by immunoblotting showing higher expression of the enzyme in cerebellum (Fig 3B, insert).

3.5. Assay Specificity

In order to evaluate the functionality and specificity of the assay we tested two GS modulators: MSO, a specific inhibitor of the enzyme, and peroxide, a general oxidant. First, we tested the inhibitors MSO and peroxide (both 5 mM) in homogenates of astrocyte culture for 1h, followed by GS activity assay (Fig 4). In another set of experiments we tested both inhibitors MSO (1mM) and peroxide (50 µM) in astrocytes culture treated during 3 h, followed by GS activity assay (Fig 5). In both situations we observed a statistical reduction in GS activity. It is important to mention that neither MSO nor hydrogen peroxide caused a reduction of GS expression as seen in immunoblotting analysis (Fig 5, insert).

4. Discussion

The measurement of GS activity is essential to observe any dysfunction in glutamine-glutamate cycle and other important pathways in which this enzyme participates in the brain. In this research we standardized an assay that measures the glutamyl-transferase activity of glutamine synthetase in astrocytes cell culture, C6 lineage and different brain tissue. Here, we show a sensible assay, detecting little quantities of product (0.156 mM) and high linearity with $R^2 = 0.99$ (Fig 1). Furthermore, the technique was very precise showing an intra-assay and inter-assay CV lower than 10%, which is adequate for enzymatic assays [32, 33]. GS transferase activity remained linear in range of protein quantity (from 18.4 to 55.2 µg of protein in cell culture and from 7.6 to 121.1 µg of protein in hippocampal slices) and time of incubation (5 to 30 min for both samples) (Fig 2). The characterization of GS assay favors its wide use in the brain research area,

providing a good method to study the enzyme in physiologic condition state and neurodegenerative diseases.

In addition, it was shown the applicability of the assay in different cerebral structures, in astrocytes culture and in C6 glioma cell line (Fig 3). This assay showed to be highly sensible, detecting GS activity even in cells with little amount of enzyme, such as C6 glioma cell line. It was shown that ammonia is differentially metabolized, depending on brain region [34, 35], probably due to differences in astrocytes GS content or activity from different regions of the CNS [36]. In fact, in our investigation, cerebellum showed greater basal activity of GS when compared with other regions analyzed, and this correspond with greater GS immunocontent as showed in western blot analysis. Interestingly, Cao Danh and coauthor (1985) also obtained high GS activity in cerebellum of rats compared with similar brain areas analyzed [37].

In our results, GS activity was reduced with MSO or peroxide treatment with no alteration in the enzyme content. These data, not only demonstrate the specificity of the assay, but show the importance to measure the activity of the enzyme rather than only its expression. A commitment in enzyme activity may provide more information about some physiologic alteration, such as oxidative damage, which results in the enzymatic impairment.

It is known that enzymatic activity is highly dependent on its structure; and any conformation change may interfere in its activity. In fact, freezing and thawing may alter protein structure, which can be misinterpreted in activity assays. Here we show that GS activity in dry freezing samples and in homogenates of cell culture was not affected by freezing and thawing. The enzyme was stable up to 1 week, frozen either in - 20°C or -80°C. It is important to say that the addition of protease inhibitor (PMSF, EGTA and EDTA) was essential for the maintenance of activity in culture sample homogenates. Without the addition of these inhibitors, cell culture samples were not stable even for 24 h frozen (data not shown). Ensuring the stability of the enzyme after thawing is extremely important to the reliability of the results, and provides better flexibility to the researcher to do the analysis after experiment.

5. Conclusion

Despite being commonly used, the GS transferase activity assay it was little standardized in cerebral tissue [27]. Considering that may be differences in GS activity from different organs it is important to characterize an assay specific for cerebral tissue [28, 29]. Here, we characterized a colorimetric assay that measures transferase activity of GS showing accuracy, sensibility and linearity. We demonstrate that it is applicable in many structures of the CNS and in cell culture. GS transferase activity assay was shown to be highly sensible to MSO treatment without changing the expression of the enzyme, showing specificity. Furthermore, the evaluation of enzymatic activity after freezing showed that GS is stable up to one week in dry tissue or cell culture homogenates. This assay has the advantage to be less susceptible to interference than synthetase reaction, faster and methodologically safer when compared to radioactive assay. The literature demonstrates that GS is involved to the pathogenesis of several neurological disorders, such as HE and AD, and changes in the activity of this enzyme are a useful marker for astroglial functionality in acute brain injury and neurodegeneration disorders. Herein, we standardized in brain tissue and astrocyte culture a reliable, simple and cheaper GS activity assay, potentially very useful for the investigation of this enzyme in physiological and pathological situations.

Acknowledgements: This work was supported by Conselho Nacional de Desenvolvimento Científico e Tecnológico (CNPq), Coordenação de Aperfeiçoamento de Pessoal de Nível Superior (CAPES), Fundação de Amparo à Pesquisa do Estado do Rio Grande do Sul (FAPERGS) and Instituto Nacional de Ciência e tecnologia (INCT).

6. References

[1] G. Pesole, M.P. Bozzetti, C. Lanave, G. Preparata, C. Saccone, Glutamine synthetase gene evolution: a good molecular clock, Proc Natl Acad Sci U S A, 88 (1991) 522-526.

[2] Y. Kumada, D.R. Benson, D. Hillemann, T.J. Hosted, D.A. Rochefort, C.J. Thompson, W. Wohlleben, Y. Tateno, Evolution of the glutamine synthetase gene, one of the oldest existing and functioning genes, Proc Natl Acad Sci U S A, 90 (1993) 3009-3013.

[3] Y. Wang, J. Kudoh, R. Kubota, S. Asakawa, S. Minoshima, N. Shimizu, Chromosomal mapping of a family of human glutamine synthetase genes: functional gene (GLUL) on 1q25, pseudogene (GLULP) on 9p13, and three related genes (GLULL1, GLULL2, GLULL3) on 5q33, 11p15, and 11q24, Genomics, 37 (1996) 195-199.

[4] A. Meister, Glutamine synthetase from mammalian tissues, Methods Enzymol, 113 (1985) 185-199.

[5] K. Chan, S.M. Busque, M. Sailer, C. Stoeger, S. Bröer, H. Daniel, I. Rubio-Aliaga, C.A. Wagner, Loss of function mutation of the Slc38a3 glutamine transporter reveals its critical role for amino acid metabolism in the liver, brain, and kidney, Pflugers Arch, 468 (2016) 213-227.

[6] C.F. Rose, A. Verkhratsky, V. Parpura, Astrocyte glutamine synthetase: pivotal in health and disease, Biochem Soc Trans, 41 (2013) 1518-1524.

[7] A.J. Cooper, The role of glutamine synthetase and glutamate dehydrogenase in cerebral ammonia homeostasis, Neurochem Res, 37 (2012) 2439-2455.

[8] A.T. Holten, V. Gundersen, Glutamine as a precursor for transmitter glutamate, aspartate and GABA in the cerebellum: a role for phosphate-activated glutaminase, J Neurochem, 104 (2008) 1032-1042.

[9] H.G. Bernstein, J. Bannier, G. Meyer-Lotz, J. Steiner, G. Keilhoff, H. Dobrowolny, M. Walter, B. Bogerts, Distribution of immunoreactive glutamine synthetase in the adult human and mouse brain. Qualitative and quantitative observations with special

emphasis on extra-astroglial protein localization, J Chem Neuroanat, 61-62 (2014) 33-50.

[10] W. Cammer, Glutamine synthetase in the central nervous system is not confined to astrocytes, J Neuroimmunol, 26 (1990) 173-178.

[11] Y. Trabelsi, M. Amri, H. Becq, F. Molinari, L. Aniksztejn, The conversion of glutamate by glutamine synthase in neocortical astrocytes from juvenile rat is important to limit glutamate spillover and peri/extrasynaptic activation of NMDA receptors, Glia, 65 (2017) 401-415.

[12] A.R. Jayakumar, M.D. Norenberg, Glutamine Synthetase: Role in Neurological Disorders, Adv Neurobiol, 13 (2016) 327-350.

[13] C.K. Petito, M.C. Chung, L.M. Verkhovsky, A.J. Cooper, Brain glutamine synthetase increases following cerebral ischemia in the rat, Brain Res, 569 (1992) 275-280.

[14] M. Kulijewicz-Nawrot, E. Syková, A. Chvátal, A. Verkhratsky, J.J. Rodríguez, Astrocytes and glutamate homoeostasis in Alzheimer's disease: a decrease in glutamine synthetase, but not in glutamate transporter-1, in the prefrontal cortex, ASN Neuro, 5 (2013) 273-282.

[15] L.C. Ribeiro, A. Quincozes-Santos, M.C. Leite, R.T. Abib, J. Kleinkauf-Rocha, R. Biasibetti, L.N. Rotta, S.T. Wofchuk, M.L. Perry, C.A. Gonçalves, C. Gottfried, Caloric restriction increases hippocampal glutamate uptake and glutamine synthetase activity in Wistar rats, Neurosci Res, 64 (2009) 330-334.

[16] C. Bernardi, A.C. Tramontina, P. Nardin, R. Biasibetti, A.P. Costa, A.F. Vizueti, C. Batassini, L.S. Tortorelli, K.M. Wartchow, M.F. Dutra, L. Bobermin, P. Sesterheim, A. Quincozes-Santos, J. de Souza, C.A. Gonçalves, Treadmill exercise induces hippocampal astroglial alterations in rats, Neural Plast, 2013 (2013) 709732.

[17] S.H. Liaw, I. Kuo, D. Eisenberg, Discovery of the ammonium substrate site on glutamine synthetase, a third cation binding site, Protein Sci, 4 (1995) 2358-2365.

[18] A. Meister, The specificity of glutamine synthetase and its relationship to substrate conformation at the active site, Adv Enzymol Relat Areas Mol Biol, 31 (1968) 183-218.

[19] R. Minet, F. Villie, M. Marcollet, D. Meynial-Denis, L. Cynober, Measurement of glutamine synthetase activity in rat muscle by a colorimetric assay, Clin Chim Acta, 268 (1997) 121-132.

[20] W.B. Rowe, A. Meister, Studies on the inhibition of glutamine synthetase by methionine sulfone, Biochemistry, 12 (1973) 1578-1582.

[21] B.H. Juurlink, Glutamine synthetase and glutamyltransferase activities in the mouse astrocyte *in vitro*, Neurochem Res, 7 (1982) 905-910.

[22] S.C. Dennis, J.C. Lai, J.B. Clark, The distribution of glutamine synthetase in subcellular fractions of rat brain, Brain Res, 197 (1980) 469-475.

[23] E.R. Stadtman, B.M. Shapiro, A. Ginsburg, H.S. Kingdon, M.D. Denton, Regulation of glutamine synthetase activity in Escherichia coli, Brookhaven Symp Biol, 21 (1968) 378-396.

[24] H. Yamamoto, H. Konno, T. Yamamoto, K. Ito, M. Mizugaki, Y. Iwasaki, Glutamine synthetase of the human brain: purification and characterization, J Neurochem, 49 (1987) 603-609.

[25] R.A. Ronzio, S. Wilk, W.B. Rowe, A. Meister, Preparation and studies on the characterization of sheep brain glutamine synthetase, Biochemistry, 8 (1969) 2670-2674.

[26] E. Ehrenfeld, S.J. Marble, A. Meister, ENZYMATIC SYNTHESIS OF GAMMA-GLUTAMYLHYDROXAMIC ACID FROM GLUTAMIC ACID AND HYDROXYLAMINE, J Biol Chem, 238 (1963) 3711-3716.

[27] N. Seiler, J. Reid, B. Knödgen, A sensitive method for the assay of glutamine synthetase, Neurochem Res, 15 (1990) 301-305.

[28] K. Iqbal, J.H. Ottaway, Glutamine synthetase in muscle and kidney, Biochem J, 119 (1970) 145-156.

[29] T. Böttcher, M. Goiny, J. Bering, S. Domhof, R. Nau, U. Ungerstedt, Regional differences in glutamine synthetase inhibition by L-methionine sulfoximine: a microdialysis study in the rabbit brain, Exp Brain Res, 150 (2003) 194-200.

[30] C. Gottfried, F. Tramontina, D. Gonçalves, C.A. Gonçalves, E. Moriguchi, R.D. Dias, S.T. Wofchuk, D.O. Souza, Glutamate uptake in cultured astrocytes depends on age: a study about the effect of guanosine and the sensitivity to oxidative stress induced by H(2)O(2), Mech Ageing Dev, 123 (2002) 1333-1340.

[31] G.L. Peterson, A simplification of the protein assay method of Lowry et al. which is more generally applicable, Anal Biochem, 83 (1977) 346-356.

[32] V.V. Daitx, J. Mezzalira, V.a.C. Moraes, A.C. Breier, J. Cé, J.C. Coelho, Comparing the alpha-galactosidase A biochemical properties from healthy individuals and Fabry disease patients, Clin Chim Acta, 445 (2015) 60-64.

[33] Z. Lukacs, P. Nieves Cobos, A. Keil, R. Hartung, E. Mengel, M. Beck, M. Deschauer, F. Hanisch, R. Santer, Dried blood spots in the diagnosis of lysosomal storage disorders--possibilities for newborn screening and high-risk population screening, Clin Biochem, 44 (2011) 476.

[34] E.A. Kosenko, E.E. Beloushko, I.G. Kaminskiĭ, [Differences between cerebellum and hippocampus in antioxidant system], Biomed Khim, 60 (2014) 469-472.

[35] E.A. Kosenko, L.A. Tikhonova, V.P. Reddy, G. Aliev, Y.G. Kaminsky, Differential up-regulation of ammonia detoxifying enzymes in cerebral cortex, cerebellum, hippocampus, striatum and liver in hyperammonemia, CNS Neurol Disord Drug Targets, 13 (2014) 1089-1095.

[36] A.J. Patel, M.D. Weir, A. Hunt, C.S. Tahourdin, D.G. Thomas, Distribution of glutamine synthetase and glial fibrillary acidic protein and correlation of glutamine synthetase with glutamate decarboxylase in different regions of the rat central nervous system, Brain Res, 331 (1985) 1-9.

[37] H. Cao Danh, M. Strolin Benedetti, P. Dostert, Age-related changes in glutamine synthetase activity of rat brain, liver and heart, Gerontology, 31 (1985) 95-100.

[38] V. Felipo, R.F. Butterworth, Neurobiology of ammonia, Prog Neurobiol, 67 (2002) 259-279.

Table 1 Frozen stability of the enzyme.

	Astrocytes		Hippocampal slices	
	-20°C	-80°C	-20°C	-80°C
Fresh	2.5±0.2	2.5±0.2	2.2 ±0.2	1.92±0.27
1 day	2.4±0.3	2.5±0.3	1.7±0.3	1.80±0.17
1 week	2.0±0.1	2.2±0.1	2.3±0.5	1.77±0.25

Legends of figures

Fig 1. Sensibility and linearity of the assay. Representative curve of standard quantities of γ-glutamylhydroxamate acid ranged from 0.156 mM to 20 mM containing the total incubation mixture. The absorbance was measured at 540 nm. The curve's correlation coefficient is shown.

Fig 2. Time of incubation and protein quantity linearity in astrocytes and hippocampal slices. The same samples of astrocytes culture (A) or hippocampal slices (B) were incubated at different time intervals, ranged from 5 to 30 minutes. For standard quantities of protein several dilution of the same sample were made in astrocytes culture (C) and in hippocampal slices (D) and incubated for 15 min. Glutamine synthetase activity was expressed as μmol/h/mg prot. The correlation coefficient (R^2) was calculated for each curve.

Fig 3. Applicability of the assay in CNS. GS transferase activity was measured in (A) astrocyte culture and C6 cell line or (B) in cerebral cortex (CX), hippocampus (HC), cerebellum (CE), striatum (ST) and hypothalamus (HT) of Wistar rats. Imunocontent of GS is shown in inserts in A and B. Each value is the mean (± standard error) of at least 5 independent experiments performed in triplicate or five rats. * represent significantly difference, in (A) t-test and in (B) one way ANOVA followed by Duncan's test, with a significance level of $p < 0.05$).

Fig 4. GS activity is inhibited *in vitro*. Astrocytes previously homogenized were incubated with 5 mM of MSO or peroxide at 37°C and GS activity was measured after 1h. Each value is the mean (± standard error) of at least 5 independent experiments

performed in triplicate. * significantly different (one way ANOVA followed by Duncan's test, with a significance level of $p < 0.05$).

Fig 5. GS activity is inhibited in treated astrocytes culture. MSO 1 mM or 50 µM of peroxide were incubated in astrocytes culture at 37°C and GS activity was measured after 3h. Immunocontent of GS is shown in insert. Each value is the mean (± standard error) of at least 5 independent experiments performed in triplicate. * significantly different (one way ANOVA followed by Duncan's test, with a significance level of $p < 0.05$).

Figure 1

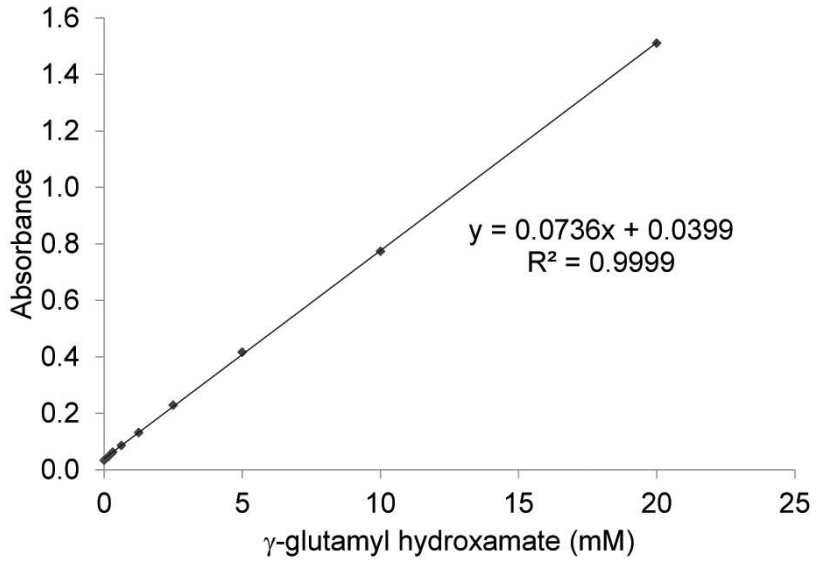
1.6
1.4
1.2
1.0
0.8
0.6
0.4
0.2
0.0
Absorbance
0
5
10
15
20
25
γ-glutamyl hydroxamate (mM)
y = 0.0736x + 0.0399
R² = 0.9999

Figure 2

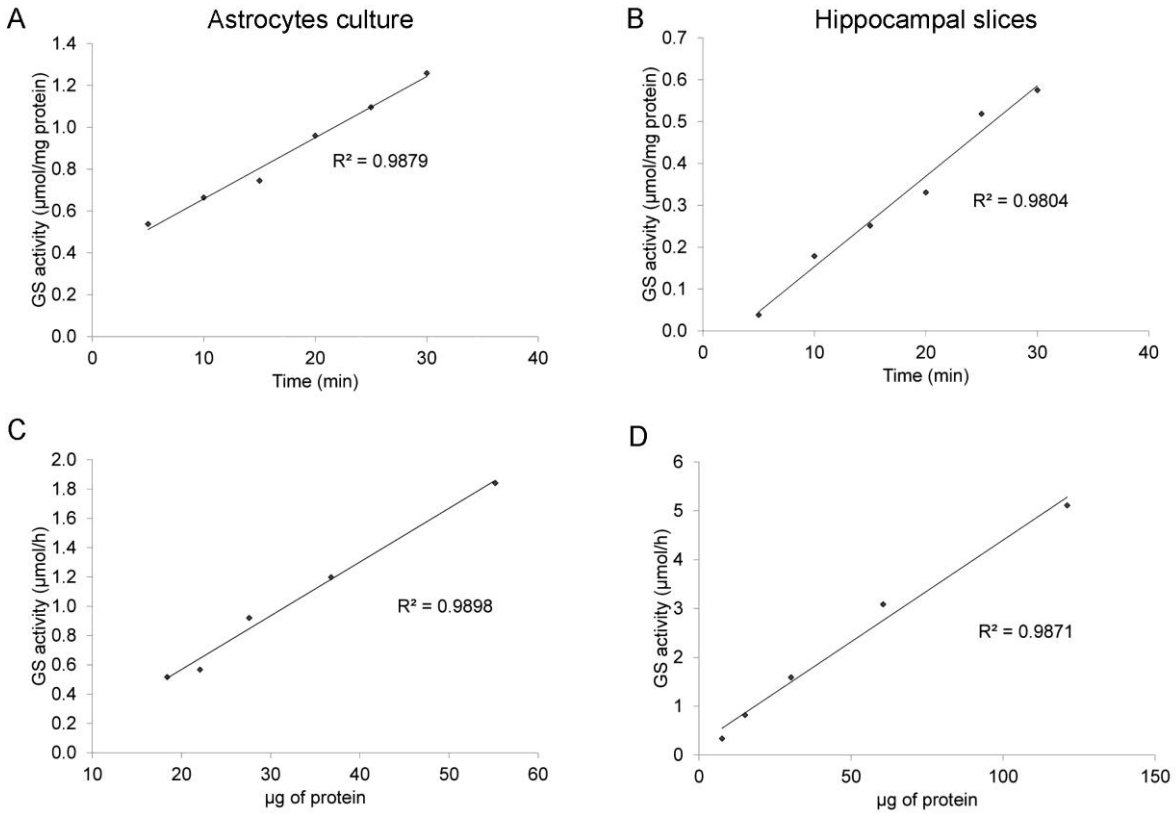
A
Astrocytes culture
GS activity (µmol/mg protein)
Time (min)
R² = 0.9879
B
Hippocampal slices
GS activity (µmol/mg protein)
Time (min)
R² = 0.9804
C
GS activity (µmol/h)
µg of protein
R² = 0.9898
D
GS activity (µmol/h)
µg of protein
R² = 0.9871

Figure 3

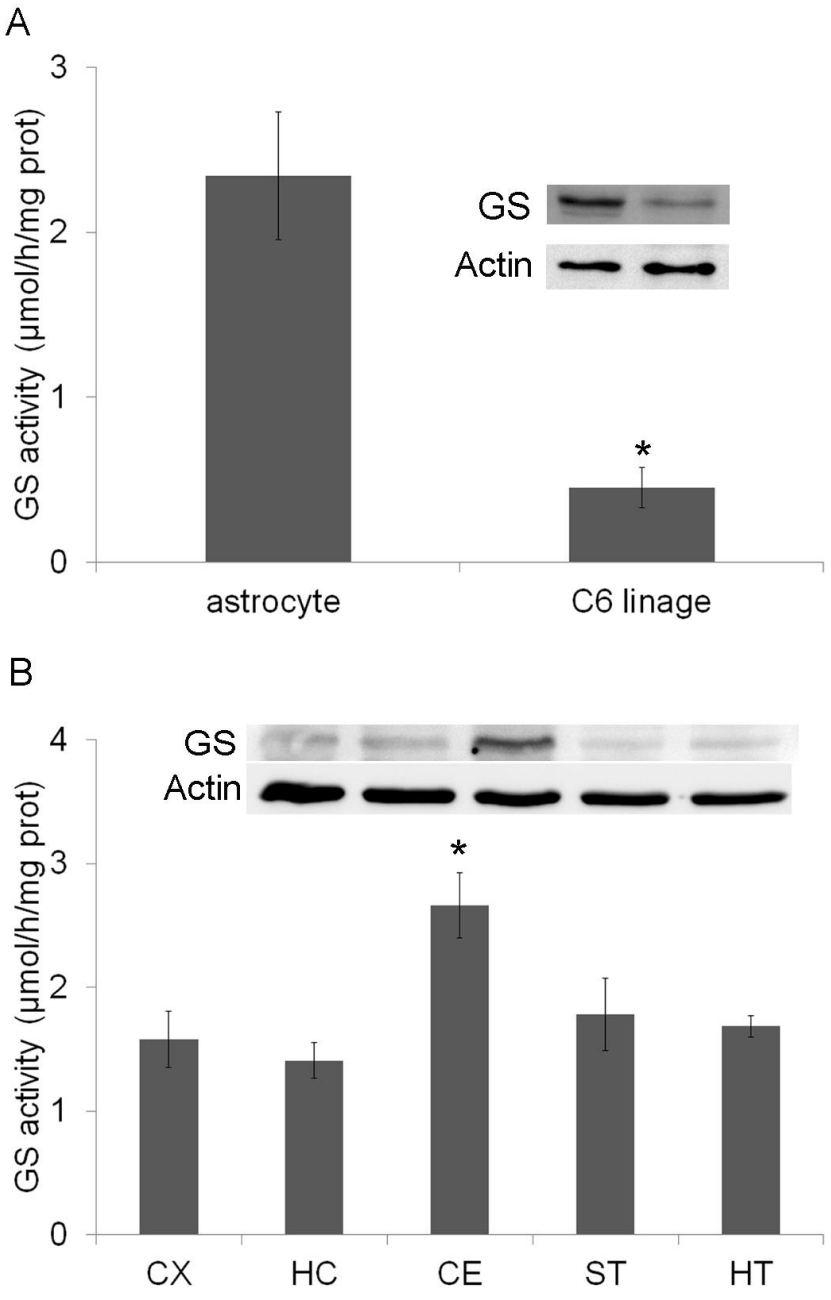
A
GS activity (µmol/h/mg prot)
3
2
1
0
GS
Actin
*
astrocyte
C6 linage
B
GS activity (µmol/h/mg prot)
4
3
2
1
0
GS
Actin
*
CX
HC
CE
ST
HT

Figure 4

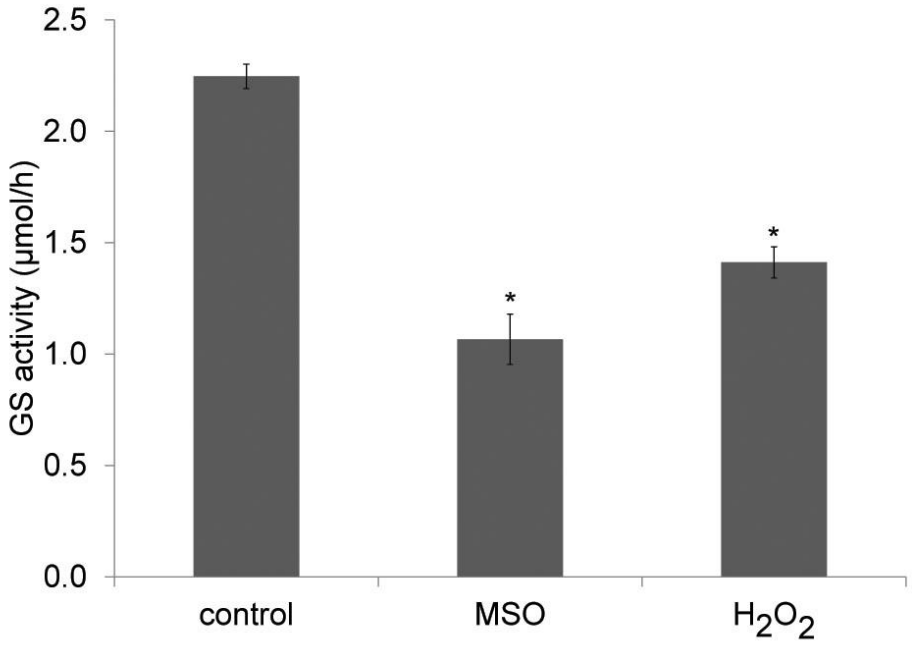

Figure 5

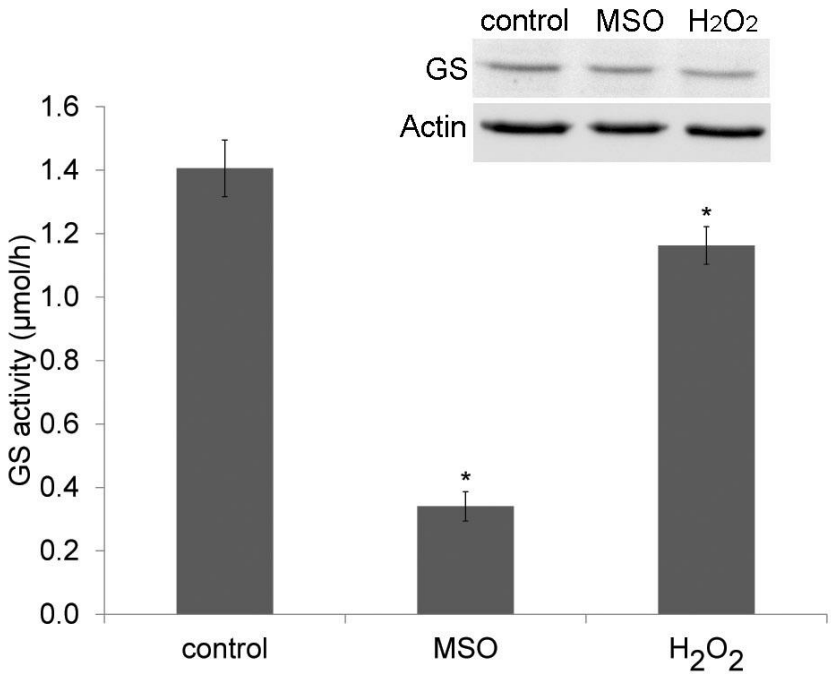
control
MSO
H2O2
GS
Actin
GS activity (µmol/h)
1.6
1.4
1.2
1.0
0.8
0.6
0.4
0.2
0.0
*
*
control
MSO
H2O2

4. Discussão

4.1. Caracterização molecular e funcional de cultura primária de astrócitos, astrócitos imortalizados e glioma C6.

Este trabalho teve como principal objetivo comparar três diferentes modelos de cultura de astrócitos - cultura primária (CP), astrócitos imortais (AI) e linhagem C6 (C6) no que diz respeito às propriedades moleculares e, principalmente, funcionais de cada tipo celular. Uma análise completa e a integração das características de cada célula em um único estudo permitiu a comparação direta, uma vez que as condições de cultivo foram mantidas as mesmas. Desta forma, foi possível avaliar o modelo mais adequado de estudo para astrócitos em cultura, avaliando-se as desvantagens e vantagens de cada tipo celular.

4.1.1. Avaliação da morfologia basal e plasticidade após estímulo

Varias funções dos astrócitos dependem da sua capacidade de alteração morfológica, uma vez que quando emitem processos conseguem regular o microambiente extracelular, ou mesmo interferir na atividade sináptica dos neurônios (Ostroff et al. 2014, De Pittà et al. 2016). A capacidade das células em cultivo de responder a certos estímulos com alterações morfológicas e emissão de processos é uma ferramenta muito eficiente e utilizada para a avaliação das funções astrocíticas. Neste trabalho, observamos que em estado basal CP e AI apresentavam morfologia mais similar, mostrando formato poligonal e citoesqueleto de actina mais regular (Fig 1, capítulo I). Já a linhagem C6, mostrou aspecto mais alongado, triangular e com uma rede de filamentos de actina mais irregular. Um estudo anterior, já havia registrado diferenças na estrutura do citoesqueleto entre CP e C6, destacando um aspecto mais

desorganizado nos filamentos de actina em C6, justificado por ser uma célula de propriedades invasivas (Zhou et al. 2008). No entanto, quando o estímulo de forskolina foi testado nestas células, AI não foram capazes de alterar a sua morfologia, como foi observado em CP e C6. A forskolina é um estímulo clássico que induz alterações morfológicas por um aumento intracelular dos níveis de AMPc (Frizzo *et al.* 2004). De uma forma semelhante, outro estudo mostrou a incapacidade de AI alterarem a expressão de GFAP em resposta a dibutiril AMPc em comparação com CP e C6 (Geller & Dubois-Dalcq 1988). Estes resultados indicam a restrição do uso de AI para estudo de alterações morfológicas em cultura. Em contraposição, CP e C6 apresentaram alta capacidade de mudança morfológica, contraindo o corpo celular e emitindo processos longos após estímulo com forskolina. Embora C6 tenha respondido ao estímulo, é importante ressaltar que os processos vistos em CP foram mais proeminentes. Foi visto que o subcultivo de cultura de astrócitos primários induziu uma mudança morfológica, reduzindo a quantidade de processos aparentes (Passaquin *et al.* 1994). Este resultado indica que o processo de subcultivo pode afetar a capacidade de resposta morfológica da célula, como no caso de AI e C6. Além disso, as linhagens apresentaram redução no nível de GFAP e vimentina, o que é considerado essencial para a indução de hipertrofia em astrócitos (Wilhelmsson *et al.* 2004).

4.1.2. Perfil molecular dos diferentes modelos de astrócitos

O perfil molecular dos astrócitos é bastante heterogêneo, dependendo da origem, local ou mesmo contexto patológico onde se encontra. Apesar disso, algumas proteínas características são usadas como marcadores moleculares deste tipo celular. Sabe-se que durante o desenvolvimento astrócitos reduzem os níveis de vimentina e aumentam os de

GFAP (Menet *et al.* 2001). De acordo com os dados do nosso estudo os três modelos de astrócitos mostram razão aumentada de GFAP / vimentina.

Neste trabalho avaliamos o conteúdo intracelular de GFAP e S100B, que são proteínas altamente usadas como marcadores astrogliais (Eng 1985, Van Eldik & Wainwright 2003, Brozzi *et al.* 2009). Ambas as proteínas foram detectadas nos três modelos de cultura de astrócitos, embora em quantidades significativamente menores nos AI e C6 (Fig 2, Capítulo I). Resultados similares já haviam sido relatados para os modelos de astrócitos, porém muitas vezes negligenciando a diferença em relação à quantidade de proteína (Raju et al. 1980, Tabuchi et al. 1982, Groves *et al.* 1993, Morikawa et al. 2001, Furihata et al. 2016). Além destes marcadores clássicos, também foi avaliado a presença da proteína ALDH1L1 que vem sendo usada como um novo marcador astroglial específico (Yang et al. 2011, Souza *et al.* 2013). Embora esta proteína participe do metabolismo do folato, estando relacionada com divisão e crescimento celular (Krupenko 2009) observamos níveis reduzidos em AI e C6 em comparação com CP. O mesmo resultado foi encontrado para AQP4, proteína altamente expressa em astrócitos (Papadopoulos & Verkman 2013). Uma possível explicação para a redução nos níveis de proteínas marcadores de astrócitos em AI e C6 seria as altas taxas proliferativas destas células, as quais devem investir menos no perfil de diferenciação, em comparação com CP cuja taxa crescimento é bem menor.

A quantidade de canais de potássio Kir4.1 foi similar entre os três tipos celulares. Trabalhos anteriores mostraram que a condutância de potássio é muita baixa em gliomas em comparação com células diferenciadas. No entanto, este comprometimento não se deve a uma redução nos níveis de expressão dos canais, mas sim em uma diferença de localidade. Em gliomas os canais de potássio estão proeminentemente expressões no núcleo ao invés da membrana celular (Olsen &

Sontheimer 2008). Portanto, a expressão equivalente do canal Kir4.1 em AI e C6 em comparação com CP pode não representar a funcionalidade dos transportadores de potássio.

4.1.3. Caracterização funcional do metabolismo do glutamato em modelo de astrócitos

Os astrócitos desempenham um papel essencial no metabolismo do glutamato, sendo importante para a depuração deste aminoácido da fenda sináptica, evitando assim a excitotoxicidade. Qualquer disfunção nos transportadores de glutamato ou mesmo na atividade da GS pode comprometer as funções cerebrais e está relacionada com o desenvolvimento de doenças neurodegenerativas (Benarroch 2010). De fato, a atividade da GS está intimamente ligada com a funcionalidade dos transportadores. Foi visto que uma inibição na atividade da GS compromete a depuração de glutamato pelos EAATs (Trabelsi et al. 2017). Os nossos resultados mostram que tanto AI quanto C6 são positivos para EAAT1, EAAT2 e GS, porém apresentam níveis reduzidos em comparação com CP (Fig 3 , Capítulo I). Além disso, observamos que não apenas a quantidade, mas também a funcionalidade destas proteínas está reduzida, avaliada pela captação de glutamato e atividade da GS. A presença de transportadores de glutamato em linhagens de astrócitos não é clara. Embora alguns estudos tenham detectado a presença de transportadores de glutamato, a funcionalidade destes não foi avaliada (Baber & Haghighat 2010, Furihata et al. 2016). Já outros estudos não detectaram a presença destes transportadores (Palos *et al.* 1996, Vanhoutte & Hermans 2008). Estas diferenças podem estar relacionadas ao número de passagens celulares, pelo menos no que diz respeito às células C6. As células negativas para EAAT2 foram observadas em um estudo com C6 de baixas passagens, em oposição às células do nosso estudo, as quais foram subcultivadas pelo menos 100 vezes. Pouco se sabe sobre o processo de

transição da linhagem C6, a qual, ao longo das passagens reduz características tumorais para expressar fatores mais similares a um astrócitos diferenciado. Apesar disso, este processo parece ser fundamental para a sua diferenciação. Foi visto em trabalhos anteriores que a super-expressão de EAAT2 em células C6, reduziu a taxa proliferativa após estímulo com glutamato (Vanhoutte & Hermans 2008), indicando a relação inversa entre a presença de transportador de glutamato com a proliferação celular.

Outra característica importante dos astrócitos é a regulação e manutenção de defesas antioxidantes. Estas células são ricas em GSH, um tripeptídeo composto de glutamato, cisteína e glicina, considerado o principal antioxidante cerebral. Além de se auto-proteger, astrócitos são capazes de suprir neurônios com precursores para a síntese de GSH para defesa contra oxidantes (Dringen & Hamprecht 1996, Dringen *et al.* 2015). Nossos resultados mostraram quantidade similar no conteúdo de GSH nos três modelos de cultura celular. Sabe-se que o glutamato é um precursor da síntese de GSH (Matés *et al.* 2002). Contudo, os nossos dados mostraram que as linhagens celulares captam menos glutamato em comparação com CP. Portanto, pode-se sugerir que o glutamato captado por AI e C6 destina-se mais para a síntese de GSH, comparando proporcionalmente com a CP. Em outras palavras, pode-se supor que o glutamato captado pelas linhagens seria destinado em grande parte à produção de GSH, ao invés da síntese de glutamina (Dringen 2000, McKenna 2007). O destino do glutamato uma vez dentro do astrócito, mostrou-se variado, dependente das concentrações de glutamato extracelular e de outros metabólitos (McKenna 2007). Portanto, esta via pode ser diferentemente regulada em CP e nas linhagens celulares avaliadas. Além disso, não se pode descartar outras fontes internas de glutamato, como o ciclo do ácido tricarboxílico. Ainda, a expressão do sistema antiporter Xc cisteína-glutamato mostrou-se aumentada em gliomas em comparação com astrócitos normais, contribuindo para o crescimento e

expansão celular. Este sistema também pode contribuir para a síntese de GSH, uma vez que promove a entrada de seu substrato cisteína na célula (Bridges *et al.* 2012). Altos níveis de GSH são necessários em células tumorais como uma defesa antioxidante devido ao alto metabolismo oxidativo destas células (Marie & Shinjo 2011). Além do mais, a GSH tem sido relacionada com a proliferação celular, interferindo na atividade da telomerase (Pallardó *et al.* 2009). Portanto, é pertinente pensar que células proliferativas tenham a via de produção de GSH mais ativa.

4.1.4. Comparação do metabolismo energético e comunicação por junção gap em modelos de astrócitos

Os astrócitos são considerados elementos chave no metabolismo da glicose, captando-a pelos pés-terminais em contato com vasos sanguíneos e redistribuindo-a aos neurônios. O GLUT-1 é o principal transportador de glicose em astrócitos (Pellerin 2008). A glicose captada pode ser armazenada na forma de glicogênio e/ou convertida a lactato para exportação aos neurônios (Bouzier-Sore & Pellerin 2013). Em relação à expressão do transportador de glicose, AI e C6 apresentaram baixa quantidade de GLUT-1 quando comparada aos níveis da CP. Porém, a funcionalidade deste transportador, avaliado pela captação de glicose, foi significativamente maior em células C6 do que AI e CP (Fig 4, Capítulo I). De acordo com este resultado, outro trabalho mostrou que células C6 utilizam mais glicose e produzem menos lactato em condições basais quando comparadas com astrócitos normais (Haghighat & McCandless 1997a, Haghighat & McCandless 1997b). Os autores sugerem que a glicose captada pela C6 pode ser destinada a outras vias, como a das pentoses-fosfato para a síntese de nucleotídeos. Se considerarmos esta hipótese, a via das pentoses-fosfato serve também para a produção de NADPH, o qual pode ser utilizado pela glutationa redutase para a manutenção dos níveis de GSH (Dringen et al. 2015). Além disso, sabe-se que o

metabolismo energético é um dos principais processos afetados durante a transição de células normais para as células tumorais, e é um determinante para a manutenção da proliferação celular (Marie & Shinjo 2011). Tendo-se em conta que as células C6 são originadas a partir de um glioma, pode ser facilmente assumido que estas células ainda mantenham algumas características das células tumorais, como por exemplo, a alta taxa de proliferação e o alto consumo de glicose. É interessante notar que, embora os AI tenham uma alta taxa proliferativa, não apresentaram uma maior captação de glicose, assim como as C6. Os astrócitos imortalizados originam-se de um astrócito normal e não de uma célula maligna, o que pode implicar em outras vias metabólicas ativadas distintas de um tumor.

Além disso, o metabolismo da glicose está relacionado à comunicação por junção gap, uma vez que substratos energéticos podem ser transferidos de célula a célula por meio destas estruturas (Rouach et al. 2002). Por outro lado, as junções gap estão também relacionadas às taxas de proliferação celular. As linhagens tumorais são normalmente desprovidas de junção gap, uma vez que moléculas promotoras de tumor as inibem (Budunova & Williams 1994). De fato, células C6 apresentam baixos níveis de comunicação por junção gap, e são normalmente usadas como controle negativo para esse tipo de ensaio (Leite et al. 2009, Tabernero et al. 2006). De acordo com isto, tanto células C6 quanto AI apresentaram baixos níveis de Cx43 em comparação com CP (Fig 5, Capítulo I). Foi visto que um aumento da expressão de conexinas em células C6, através de transfecção, diminui a captação de glicose e a taxa proliferativa destas células, ao mesmo tempo que inibidores de junção gap aumentam a captação de glicose (Tabernero et al. 2006). Assim, os altos níveis de captação de glicose, observados nas células C6, podem também ser explicados pelo baixo nível de junção gap.

4.1.5. Avaliação de resposta nos modelos de cultura de astrócitos

Alguns resultados contraditórios são encontrados na literatura quando diferentes modelos de cultura de astrócitos são submetidos ao mesmo estímulo. Por exemplo, o tratamento com glicose diminui a secreção de S100B em CP, porém aumenta em C6 (Nardin et al. 2007). O tratamento com amônia induz diferente resposta energética em CP e C6 (Haghighat & McCandless 1997b), assim como os baixos níveis de comunicação por junção gap em C6 induzem um aumento na captação de glicose (Tabernero et al. 2006). Ainda, astrócitos imortalizados não responderam ao tratamento com dibutiril AMPc em relação aos níveis de GFAP (Morikawa et al. 2001), assim como não responderam ao tratamento com dopamina em relação aos níveis de NGF em comparação com astrócitos normais (Geller & Dubois-Dalcq 1988). Essas variações dificultam a análise dos dados e questionam a validade dos modelos. É importante salientar que, além da variação biológica de cada tipo celular, resultados contraditórios podem ser devido as diferentes condições de cultivo, como o protocolo de cultivo, composição do meio e o número de subcultivos no caso de linhagens (Lange et al. 2012). Estas variações podem interferir na expressão de genes e variação morfológica (Passaquin et al. 1994). Recentemente foi observado que a composição da matriz extracelular determina a resposta de astrócitos a estímulos mecânicos e inflamatórios (Johnson *et al.* 2015). Neste trabalho, considerando que mantivemos as mesmas condições de cultivo para os três modelos, podemos garantir que os efeitos observados foram decorrentes apenas da variação biológica de cada célula. Os estímulos utilizados já eram conhecidos na literatura por causar alterações funcionais em astrócitos de cultura primária. Em geral, os resultados mostraram que CP e C6 respondem de forma semelhante ao mesmo estímulo, quanto à secreção de S100B, ao metabolismo oxidativo de GSH, à atividade da glutamina sintetase e à captação de glicose (Tabela 1, Capítulo I). Portanto, apesar de apresentarem frequentemente

diferenças na quantidade basal de proteína, as vias ativadas pelo mesmo estímulo parecem ser semelhantes. Em contraste, os AI com a transfecção utilizada nesse estudo mostraram pouca reatividade nos ensaios testados, apenas respondendo para o estímulo relacionado à captação de glicose, indicando não ser um bom modelo para o estudo de características específicas de astrócitos. Recentemente foi demonstrado que astrócitos expressam duas isoformas da p53, as quais tem efeitos opostos sobre a neuroprotecção mediada por astrócitos e a neurodegeneração (Turnquist *et al.* 2016). Deste modo, uma inibição da p53, como ocorre no processo de transfecção e imortalização dos astrócitos, pode afetar a funcionalidade destes genes, mudando portanto, a capacidade de resposta destas células.

4.1.6. Escolha do modelo de cultura de astrócitos

Nesta parte do trabalho, apresentamos uma análise integrativa e comparativa de três modelos de cultura de astrócitos: cultura primária, astrócitos imortais e linhagem C6. Analisamos, em condição basal, não apenas o perfil de expressão proteica de cada modelo celular, mas também a funcionalidade destas proteínas quanto ao metabolismo do glutamato e da glicose e a comunicação celular. Além disso, a variação morfológica ou respostas bioquímicas após a indução do mesmo estímulo também foi avaliado.

A taxa de proliferação é uma das principais diferenças entre CP e as linhagens celulares. Esta variação pode explicar algumas diferenças basais relacionadas ao perfil de expressão proteica. A alta taxa de crescimento das linhagens celulares acarreta em um maior investimento em proteínas proliferativas, ao invés de proteínas relacionadas à diferenciação. Logo, estas células podem apresentar um fenótipo de diferenciação incompleta, o que justificaria os baixos níveis de proteínas marcadoras de astrócitos. De fato, os níveis de qualquer proteína específica dentro da célula são dinâmicos. A expressão de genes pode variar dependendo da densidade celular ou do tempo de

transição do ciclo celular. Por exemplo, espera-se uma diminuição dos genes associados à proliferação e um aumento de genes associados à diferenciação em células confluentes (Frisa & Jacobberger 2002). A redução da taxa de proliferação induzida, por exemplo, pela retirada do soro, pode fazer com que a célula adote um status mais diferenciado. Portanto, é importante manter um padrão de confluência para os estudos em cultivo celular de forma a alcançar a estabilidade da expressão gênica.

Em geral, nossos resultados mostraram que os dois modelos de linhagens celulares (AI e C6) foram positivos para proteínas características de astrócitos, porém com perfil de expressão em quantidade muito menor. Embora AI apresente uma taxa de crescimento mais lenta do que as células C6 e uma morfologia basal mais similar com CP, não se revelou um modelo reprodutível das funções astrocíticas clássicas, uma vez que não respondeu a maioria dos estímulos testados. Em contraste, as células C6, apesar de sua origem tumoral, foram capazes de apresentar características diferenciadas, apresentando resposta similar aos astrócitos de cultura primária quando submetidas ao mesmo estímulo.

Com base nos nossos dados, embora o CP seja uma técnica mais demorada e custosa, o uso como modelo reprodutivo para o estudo de astrócitos é sem dúvida preferencial. A linhagem C6, embora apresente algumas limitações, reproduziu os astrócitos funcionalmente na maioria dos testes. Além disso, o cultivo destas células é um processo metodologicamente mais rápido, de baixo custo e sem o uso de animais. Todas estas questões devem ser consideradas para a escolha de um modelo adequado para o estudo de astrócitos.

No que diz respeito aos dados relacionados à S100B, que é uma das principais proteínas características deste tipo celular, CP e C6 apresentaram níveis basais diferentes, porém quando submetidas ao mesmo estímulo apresentaram resposta

semelhante, reduzindo a secreção da proteína em 24h de estimulo com LPS. Contudo, os níveis reduzidos de proteínas em condições basais apresentados em C6 pode dificultar o estudo, uma vez que o os dados ficam muito próximos ao limite de detecção da técnica, muitas vezes gerando resultados negativos. Por este motivo, para a continuidade do nosso estudo, escolhemos a CP para investigar a capacidade de internalização da proteína S100B e as vias intracelulares de destino.

4.2. Internalização tempo-dependente da S100B extracelular e análise da movimentação de vesículas em cultura de astrócitos

De forma a compreender os mecanismos moleculares que os astrócitos adotam para a manutenção da homeostase cerebral e ainda, para entender os efeitos causados pela S100B extracelular, estudamos o processo de internalização da proteína S100B marcada com fluorescência em CP. Os resultados deste estudo revelaram que os astrócitos captam a S100B extracelular de maneira tempo dependente via endocitose mediada pela ligação ao RAGE. Ao longo do tempo, as vesículas capturadas S100B-Alexa^{488} positivas exibem mobilidade direcional, indicando que as vesículas ficam funcionalmente aderidas ao citoesqueleto (Potokar *et al.* 2007). Além disso, a mobilidade das vesículas S100B-Alexa^{488} positivas parecem ser reguladas pela alteração intracelular de cálcio induzido por ATP, tal como foi determinado previamente para vesículas endolisossomais, peptidérgicas e vesículas secretórias glutamatérgicas em astrócitos (Stenovec *et al.* 2007, Potokar *et al.* 2008, Potokar *et al.* 2010).

4.2.1. Mecanismo de internalização da S100B em cultura de astrócitos

A ligação da proteína S100B com o fluoróforo Alexa permitiu avaliar de forma eficiente a captação extracelular desta proteína em cultura de astrócitos (Fig 1, Capítulo

II). Pela primeira vez, mostrou-se que estas células são capazes de internalizar a proteína S100B de forma efetiva em apenas 15 min de incubação e, que o número de partículas captadas aumenta com o tempo de incubação (Fig. 2, Capítulo II). Além disso, de forma a se entender melhor o mecanismo de endocitose, foi comparado o processo de internalização de S100B-Alexa^{488} com Dextran^{546}, um polissacarídeo comumente usado para determinar mecanismo de endocitose inespecífica (Lim & Gleeson 2011). Esta comparação permitiu verificar que a internalização inicial das duas moléculas ocorria de forma diferente em relação ao tempo e estrutura, porém, acabavam no mesmo compartimento em tempos prolongados, evidenciado pelo alto grau de colocalização observado em 24h de incubação. Inicialmente, a S100B-Alexa^{488} foi captada em uma taxa relativamente mais baixa do que Dextran^{546}, além de apresentar baixo grau de colocalização entre as duas moléculas. Além disso, a estimativa do diâmetro das vesículas em 15 min de incubação mostrou-se diferente. Adicionalmente, o peso molecular destas duas moléculas são diferentes, sendo a S100B homodimérica e funcional no tamanho de 21 kDa, enquanto que o Dextran apresenta a metade do peso com 10 kDa. Todos estes dados nos sugeriram um mecanismo distinto de internalização entre S100B-Alexa^{488} e Dextran^{546}. A formação da via endocítica pode ser constitutiva ou mesmo ser ativada pela ligação a um receptor (González *et al.* 2007). Trabalhos prévios mostraram que a endocitose de dextran ocorre de forma inespecífica por um processo mediado por pinocitose (Commisso *et al.* 2013, Thilo *et al.* 1995). Sabendo-se que a maioria dos efeitos extracelulares da S100B são mediados via RAGE (Donato *et al.* 2013), neste trabalho verificamos se a internalização da S100B ocorreria por um processo mediado por receptor. De fato, a internalização da S100B-Alexa^{488} foi reduzida quase pela metade com a inibição do receptor RAGE, enquanto que a internalização do Dextran^{546} não foi comprometida (Fig. 3, Capítulo II). Portanto, foi

possível verificar que a internalização de S100B é mediada pela ligação ao RAGE, pelo menos em parte. De acordo com isso, os efeitos extracelulares da S100B, tanto tróficos quanto tóxicos, podem ser dependentes da interação com RAGE (Leclerc et al. 2009, Donato et al. 2009, Huttunen et al. 2000). A concentração da proteína no espaço extracelular parece ser um fator importante no desencadeamento desses efeitos (Donato 2007). A endocitose ativada por receptor pode ser mediada tanto por clatrina quanto por caveolina (Mayor & Pagano 2007). Foi visto que o tratamento com S100B em células de Schwann promove a fosforilação e ativação de caveolina-1 seguida da internalização de RAGE (Perrone *et al.* 2008). Estes dados sugerem que a S100B também pode ser internalizada por uma forma de endocitose dependente de caveolina-1, contudo, isso implicaria em maiores investigações. No nosso trabalho, mostramos que tanto a internalização de S100B-Alexa^{488} quanto de Dextran^{546} são dependentes de dinamina, uma proteína que está envolvida no processo de endocitose mediado tanto por caveolina, quanto por clatrina e sua atuação é essencial para a cisão da vesícula com a membrana plasmática (Mayor & Pagano 2007).

4.2.2. Caracterização das vesículas S100B-Alexa^{488} positivas

Uma vez endocitada, a S100B pode ter vários destinos intracelulares. Neste trabalho mostramos que a S100B-Alexa^{488} está presente em vesículas do compartimento endocítico, as quais participam no transporte intracelular de moléculas e degradação (Fig 4, Capítulo II). A presença da S100B endógena em compartimentos vesiculares já tinha sido sugerida por trabalhos prévios (Davey et al. 2001, Perrone et al. 2008), porém a caracterização destas vesículas tinha sido pouco estudada. Os nossos dados mostraram que a S100B-Alexa^{488} internalizada colocaliza fortemente com Dextran^{546} após a incubação prolongada (51% após 3 h). Por sua vez, em outros trabalhos foi observado

que Dextran^{546} colocaliza fortemente com marcadores de endossomos tardios - LAMP1 e proteínas Rab7 - representando vesículas terminais do compartimento endolisossomal (Humphries *et al.* 2011, Vardjan *et al.* 2012). Da mesma forma que o Dextran, as vesículas S100B-Alexa^{488} positivas colocalizaram fortemente com LysoTracker (56%), marcador de compartimentos ácidos, o qual também verificou-se que colocaliza com EEA1 e LAMP1, marcadores de endossomos recentes e tardio, respectivamente (Potokar et al. 2010). Além disso, uma porção das vesículas marcadas para S100B, colocalizaram com EAA1 (9%) e LAMP1 (10%). É importante salientar que a via endolisossomal consiste em subpopulações distintas de vesículas, caracterizadas por diferentes proteínas de membrana, podendo apresentar vesículas positivas apenas para Rab7 ou apenas para LAMP1, ou ainda positivas para ambos LAMP1/Rab7. Por sua vez, cada uma destas vesículas apresentam diferentes dinâmicas intracelulares (Humphries et al. 2011, Szymanski *et al.* 2011). Da mesma forma, em células epiteliais humanas foram encontradas duas sub-populações de vesículas endocíticas de reciclagem: uma positiva para Rab11 e transferrina; e outra positiva para Rab11 e *Neisseria meningitidis adhesin A* (proteína de bactéria). Estas duas subpopulações tiveram comportamentos diferentes em relação ao mesmo tratamento (Bozza *et al.* 2014). No nosso trabalho mostramos que a maior parte das vesículas S100B-Alexa^{488} colocalizam com Dextran^{546} e Lisotracker, e menos com os marcadores EEA1 e LAMP1. A baixa colocalização com LAMP1 é intrigante, uma vez que foi visto que tanto Dextran quanto lysotracker colocalizam fortemente com LAMP1 (Potokar et al. 2010, Vardjan et al. 2012). No entanto, isto pode ser explicado pela forma usada para estimar a colocalização. Ou seja, a forma que foi expressa, a colocalização mostra que apenas uma pequena fração de vesículas LAMP1 internalizam S100B, porém não que a maioria da S100B não se localiza em vesículas positivas para LAMP1. De fato, se a

S100B fosse usada como o sinal de referência, a colocalização entre S100B e LAMP1 aumentaria para 39,35 ± 1,54% (n=72) em 1h de incubação, e ainda mais, 78,65 ± 1,26% (n = 82) em 24 h de incubação (resultados não mostrados). Estas análises indicaram, que na verdade, a maior parte das vesículas positivas para S100B continham LAMP1. Além disso, é importante se levar em conta que a composição molecular das vesículas endocíticas é dinâmica e deve variar cada vez que uma vesícula se fusiona uma com outra (Gould & Lippincott-Schwartz 2009, Scott et al. 2014). Portanto, é esperado que a colocalização das vesículas positivas para S100B com marcadores endocíticos não permaneça constante ao longo do tempo, como evidenciado na Fig 2A e C do Capítulo II dos nossos resultados.

4.2.3. A mobilidade das vesículas S100B-Alexa^{488} é alterada pelo estímulo com ATP

A avaliação da mobilidade das vesículas S100B-Alexa^{488} mostrou um aumento de direcionalidade ao longo do tempo de incubação (Fig. 5, Capítulo II). Esta análise é realizada através da avaliação do deslocamento máximo da vesícula e o comprimento total percorrido (Potokar *et al.* 2005). Com estas informações é possível avaliar a direcionalidade da vesícula dividindo-se o deslocamento máximo pelo comprimento total percorrido. Um aumento de direcionalidade da vesícula também foi observado em vesículas positivas para vírus transmitido por carrapato em astrócitos (Potokar *et al.* 2014). Este aumento na mobilidade pode ser explicado pelo progressivo acoplamento das vesículas ao citoesqueleto, o qual geralmente serve como suporte para o tráfego de vesículas (Potokar et al. 2007, Potokar et al. 2010, Vardjan et al. 2012, Potokar *et al.* 2013). No entanto, a mobilidade da vesícula S100B-Alexa^{488} foi reduzida com o tratamento de ATP, o qual aumenta as concentrações citosólicas de cálcio (Fig. 6,

Capítulo II). Esta resposta é característica de vesículas endossomais de astrócito, uma vez que o mesmo efeito foi observado em vesículas marcadas com Lysotracker (Potokar et al. 2010) e Dextran (Vardjan et al. 2012). De fato, um aumento transitório de cálcio pode afetar a integridade do citoesqueleto, principalmente de microtúbulos e/ou actina, onde encontram-se proteínas motoras que impulsionam as vesículas (Soldati & Schliwa 2006). Da mesma forma, um aumento prolongado das concentrações de cálcio foi capaz de induzir o desacoplamento parcial de microtúbulos em astrócitos (Stenovec *et al.* 2014). Apesar disso, foi verificado que o desacoplamento de microtúbulos ocorre em concentrações de cálcio bem maiores (1-4 µM) (Schliwa *et al.* 1981) do que o estimulo induzido por ATP (100 µM) é capaz de causar (780 ±120nM) (Salter & Hicks 1994). Portanto, é mais provável que outro mecanismo esteja envolvido na redução de mobilização destas vesículas. Ainda, foi observado que os endossomos marcados com Lisotracker apresentam uma redução mais acentuada na direcionalidade quando comparadas com vesículas peptidérgicas estimuladas com ATP (Stenovec *et al.* 2016). Portanto, é possível que alguns tipos de vesículas se desconectem mais facilmente do citoesqueleto devido a uma diferença de composição de proteínas na membrana e interação com o citoesqueleto.

Em relação ao significado da redução da mobilidade da vesícula após estímulo são geradas algumas hipóteses. Nos astrócitos são encontrados vários tipos de vesículas além das endossomais, incluindo vesículas de aminoácidos (Ex. glutamatérgicas), vesículas peptidérgicas (Ex. ANP- peptídeo natriurético atrial), e vesículas nucleotídicas (ex. ATP). Além das diferenças em conteúdo, estas vesículas apresentam tamanhos e dinâmicas diferentes (Guček *et al.* 2012). Sabe-se, por exemplo, que vesículas endossomais e peptidérgicas apresentam uma natureza mais lenta quando comparadas a vesículas glutamatérgicas. As vesículas de glutamato aumentam sua mobilidade com

um estímulo de cálcio, aumentando a fusão com a membrana plasmática e a liberação de glutamato. Já as vesículas endossomais, como é o caso das vesículas S100B positivas, podem apresentar a característica chamada “kiss and run” (beijar e fugir), onde um comprometimento da mobilidade em função da variação de cálcio, poderia aumentar o tempo de fusão com a membrana plasmática, de forma a liberar mais carga intravesicular (Parpura *et al.* 2010, Parpura & Zorec 2010). Interessantemente, o estímulo com AMPc ou cálcio aumenta a secreção endógena de S100B em glioblastomas e esta secreção tem sido sugerida ser na forma de vesículas (Davey et al. 2001, Mbele et al. 2002). Além disso, foi visto que a inibição da proteína cinase src, envolvida no processo de endocitose, diminui a secreção de S100B em células de Schwann, o que poderia indicar que uma inibição da internalização da S100B também induziria uma inibição de sua secreção (Perrone et al. 2008). Contudo, mais estudos seriam necessários para verificar este processo com vesículas de S100B internalizadas.

4.2.4. Regulação da S100B por endocitose

Nesta parte do trabalho mostramos que astrócitos em cultura são capazes de internalizar a S100B extracelular por um mecanismos de endocitose dependente de RAGE e dinamina. Uma vez internalizada a S100B segue pela via endocitica, colocalizando com importantes marcadores desta via, como Dextran e Lysotracker. Avaliamos também neste trabalho o tráfego intracelular destas vesículas, mostrando um aumento de direcionalidade ao longo do tempo de incubação, o qual é afetado pelo estímulo com ATP que aumenta as concentrações de cálcio intracelular. Estes dados auxiliam na compreensão do mecanismo de sinalização extracelular da proteína S100B, assim como o papel dos astrócitos nesta regulação.

Sabe-se que a S100B apresenta efeitos contrastantes no espaço extracelular, dependente da sua concentração local. Foi visto que em concentrações nanomolares a

S100B induz crescimento de neuritos e sobrevivência neuronal em resposta a um estímulo tóxico, através da ativação de NFκB (Van Eldik & Wainwright 2003, Villarreal *et al.* 2011). No entanto, em concentrações micromolares, pode induzir efeitos tóxicos como apoptose (Hu *et al.* 1997) e um aumento de EROs por uma via dependente de MEK/ERK1/2 (Businaro et al. 2006). Particularmente em astrócitos, a S100B em baixas concentrações induz proliferação e migração em áreas agredidas (Villarreal et al. 2014, Selinfreund et al. 1991), além de prevenir alterações morfológicas e aumento de iNOS induzido por neurotoxina, via NFκB (Reali et al. 2005). Já em altas concentrações, a S100B induz a liberação de óxido nítrico e citocinas inflamatórias, através ativação da via NFκB em astrócitos (Lam et al. 2001, Hu & Van Eldik 1999, Ponath et al. 2007). A maioria dos efeitos, tanto tróficos quanto tóxicos parecem ser mediados pela ligação ao RAGE. Neste trabalho usamos 1 μM de S100B, o que é considerado uma concentração alta, podendo gerar, portanto, efeitos tóxicos. Contudo, mais estudos seriam necessários para a avaliação destes parâmetros.

In vivo, o aumento das concentrações extracelulares de S100B está associado a efeitos tóxicos, como por exemplo, após um dano traumático cerebral ou em algumas doenças neurodegenerativas como doença de Alzheimer e esquizofrenia (Rothermundt et al. 2003, Steiner et al. 2011). Portanto, a capacidade dos astrócitos de capturar o excesso de S100B extracelular pode ser interpretada como uma tentativa de recuperação do ambiente extracelular reduzindo os efeitos tóxicos da proteína, melhorando as funções do SNC. Além disso, o sistema glinfático deve auxiliar na passagem desta proteína do LCR para o soro e, qualquer comprometimento desta via poderia aumentar o papel dos astrócitos nesta função de regulação da sinalização extracelular de S100B (Plog *et al.* 2015).

Esta atividade regulatória dos astrócitos pode estar representada em alguns trabalhos, os quais mostram que ocorre um pico nos níveis de S100B no LCR após lesão cerebral traumática ou uma resposta inflamatória, seguido por uma redução subsequente nos níveis desta proteína (Berger et al. 2002, Guerra et al. 2011, Kruse *et al.* 1991). Ainda, trabalhos *in vitro* também mostram um efeito semelhante ao observado em cultura de astrócitos: citocina inflamatória (de Souza *et al.* 2013) e fluoxetina (Tramontina et al. 2008) induzem uma elevação aguda nos níveis extracelulares de S100B que são reduzidos em períodos mais longos. Esta redução dos níveis extracelulares de S100B pode ser devido a uma diminuição da secreção desta proteína por astrócitos, ou mesmo um aumento da captação de S100B por estas células. A internalização da proteína pode representar não só uma forma de recuperar a composição molecular do ambiente extracelular, mas também uma forma de sinalização e comunicação intercelular. Considerando que as concentrações extracelulares de S100B são determinantes para seu efeito trófico ou tóxico, os astrócitos devem ter a importante função da regulação fina das concentrações extracelulares desta proteína, regulando a resposta inflamatória ou trófica (Sofroniew 2015). Neste trabalho mostramos que a internalização é, em parte, dependente de RAGE, o qual medeia tanto respostas tróficas quanto tóxicas (Villarreal et al. 2014). Não se pode descartar que outras células, além dos astrócitos, podem estar envolvidas na remoção extracelular de S100B, como, por exemplo, a micróglia, a qual também expressa RAGE (Yan *et al.* 1996) e é capaz de endocitar debris extracelulares via pinocitose (Neumann *et al.* 2009), macropinocitose (Mandrekar *et al.* 2009), assim como endocitose mediada por receptor (Lee *et al.* 2008).

Portanto, a internalização da S100B pelos astrócitos pode representar uma tentativa de reduzir as concentrações extracelulares da proteína de forma a evitar alguns efeitos

tóxicos, minimizando o dano em células vizinhas. Assim como, a internalização pode representar uma forma de sinalização, onde os astrócitos captam S100B via RAGE, de forma a induzir sinais intracelulares e mediar tanto respostas tóxicas, quanto tróficas.

4.3. Padronização de ensaio colorimétrico para dosagem de atividade da GS

Além da proteína S100B, outra proteína importante para a caracterização de astrócitos é a GS. Nesta parte de nosso estudo, padronizamos um ensaio colorimétrico que mede a atividade glutamil-transferase da GS em cultura de células e em diferentes tecidos cerebrais. O estabelecimento de uma técnica confiável para a dosagem da atividade da GS é essencial para verificar disfunções que podem ocorrer no ciclo glutamina-glutamato e outras vias importantes das quais esta enzima participa no cérebro.

Neste trabalho, conseguimos mostrar um ensaio sensível, detectando baixas concentrações de produto (0,156 mM) e alta linearidade com R = 0,99 (Fig. 1, Capítulo III). Além disso, a técnica foi precisa, mostrando um coeficiente de variância intra-ensaio e inter-ensaio inferior a 10%, o que é adequado para ensaios enzimáticos (Lukacs *et al.* 2011, Daitx *et al.* 2015). A atividade transferase da GS foi linear com relação a quantidade de proteína (entre 18,4 - 55,2 μg em cultura celular e 7,6 - 121,1 μg em fatias de hipocampo), bem como ao tempo de incubação (5 a 30 min para ambas as amostras).

Além disso, o ensaio se mostrou com alta aplicabilidade, medindo a atividade da GS em diferentes estruturas cerebrais, assim como em cultura de astrócitos e na linhagem celular de glioma C6 (Fig. 3, Capítulo III). O ensaio foi altamente sensível, detectando a atividade da GS mesmo em células com pouca quantidade da enzima, como na linhagem C6. A enzima GS tem grande participação na detoxificação da amônia cerebral. Estudos prévios mostram que a amônia é metabolizada diferentemente

dependendo da região cerebral (Kosenko *et al.* 2014a, Kosenko *et al.* 2014b), provavelmente devido a diferenças no conteúdo ou atividade de GS nestas regiões (Patel *et al.* 1985). De fato, neste estudo, o cerebelo apresentou maior atividade basal de GS quando comparado com outras regiões analisadas. Corroborando com isso, Cao Danh e Coauthor (1985) também obtiveram elevada atividade de GS no cerebelo de ratos comparados com áreas cerebrais semelhantes (Cao Danh *et al.* 1985).

A atividade da GS foi comprometida pela incubação com MSO ou peróxido, devido à ligação específica do inibidor ou oxidação da enzima, respectivamente, e não devido alteração no seu conteúdo como mostrado por imunobloting (Fig 5, Capítulo III). Estes resultados não apenas demonstram a especificidade do ensaio, mas também salientam a importância de se medir a atividade da enzima, e não somente o seu conteúdo. Como no nosso exemplo, um dano oxidativo pode comprometer a atividade da enzima sem afetar o seu conteúdo. Portanto, a dosagem apenas da expressão da enzima pode refletir de forma errônea a atividade desta.

Sabe-se que a atividade enzimática é altamente dependente da estrutura da enzima e, portanto, qualquer mudança de conformação pode interferir na sua atividade. De fato, o processo de congelamento e descongelamento pode alterar a conformação da enzima e reduzir a sua atividade. Os nossos dados demonstraram que a atividade de GS foi estável após congelamento, tanto em homogeneizados de cultura celular quanto em fatias cerebrais congeladas a seco. A enzima mostrou-se estável por uma semana, congeladas tanto a -20 ° C ou -80 ° C. A adição de inibidor de protease (PMSF, EGTA e EDTA) foi essencial para a preservação da atividade em homogeneizados de amostras de cultura. Sem a adição destes inibidores, estas amostras não foram estáveis nem durante 24 h congeladas (dados não apresentados). A análise da estabilidade da enzima

é extremante importante para que o pesquisador tenha maior confiabilidade nos seus resultados. Além disso, flexibiliza o tempo de dosagem após experimento.

4.3.1. Vantagens do ensaio

A atividade transferase da GS, apesar de comumente usada, foi pouco padronizada para estruturas cerebrais. De fato, apenas um trabalho na literatura relata a padronização do ensaio de GS para medir a atividade transferase, porém, além de ser uma padronização mais simples, apresentou diferenças na composição dos substratos e usou-se cromotografia para a identificação do produto (Seiler et al. 1990). Neste trabalho caracterizamos um ensaio colorimétrico que mede com precisão, sensibilidade e linearidade a atividade transferase da GS em diferentes estruturas cerebrais, assim como em cultura de astrócitos e linhagem C6, evidenciando a sua alta aplicabilidade. Além disso, esta técnica mostrou ser específica para GS, uma vez que o MSO, seu inibidor específico, reduziu a sua atividade, mas não a quantidade de enzima. A avaliação da atividade enzimática após congelamento mostrou que é a GS é estável quando mantida a seco ou em solução de lise na presença de inibidores de protease por até uma semana. Ainda, este ensaio tem a vantagem de apresentar menos interferentes do que a reação sintetase. A técnica apresenta baixo custo e é metodologicamente mais segura quando comparado com o ensaio radioativo. A literatura demonstra que a GS está envolvida na patogênese de vários distúrbios neurológicos, tais como HE e DA, e as alterações na atividade desta enzima são um marcador útil para a funcionalidade astroglial em lesões cerebrais agudas e distúrbios neurodegenerativos. A padronização do ensaio da GS em estruturas cerebrais favorece sua ampla utilização na área de pesquisa, proporcionando um bom método para estudo da enzima tanto em situações fisiológicas quanto em situações patológicas.

5. Conclusões

De forma geral apresentamos uma análise integrativa e comparativa de três modelos de cultura celular de astrócitos: cultura primária, astrócitos imortais e linhagem C6. Estes modelos têm sido estudados de forma a se entender a fisiologia dos astrócitos e o comportamento destas células frente a diversos estímulos. De acordo com os nossos dados, e como era esperado, o modelo mais adequado para o estudo de astrócitos sem dúvida foi representado pela cultura primária de astrócitos. Esta é a forma de estudo mais clássica da literatura, com a vantagem principal de ser originada do próprio córtex cerebral de um rato. Estas células são fisiologicamente mais similares a um astrócito que seria encontrado *in vivo,* assim como foi evidenciado recentemente pela análise de expressão de genes (Hertz *et al.* 2017). É evidente que o processo de cultivo por si só já é um fator limitante e de estresse, fazendo com que a célula adote um status mais reativo, aumentando a expressão de algumas proteínas tais como a GFAP. Além disso, as células de cultura primária apresentam alto grau de variabilidade, uma vez que descendem de um sistema *in vivo* altamente heterogêneo. É importante se ter em consideração que os astrócitos tratados em cultivo representam as células mais resistentes, as quais sobreviveram a todo o processo de cultivo. Portanto, são células de certa forma selecionadas, não representando todo o grau de variabilidade de um sistema *in vivo*. Apesar disso, a proximidade destas células com o sistema *in vivo* é evidente quando se mostra que astrócitos cultivados de diferentes regiões cerebrais ou mesmo de diferentes animais apresentam expressão de proteínas diferenciadas e complexidade diferente, assim como encontrado no organismo vivo (Pinto *et al.* 2000, Zhang *et al.* 2016). De fato, no nosso estudo, a cultura primária foi o modelo que apresentou características mais acentuadas de um astrócito, respondendo facilmente a estímulos morfológicos e bioquímicos.

Os outros dois modelos de astrócitos são apresentados na literatura como uma alternativa para o estudo de astrócitos, apresentando a principal vantagem de serem células mais homogêneas e com alto poder reprodutivo, o que torna o processo mais fácil, rápido e dinâmico uma vez que as células podem ser facilmente congeladas e descongeladas. Apesar de comumente usadas, os trabalhos na literatura que mostram as propriedades destas células são esparsos, com análise de características isoladas, e frequentemente não comparadas a um astrócitos comum. Nas análises comparativas deste estudo foi possível perceber que tanto em astrócitos imortais quanto em C6 foram detectadas proteínas características de astrócitos, porém nem sempre a funcionalidade destas células respondeu de forma similar a um astrócitos. Na nossa análise, os astrócitos imortalizados não se mostraram um bom modelo para reproduzir as funções astrocíticas estudadas, porém a linhagem C6, subcultivada pelo menos 100 vezes, mostrou padrão de resposta similar a um astrócitos de cultura primária, podendo representar uma alternativa viável para o estudo destas células. A linhagem C6 pode sempre ser usada como um modelo de estudo inicial, detectando-se, de uma forma mais rápida, algumas características onde os astrócitos estariam envolvidos, de modo que possa ser analisado de uma forma mais aprofundada em um estudo posterior em astrócitos de cultura primária.

Considerando os astrócitos de cultura primária como um bom modelo para o estudo das propriedades astrocíticas, neste trabalho também avaliamos o envolvimento destas células na manutenção do ambiente extracelular, principalmente no que diz respeito às concentrações extracelulares da proteína S100B. Pela primeira vez foi mostrado que astrócitos são capazes de captar a S100B extracelular, podendo representar um mecanismo de controle da sinalização extracelular desta proteína.

Considerando-se que os níveis extracelulares são determinantes para a sua ação trófica ou toxica, é importante que suas concentrações sejam finamente reguladas. A S100B foi captada pelos astrócitos de modo RAGE dependente, podendo representar também uma forma de sinalização, ativando vias intracelulares, como a da NFκB, as quais podem estimular a liberação de citocinas como foi demonstrado para IL-1β, IL-6 e TNFα (Donato et al. 2009). Além disso, as vesículas positivas para S100B foram caracterizadas, estando presentes em vesículas do sistema endolisossomal o qual tem um importante papel no tráfico de proteínas e posterior degradação. Variações de cálcio intracelulares inibiram a mobilidade destas vesículas, o que poderia implicar em mais tempo de fusão destas vesículas com a membrana plasmática para a liberação do conteúdo interno. Porém, para a confirmação desta hipótese mais estudos seriam necessários.

Finalmente, um ensaio colorimétrico para a dosagem da atividade da GS foi padronizado. Esta enzima é altamente expressa em astrócitos e sua atividade é essencial para diversas funções cerebrais, como a manutenção do ciclo glutamina-glutamato. Portanto, a padronização de uma técnica sensível, precisa e específica para esta enzima é essencial para avaliar sua atividade em diferentes condições experimentais. Além disso, o ensaio mostrou-se versátil, na medida em que foi aplicável tanto em cultura celular (cultura primária de astrócitos e C6) quanto em diferentes estruturas cerebrais. A atividade glutamil-transferase mostrou ser específica para GS, uma vez que o inibidor para esta enzima, MSO, reduziu drasticamente sua atividade. Testes de congelamento mostraram preservação da atividade da enzima, sob determinadas condições de armazenamento, garantindo uma maior flexibilidade para dosagem após experimento.

Por fim, nesta tese demonstramos a importância da escolha de um modelo *in vitro* de cultura de células para o estudo de astrócitos. Destacamos as diferenças moleculares

e funcionais entre cada tipo celular e suas limitações. Com este estudo inicial foi possível escolher o modelo mais adequado para o estudo dos efeitos extracelulares da proteína S100B. Demostramos que astrócitos de cultura primária são capazes de captar a S100B extracelular, podendo representar uma forma de prevenção dos efeitos tóxicos desta proteína sobre células neuronais. Estes dados podem ser usados para o estudo de estratégias terapêuticas no controle dos efeitos tóxicos induzidos pela S100B em doenças neurodegenerativas. Além disso, destacamos o papel dos astrócitos no metabolismo cerebral e controle da homeostase extracelular.

6. Perspectivas

- Realizar uma curva de concentração da S100B-Alexa^{488} exógena e avaliar o mecanismo de internalização e dependência com RAGE;

- Avaliação da captação de S100B-Alexa^{488} por outros tipos celulares;

- Estudar as vias intracelulares ativadas no tratamento com S100B-Alexa^{488};

- Avaliar mecanismos de secreção da S100B-Alexa^{488} para o espaço extracelular realizando estímulos com cálcio e com inibidores de endocitose e exocitose;

- Comparação entre secreção de S100B-Alexa^{488} internalizada com S100B endógena;

7. Referências Bibliográficas

Adami, C., Bianchi, R., Pula, G. and Donato, R. (2004) S100B-stimulated NO production by BV-2 microglia is independent of RAGE transducing activity but dependent on RAGE extracellular domain. *Biochim Biophys Acta,* **1742,** 169-177.

Ahuja, D., Sáenz-Robles, M. T. and Pipas, J. M. (2005) SV40 large T antigen targets multiple cellular pathways to elicit cellular transformation. *Oncogene,* **24,** 7729-7745.

Baber, Z. and Haghighat, N. (2010) Glutamine synthetase gene expression and glutamate transporters in C6-glioma cells. *Metab Brain Dis,* **25,** 413-418.

Basso, M. and Bonetto, V. (2016) Extracellular Vesicles and a Novel Form of Communication in the Brain. *Front Neurosci,* **10,** 127.

Beenhakker, M. P. and Huguenard, J. R. (2010) Astrocytes as gatekeepers of GABAB receptor function. *J Neurosci,* **30,** 15262-15276.

Benarroch, E. E. (2010) Glutamate transporters: diversity, function, and involvement in neurologic disease. *Neurology,* **74,** 259-264.

Benda, P., Lightbody, J., Sato, G., Levine, L. and Sweet, W. (1968) Differentiated rat glial cell strain in tissue culture. *Science,* **161,** 370-371.

Bennett, M. V., Contreras, J. E., Bukauskas, F. F. and Sáez, J. C. (2003) New roles for astrocytes: gap junction hemichannels have something to communicate. *Trends Neurosci,* **26,** 610-617.

Berger, R. P., Pierce, M. C., Wisniewski, S. R., Adelson, P. D., Clark, R. S., Ruppel, R. A. and Kochanek, P. M. (2002) Neuron-specific enolase and S100B in

cerebrospinal fluid after severe traumatic brain injury in infants and children. *Pediatrics,* **109,** E31.

Bernardi, C., Tramontina, A. C., Nardin, P. et al. (2013) Treadmill exercise induces hippocampal astroglial alterations in rats. *Neural Plast,* **2013,** 709732.

Bernstein, H. G., Bannier, J., Meyer-Lotz, G., Steiner, J., Keilhoff, G., Dobrowolny, H., Walter, M. and Bogerts, B. (2014) Distribution of immunoreactive glutamine synthetase in the adult human and mouse brain. Qualitative and quantitative observations with special emphasis on extra-astroglial protein localization. *J Chem Neuroanat,* **61-62,** 33-50.

Bezzi, P. and Volterra, A. (2001) A neuron-glia signalling network in the active brain. *Curr Opin Neurobiol,* **11,** 387-394.

Boksha, I. S., Tereshkina, E. B. and Burbaeva, G. S. (2000) Glutamine synthetase and glutamine synthetase-like protein from human brain: purification and comparative characterization. *J Neurochem,* **75,** 2574-2582.

Böttcher, T., Goiny, M., Bering, J., Domhof, S., Nau, R. and Ungerstedt, U. (2003) Regional differences in glutamine synthetase inhibition by L-methionine sulfoximine: a microdialysis study in the rabbit brain. *Exp Brain Res,* **150,** 194-200.

Bouzier-Sore, A. K. and Pellerin, L. (2013) Unraveling the complex metabolic nature of astrocytes. *Front Cell Neurosci,* **7,** 179.

Bozza, G., Capitani, M., Montanari, P. et al. (2014) Role of ARF6, Rab11 and external Hsp90 in the trafficking and recycling of recombinant-soluble Neisseria meningitidis adhesin A (rNadA) in human epithelial cells. *PLoS One,* **9,** e110047.

Bridges, R. J., Natale, N. R. and Patel, S. A. (2012) System xc⁻ cystine/glutamate antiporter: an update on molecular pharmacology and roles within the CNS. *Br J Pharmacol,* **165,** 20-34.

Brown, A. M. and Ransom, B. R. (2015) Astrocyte glycogen as an emergency fuel under conditions of glucose deprivation or intense neural activity. *Metab Brain Dis,* **30,** 233-239.

Brozzi, F., Arcuri, C., Giambanco, I. and Donato, R. (2009) S100B Protein Regulates Astrocyte Shape and Migration via Interaction with Src Kinase: IMPLICATIONS FOR ASTROCYTE DEVELOPMENT, ACTIVATION, AND TUMOR GROWTH. *J Biol Chem,* **284,** 8797-8811.

Budunova, I. V. and Williams, G. M. (1994) Cell culture assays for chemicals with tumor-promoting or tumor-inhibiting activity based on the modulation of intercellular communication. *Cell Biol Toxicol,* **10,** 71-116.

Businaro, R., Leone, S., Fabrizi, C., Sorci, G., Donato, R., Lauro, G. M. and Fumagalli, L. (2006) S100B protects LAN-5 neuroblastoma cells against Abeta amyloid-induced neurotoxicity via RAGE engagement at low doses but increases Abeta amyloid neurotoxicity at high doses. *J Neurosci Res,* **83,** 897-906.

Butterworth, R. F. (2014) Pathophysiology of brain dysfunction in hyperammonemic syndromes: The many faces of glutamine. *Mol Genet Metab,* **113,** 113-117.

Cahoy, J. D., Emery, B., Kaushal, A. et al. (2008) A transcriptome database for astrocytes, neurons, and oligodendrocytes: a new resource for understanding brain development and function. *J Neurosci,* **28,** 264-278.

Cao Danh, H., Strolin Benedetti, M. and Dostert, P. (1985) Age-related changes in glutamine synthetase activity of rat brain, liver and heart. *Gerontology,* **31,** 95-100.

Chan, K., Busque, S. M., Sailer, M., Stoeger, C., Bröer, S., Daniel, H., Rubio-Aliaga, I. and Wagner, C. A. (2016) Loss of function mutation of the Slc38a3 glutamine transporter reveals its critical role for amino acid metabolism in the liver, brain, and kidney. *Pflugers Arch,* **468,** 213-227.

Christopherson, K. S., Ullian, E. M., Stokes, C. C. et al. (2005) Thrombospondins are astrocyte-secreted proteins that promote CNS synaptogenesis. *Cell,* **120,** 421-433.

Cirillo, C., Capoccia, E., Iuvone, T., Cuomo, R., Sarnelli, G., Steardo, L. and Esposito, G. (2015) S100B Inhibitor Pentamidine Attenuates Reactive Gliosis and Reduces Neuronal Loss in a Mouse Model of Alzheimer's Disease. *Biomed Res Int,* **2015,** 508342.

Coco, S., Calegari, F., Pravettoni, E., Pozzi, D., Taverna, E., Rosa, P., Matteoli, M. and Verderio, C. (2003) Storage and release of ATP from astrocytes in culture. *J Biol Chem,* **278,** 1354-1362.

Commisso, C., Davidson, S. M., Soydaner-Azeloglu, R. G. et al. (2013) Macropinocytosis of protein is an amino acid supply route in Ras-transformed cells. *Nature,* **497,** 633-637.

Conner, S. D. and Schmid, S. L. (2003) Regulated portals of entry into the cell. *Nature,* **422,** 37-44.

Cooper, A. J. (2012) The role of glutamine synthetase and glutamate dehydrogenase in cerebral ammonia homeostasis. *Neurochem Res,* **37,** 2439-2455.

Daitx, V. V., Mezzalira, J., Moraes, V. a. C., Breier, A. C., Cé, J. and Coelho, J. C. (2015) Comparing the alpha-galactosidase A biochemical properties from healthy individuals and Fabry disease patients. *Clin Chim Acta,* **445,** 60-64.

Davey, G. E., Murmann, P. and Heizmann, C. W. (2001) Intracellular Ca2+ and Zn2+ levels regulate the alternative cell density-dependent secretion of S100B in human glioblastoma cells. *J Biol Chem,* **276,** 30819-30826.

De Pittà, M., Brunel, N. and Volterra, A. (2016) Astrocytes: Orchestrating synaptic plasticity? *Neuroscience,* **323,** 43-61.

de Souza, D. F., Leite, M. C., Quincozes-Santos, A., Nardin, P., Tortorelli, L. S., Rigo, M. M., Gottfried, C., Leal, R. B. and Gonçalves, C. A. (2009) S100B secretion is stimulated by IL-1beta in glial cultures and hippocampal slices of rats: Likely involvement of MAPK pathway. *J Neuroimmunol,* **206,** 52-57.

de Souza, D. F., Wartchow, K., Hansen, F., Lunardi, P., Guerra, M. C., Nardin, P. and Gonçalves, C. A. (2013) Interleukin-6-induced S100B secretion is inhibited by haloperidol and risperidone. *Prog Neuropsychopharmacol Biol Psychiatry,* **43,** 14-22.

Deitmer, J. W. and Rose, C. R. (2010) Ion changes and signalling in perisynaptic glia. *Brain Res Rev,* **63,** 113-129.

Dennis, S. C., Lai, J. C. and Clark, J. B. (1980) The distribution of glutamine synthetase in subcellular fractions of rat brain. *Brain Res,* **197,** 469-475.

Donato, R. (2001) S100: a multigenic family of calcium-modulated proteins of the EF-hand type with intracellular and extracellular functional roles. *Int J Biochem Cell Biol,* **33,** 637-668.

Donato, R. (2003) Intracellular and extracellular roles of S100 proteins. *Microsc Res Tech,* **60,** 540-551.

Donato, R. (2007) RAGE: a single receptor for several ligands and different cellular responses: the case of certain S100 proteins. *Curr Mol Med,* **7,** 711-724.

Donato, R., Cannon, B. R., Sorci, G., Riuzzi, F., Hsu, K., Weber, D. J. and Geczy, C. L. (2013) Functions of S100 proteins. *Curr Mol Med,* **13,** 24-57.

Donato, R. and Heizmann, C. W. (2010) S100B Protein in the Nervous System and Cardiovascular Apparatus in Normal and Pathological Conditions. *Cardiovasc Psychiatry Neurol,* **2010,** 929712.

Donato, R., Sorci, G., Riuzzi, F., Arcuri, C., Bianchi, R., Brozzi, F., Tubaro, C. and Giambanco, I. (2009) S100B's double life: intracellular regulator and extracellular signal. *Biochim Biophys Acta,* **1793,** 1008-1022.

Dringen, R. (2000) Metabolism and functions of glutathione in brain. *Prog Neurobiol,* **62,** 649-671.

Dringen, R., Brandmann, M., Hohnholt, M. C. and Blumrich, E. M. (2015) Glutathione-Dependent Detoxification Processes in Astrocytes. *Neurochem Res,* **40,** 2570-2582.

Dringen, R. and Hamprecht, B. (1996) Glutathione content as an indicator for the presence of metabolic pathways of amino acids in astroglial cultures. *J Neurochem,* **67,** 1375-1382.

Edwards, M. M. and Robinson, S. R. (2006) TNF alpha affects the expression of GFAP and S100B: implications for Alzheimer's disease. *J Neural Transm,* **113,** 1709-1715.

Ehrenfeld, E., Marble, S. J. and Meister, A. (1963) ENZYMATIC SYNTHESIS OF GAMMA-GLUTAMYLHYDROXAMIC ACID FROM GLUTAMIC ACID AND HYDROXYLAMINE. *J Biol Chem,* **238,** 3711-3716.

El-Sayed, A. and Harashima, H. (2013) Endocytosis of gene delivery vectors: from clathrin-dependent to lipid raft-mediated endocytosis. *Mol Ther,* **21,** 1118-1130.

Eng, L. F. (1985) Glial fibrillary acidic protein (GFAP): the major protein of glial intermediate filaments in differentiated astrocytes. *J Neuroimmunol,* **8,** 203-214.

Frisa, P. S. and Jacobberger, J. W. (2002) Cell density related gene expression: SV40 large T antigen levels in immortalized astrocyte lines. *BMC Cell Biol,* **3,** 10.

Frizzo, J. K., Tramontina, A. C., Tramontina, F., Gottfried, C., Leal, R. B., Donato, R. and Gonçalves, C. A. (2004) Involvement of the S100B in cAMP-induced cytoskeleton remodeling in astrocytes: a study using TRTK-12 in digitonin-permeabilized cells. *Cell Mol Neurobiol,* **24,** 833-840.

Furihata, T., Ito, R., Kamiichi, A., Saito, K. and Chiba, K. (2016) Establishment and characterization of a new conditionally immortalized human astrocyte cell line. *J Neurochem,* **136,** 92-105.

Geller, H. M. and Dubois-Dalcq, M. (1988) Antigenic and functional characterization of a rat central nervous system-derived cell line immortalized by a retroviral vector. *J Cell Biol,* **107,** 1977-1986.

Gonçalves, C. A., Leite, M. C. and Nardin, P. (2008) Biological and methodological features of the measurement of S100B, a putative marker of brain injury. *Clin Biochem,* **41,** 755-763.

Gonzalez, M. e. L., Malemud, C. J. and Silver, J. (1993) Role of astroglial extracellular matrix in the formation of rat olfactory bulb glomeruli. *Exp Neurol,* **123,** 91-105.

González, M. I., Krizman-Genda, E. and Robinson, M. B. (2007) Caveolin-1 regulates the delivery and endocytosis of the glutamate transporter, excitatory amino acid carrier 1. *J Biol Chem,* **282,** 29855-29865.

Gordon, G. R., Mulligan, S. J. and MacVicar, B. A. (2007) Astrocyte control of the cerebrovasculature. *Glia,* **55,** 1214-1221.

Gould, G. W. and Lippincott-Schwartz, J. (2009) New roles for endosomes: from vesicular carriers to multi-purpose platforms. *Nat Rev Mol Cell Biol,* **10,** 287-292.

Groves, A. K., Entwistle, A., Jat, P. S. and Noble, M. (1993) The characterization of astrocyte cell lines that display properties of glial scar tissue. *Dev Biol,* **159,** 87-104.

Gruenberg, J. and van der Goot, F. G. (2006) Mechanisms of pathogen entry through the endosomal compartments. *Nat Rev Mol Cell Biol,* **7,** 495-504.

Guček, A., Vardjan, N. and Zorec, R. (2012) Exocytosis in astrocytes: transmitter release and membrane signal regulation. *Neurochem Res,* **37,** 2351-2363.

Guerra, M. C., Tortorelli, L. S., Galland, F., Da Ré, C., Negri, E., Engelke, D. S., Rodrigues, L., Leite, M. C. and Gonçalves, C. A. (2011) Lipopolysaccharide modulates astrocytic S100B secretion: a study in cerebrospinal fluid and astrocyte cultures from rats. *J Neuroinflammation,* **8,** 128.

Haghighat, N. (2005) Estrogen (17beta-estradiol) enhances glutamine synthetase activity in C6-glioma cells. *Neurochem Res,* **30,** 661-667.

Haghighat, N. and McCandless, D. W. (1997a) Effect of 6-aminonicotinamide on metabolism of astrocytes and C6-glioma cells. *Metab Brain Dis,* **12,** 29-45.

Haghighat, N. and McCandless, D. W. (1997b) Effect of ammonium chloride on energy metabolism of astrocytes and C6-glioma cells in vitro. *Metab Brain Dis,* **12,** 287-298.

Halassa, M. M., Fellin, T., Takano, H., Dong, J. H. and Haydon, P. G. (2007) Synaptic islands defined by the territory of a single astrocyte. *J Neurosci,* **27,** 6473-6477.

Hertz, L., Chen, Y. and Song, D. (2016) Astrocyte Cultures Mimicking Brain Astrocytes in Gene Expression, Signaling, Metabolism and K(+) Uptake and

Showing Astrocytic Gene Expression Overlooked by Immunohistochemistry and In Situ Hybridization. *Neurochem Res*.

Hertz, L., Chen, Y. and Song, D. (2017) Astrocyte Cultures Mimicking Brain Astrocytes in Gene Expression, Signaling, Metabolism and K(+) Uptake and Showing Astrocytic Gene Expression Overlooked by Immunohistochemistry and In Situ Hybridization. *Neurochem Res,* **42,** 254-271.

Herzfeld, A. (1973) The distribution between gamma-glutamylhydrozamate synthetase and L-glutamine-hydroxylamine glutamyltransferase activities in rat tissues. Studies in vitro. *Biochem J,* **133,** 49-57.

Holten, A. T. and Gundersen, V. (2008) Glutamine as a precursor for transmitter glutamate, aspartate and GABA in the cerebellum: a role for phosphate-activated glutaminase. *J Neurochem,* **104,** 1032-1042.

Hu, J., Castets, F., Guevara, J. L. and Van Eldik, L. J. (1996) S100 beta stimulates inducible nitric oxide synthase activity and mRNA levels in rat cortical astrocytes. *J Biol Chem,* **271,** 2543-2547.

Hu, J., Ferreira, A. and Van Eldik, L. J. (1997) S100beta induces neuronal cell death through nitric oxide release from astrocytes. *J Neurochem,* **69,** 2294-2301.

Hu, J. and Van Eldik, L. J. (1999) Glial-derived proteins activate cultured astrocytes and enhance beta amyloid-induced glial activation. *Brain Res,* **842,** 46-54.

Humphries, W. H., Szymanski, C. J. and Payne, C. K. (2011) Endo-lysosomal vesicles positive for Rab7 and LAMP1 are terminal vesicles for the transport of dextran. *PLoS One,* **6,** e26626.

Huttunen, H. J., Kuja-Panula, J., Sorci, G., Agneletti, A. L., Donato, R. and Rauvala, H. (2000) Coregulation of neurite outgrowth and cell survival by amphoterin and

S100 proteins through receptor for advanced glycation end products (RAGE) activation. *J Biol Chem,* **275,** 40096-40105.

Hyder, F., Patel, A. B., Gjedde, A., Rothman, D. L., Behar, K. L. and Shulman, R. G. (2006) Neuronal-glial glucose oxidation and glutamatergic-GABAergic function. *J Cereb Blood Flow Metab,* **26,** 865-877.

Iqbal, K. and Ottaway, J. H. (1970) Glutamine synthetase in muscle and kidney. *Biochem J,* **119,** 145-156.

Jayakumar, A. R. and Norenberg, M. D. (2016) Glutamine Synthetase: Role in Neurological Disorders. *Adv Neurobiol,* **13,** 327-350.

Johnson, K. M., Milner, R. and Crocker, S. J. (2015) Extracellular matrix composition determines astrocyte responses to mechanical and inflammatory stimuli. *Neurosci Lett,* **600,** 104-109.

Juurlink, B. H. (1982) Glutamine synthetase and glutamyltransferase activities in the mouse astrocyte in vitro. *Neurochem Res,* **7,** 905-910.

Kettenmann, H. and Verkhratsky, A. (2008) Neuroglia: the 150 years after. *Trends Neurosci,* **31,** 653-659.

Khandelwal, P. J., Herman, A. M. and Moussa, C. E. (2011) Inflammation in the early stages of neurodegenerative pathology. *J Neuroimmunol,* **238,** 1-11.

Kimelberg, H. K. and Nedergaard, M. (2010) Functions of astrocytes and their potential as therapeutic targets. *Neurotherapeutics,* **7,** 338-353.

King, L. S., Kozono, D. and Agre, P. (2004) From structure to disease: the evolving tale of aquaporin biology. *Nat Rev Mol Cell Biol,* **5,** 687-698.

Kinney, G. A. and Spain, W. J. (2002) Synaptically evoked GABA transporter currents in neocortical glia. *J Neurophysiol,* **88,** 2899-2908.

Kleindienst, A., Schmidt, C., Parsch, H., Emtmann, I., Xu, Y. and Buchfelder, M. (2010) The Passage of S100B from Brain to Blood Is Not Specifically Related to the Blood-Brain Barrier Integrity. *Cardiovasc Psychiatry Neurol,* **2010,** 801295.

Kosenko, E. A., Beloushko, E. E. and Kaminskiĭ, I. G. (2014a) [Differences between cerebellum and hippocampus in antioxidant system]. *Biomed Khim,* **60,** 469-472.

Kosenko, E. A., Tikhonova, L. A., Reddy, V. P., Aliev, G. and Kaminsky, Y. G. (2014b) Differential up-regulation of ammonia detoxifying enzymes in cerebral cortex, cerebellum, hippocampus, striatum and liver in hyperammonemia. *CNS Neurol Disord Drug Targets,* **13,** 1089-1095.

Krupenko, S. A. (2009) FDH: an aldehyde dehydrogenase fusion enzyme in folate metabolism. *Chem Biol Interact,* **178,** 84-93.

Kruse, A., Cesarini, K. G., Bach, F. W. and Persson, L. (1991) Increases of neuron-specific enolase, S-100 protein, creatine kinase and creatine kinase BB isoenzyme in CSF following intraventricular catheter implantation. *Acta Neurochir (Wien),* **110,** 106-109.

Kumada, Y., Benson, D. R., Hillemann, D., Hosted, T. J., Rochefort, D. A., Thompson, C. J., Wohlleben, W. and Tateno, Y. (1993) Evolution of the glutamine synthetase gene, one of the oldest existing and functioning genes. *Proc Natl Acad Sci U S A,* **90,** 3009-3013.

Lam, A. G., Koppal, T., Akama, K. T., Guo, L., Craft, J. M., Samy, B., Schavocky, J. P., Watterson, D. M. and Van Eldik, L. J. (2001) Mechanism of glial activation by S100B: involvement of the transcription factor NFkappaB. *Neurobiol Aging,* **22,** 765-772.

Lange, S. C., Bak, L. K., Waagepetersen, H. S., Schousboe, A. and Norenberg, M. D. (2012) Primary cultures of astrocytes: their value in understanding astrocytes in health and disease. *Neurochem Res,* **37,** 2569-2588.

Laterra, J. and Goldstein, G. W. (1991) Astroglial-induced in vitro angiogenesis: requirements for RNA and protein synthesis. *J Neurochem,* **57,** 1231-1239.

Leclerc, E., Fritz, G., Vetter, S. W. and Heizmann, C. W. (2009) Binding of S100 proteins to RAGE: an update. *Biochim Biophys Acta,* **1793,** 993-1007.

Lee, H. J., Suk, J. E., Bae, E. J. and Lee, S. J. (2008) Clearance and deposition of extracellular alpha-synuclein aggregates in microglia. *Biochem Biophys Res Commun,* **372,** 423-428.

Leis, J. A., Bekar, L. K. and Walz, W. (2005) Potassium homeostasis in the ischemic brain. *Glia,* **50,** 407-416.

Leite, M. C., Brolese, G., de Almeida, L. M., Piñero, C. C., Gottfried, C. and Gonçalves, C. A. (2006) Ammonia-induced alteration in S100B secretion in astrocytes is not reverted by creatine addition. *Brain Res Bull,* **70,** 179-185.

Leite, M. C., Galland, F., de Souza, D. F., Guerra, M. C., Bobermin, L., Biasibetti, R., Gottfried, C. and Gonçalves, C. A. (2009) Gap junction inhibitors modulate S100B secretion in astrocyte cultures and acute hippocampal slices. *J Neurosci Res,* **87,** 2439-2446.

Leuba, G. and Garey, L. J. (1989) Comparison of neuronal and glial numerical density in primary and secondary visual cortex of man. *Exp Brain Res,* **77,** 31-38.

Liaw, S. H., Kuo, I. and Eisenberg, D. (1995) Discovery of the ammonium substrate site on glutamine synthetase, a third cation binding site. *Protein Sci,* **4,** 2358-2365.

Lim, J. P. and Gleeson, P. A. (2011) Macropinocytosis: an endocytic pathway for internalising large gulps. *Immunol Cell Biol,* **89,** 836-843.

Lin, Y. C., Chow, C. W., Yuen, P. H. and Wong, P. K. (1997) Establishment and characterization of conditionally immortalized astrocytes to study their interaction with ts1, a neuropathogenic mutant of Moloney murine leukemia virus. *J Neurovirol,* **3,** 28-37.

Liu, X. P., Zheng, H. Y., Qu, M., Zhang, Y., Cao, F. Y., Wang, Q., Ke, D., Liu, G. P. and Wang, J. Z. (2012) Upregulation of astrocytes protein phosphatase-2A stimulates astrocytes migration via inhibiting p38 MAPK in tg2576 mice. *Glia,* **60,** 1279-1288.

Lukacs, Z., Nieves Cobos, P., Keil, A., Hartung, R., Mengel, E., Beck, M., Deschauer, M., Hanisch, F. and Santer, R. (2011) Dried blood spots in the diagnosis of lysosomal storage disorders--possibilities for newborn screening and high-risk population screening. *Clin Biochem,* **44,** 476.

Lutz, S. E., Zhao, Y., Gulinello, M., Lee, S. C., Raine, C. S. and Brosnan, C. F. (2009) Deletion of astrocyte connexins 43 and 30 leads to a dysmyelinating phenotype and hippocampal CA1 vacuolation. *J Neurosci,* **29,** 7743-7752.

Mandrekar, S., Jiang, Q., Lee, C. Y., Koenigsknecht-Talboo, J., Holtzman, D. M. and Landreth, G. E. (2009) Microglia mediate the clearance of soluble Abeta through fluid phase macropinocytosis. *J Neurosci,* **29,** 4252-4262.

Marenholz, I., Heizmann, C. W. and Fritz, G. (2004) S100 proteins in mouse and man: from evolution to function and pathology (including an update of the nomenclature). *Biochem Biophys Res Commun,* **322,** 1111-1122.

Marie, S. K. and Shinjo, S. M. (2011) Metabolism and brain cancer. *Clinics (Sao Paulo),* **66 Suppl 1,** 33-43.

Matés, J. M., Pérez-Gómez, C., Núñez de Castro, I., Asenjo, M. and Márquez, J. (2002) Glutamine and its relationship with intracellular redox status, oxidative stress and cell proliferation/death. *Int J Biochem Cell Biol,* **34,** 439-458.

Mayor, S. and Pagano, R. E. (2007) Pathways of clathrin-independent endocytosis. *Nat Rev Mol Cell Biol,* **8,** 603-612.

Mbele, G. O., Deloulme, J. C., Gentil, B. J., Delphin, C., Ferro, M., Garin, J., Takahashi, M. and Baudier, J. (2002) The zinc- and calcium-binding S100B interacts and co-localizes with IQGAP1 during dynamic rearrangement of cell membranes. *J Biol Chem,* **277,** 49998-50007.

McKenna, M. C. (2007) The glutamate-glutamine cycle is not stoichiometric: fates of glutamate in brain. *J Neurosci Res,* **85,** 3347-3358.

Megias, L., Guerri, C., Fornas, E. et al. (2000) Endocytosis and transcytosis in growing astrocytes in primary culture. Possible implications in neural development. *Int J Dev Biol,* **44,** 209-221.

Meister, A. (1968) The specificity of glutamine synthetase and its relationship to substrate conformation at the active site. *Adv Enzymol Relat Areas Mol Biol,* **31,** 183-218.

Meister, A. (1985) Glutamine synthetase from mammalian tissues. *Methods Enzymol,* **113,** 185-199.

Menet, V., Giménez y Ribotta, M., Chauvet, N., Drian, M. J., Lannoy, J., Colucci-Guyon, E. and Privat, A. (2001) Inactivation of the glial fibrillary acidic protein gene, but not that of vimentin, improves neuronal survival and neurite growth by modifying adhesion molecule expression. *J Neurosci,* **21,** 6147-6158.

Minet, R., Villie, F., Marcollet, M., Meynial-Denis, D. and Cynober, L. (1997) Measurement of glutamine synthetase activity in rat muscle by a colorimetric assay. *Clin Chim Acta,* **268,** 121-132.

Molofsky, A. V. and Deneen, B. (2015) Astrocyte development: A Guide for the Perplexed. *Glia,* **63,** 1320-1329.

Morikawa, M., Asai, K., Kokubo, M. et al. (2001) Isolation and characterization of a new immortal rat astrocyte with a high expression of NGF mRNA. *Neurosci Res,* **39,** 205-212.

Nardin, P., Tramontina, F., Leite, M. C., Tramontina, A. C., Quincozes-Santos, A., de Almeida, L. M., Battastini, A. M., Gottfried, C. and Gonçalves, C. A. (2007) S100B content and secretion decrease in astrocytes cultured in high-glucose medium. *Neurochem Int,* **50,** 774-782.

Neumann, H., Kotter, M. R. and Franklin, R. J. (2009) Debris clearance by microglia: an essential link between degeneration and regeneration. *Brain,* **132,** 288-295.

Nodin, C., Nilsson, M. and Blomstrand, F. (2005) Gap junction blockage limits intercellular spreading of astrocytic apoptosis induced by metabolic depression. *J Neurochem,* **94,** 1111-1123.

Oberheim, N. A., Takano, T., Han, X. et al. (2009) Uniquely hominid features of adult human astrocytes. *J Neurosci,* **29,** 3276-3287.

Oliveira, J. F., Sardinha, V. M., Guerra-Gomes, S., Araque, A. and Sousa, N. (2015) Do stars govern our actions? Astrocyte involvement in rodent behavior. *Trends Neurosci,* **38,** 535-549.

Olsen, M. L. and Sontheimer, H. (2008) Functional implications for Kir4.1 channels in glial biology: from K+ buffering to cell differentiation. *J Neurochem,* **107,** 589-601.

Ostendorp, T., Leclerc, E., Galichet, A., Koch, M., Demling, N., Weigle, B., Heizmann, C. W., Kroneck, P. M. and Fritz, G. (2007) Structural and functional insights into RAGE activation by multimeric S100B. *EMBO J,* **26,** 3868-3878.

Ostroff, L. E., Manzur, M. K., Cain, C. K. and Ledoux, J. E. (2014) Synapses lacking astrocyte appear in the amygdala during consolidation of Pavlovian threat conditioning. *J Comp Neurol,* **522,** 2152-2163.

Paemeleire, K. and Leybaert, L. (2000) ATP-dependent astrocyte-endothelial calcium signaling following mechanical damage to a single astrocyte in astrocyte-endothelial co-cultures. *J Neurotrauma,* **17,** 345-358.

Pallardó, F. V., Markovic, J., García, J. L. and Viña, J. (2009) Role of nuclear glutathione as a key regulator of cell proliferation. *Mol Aspects Med,* **30,** 77-85.

Palos, T. P., Ramachandran, B., Boado, R. and Howard, B. D. (1996) Rat C6 and human astrocytic tumor cells express a neuronal type of glutamate transporter. *Brain Res Mol Brain Res,* **37,** 297-303.

Papadopoulos, M. C. and Verkman, A. S. (2013) Aquaporin water channels in the nervous system. *Nat Rev Neurosci,* **14,** 265-277.

Parker, K. K., Norenberg, M. D. and Vernadakis, A. (1980) "Transdifferentiation" of C6 glial cells in culture. *Science,* **208,** 179-181.

Parpura, V., Baker, B. J., Jeras, M. and Zorec, R. (2010) Regulated exocytosis in astrocytic signal integration. *Neurochem Int,* **57,** 451-459.

Parpura, V. and Zorec, R. (2010) Gliotransmission: Exocytotic release from astrocytes. *Brain Res Rev,* **63,** 83-92.

Passaquin, A. C., Schreier, W. A. and de Vellis, J. (1994) Gene expression in astrocytes is affected by subculture. *Int J Dev Neurosci,* **12,** 363-372.

Patel, A. J., Weir, M. D., Hunt, A., Tahourdin, C. S. and Thomas, D. G. (1985) Distribution of glutamine synthetase and glial fibrillary acidic protein and correlation of glutamine synthetase with glutamate decarboxylase in different regions of the rat central nervous system. *Brain Res,* **331,** 1-9.

Pellerin, L. (2008) Brain energetics (thought needs food). *Curr Opin Clin Nutr Metab Care,* **11,** 701-705.

Pellerin, L. and Magistretti, P. J. (1994) Glutamate uptake into astrocytes stimulates aerobic glycolysis: a mechanism coupling neuronal activity to glucose utilization. *Proc Natl Acad Sci U S A,* **91,** 10625-10629.

Perea, G. and Araque, A. (2005) Glial calcium signaling and neuron-glia communication. *Cell Calcium,* **38,** 375-382.

Perrone, L., Peluso, G. and Melone, M. A. (2008) RAGE recycles at the plasma membrane in S100B secretory vesicles and promotes Schwann cells morphological changes. *J Cell Physiol,* **217,** 60-71.

Pesole, G., Bozzetti, M. P., Lanave, C., Preparata, G. and Saccone, C. (1991) Glutamine synthetase gene evolution: a good molecular clock. *Proc Natl Acad Sci U S A,* **88,** 522-526.

Petrova, T. V., Hu, J. and Van Eldik, L. J. (2000) Modulation of glial activation by astrocyte-derived protein S100B: differential responses of astrocyte and microglial cultures. *Brain Res,* **853,** 74-80.

Pinto, S. S., Gottfried, C., Mendez, A., Gonçalves, D., Karl, J., Gonçalves, C. A., Wofchuk, S. and Rodnight, R. (2000) Immunocontent and secretion of S100B in astrocyte cultures from different brain regions in relation to morphology. *FEBS Lett,* **486,** 203-207.

Plog, B. A., Dashnaw, M. L., Hitomi, E., Peng, W., Liao, Y., Lou, N., Deane, R. and Nedergaard, M. (2015) Biomarkers of traumatic injury are transported from brain to blood via the glymphatic system. *J Neurosci,* **35,** 518-526.

Ponath, G., Schettler, C., Kaestner, F., Voigt, B., Wentker, D., Arolt, V. and Rothermundt, M. (2007) Autocrine S100B effects on astrocytes are mediated via RAGE. *J Neuroimmunol,* **184,** 214-222.

Potokar, M., Korva, M., Jorgačevski, J., Avšič-Županc, T. and Zorec, R. (2014) Tick-borne encephalitis virus infects rat astrocytes but does not affect their viability. *PLoS One,* **9,** e86219.

Potokar, M., Kreft, M., Li, L., Daniel Andersson, J., Pangrsic, T., Chowdhury, H. H., Pekny, M. and Zorec, R. (2007) Cytoskeleton and vesicle mobility in astrocytes. *Traffic,* **8,** 12-20.

Potokar, M., Kreft, M., Pangrsic, T. and Zorec, R. (2005) Vesicle mobility studied in cultured astrocytes. *Biochem Biophys Res Commun,* **329,** 678-683.

Potokar, M., Stenovec, M., Gabrijel, M., Li, L., Kreft, M., Grilc, S., Pekny, M. and Zorec, R. (2010) Intermediate filaments attenuate stimulation-dependent mobility of endosomes/lysosomes in astrocytes. *Glia,* **58,** 1208-1219.

Potokar, M., Stenovec, M., Kreft, M., Kreft, M. E. and Zorec, R. (2008) Stimulation inhibits the mobility of recycling peptidergic vesicles in astrocytes. *Glia,* **56,** 135-144.

Potokar, M., Vardjan, N., Stenovec, M., Gabrijel, M., Trkov, S., Jorgačevski, J., Kreft, M. and Zorec, R. (2013) Astrocytic vesicle mobility in health and disease. *Int J Mol Sci,* **14,** 11238-11258.

Rajendran, L., Knölker, H. J. and Simons, K. (2010) Subcellular targeting strategies for drug design and delivery. *Nat Rev Drug Discov,* **9,** 29-42.

Raju, T. R., Bignami, A. and Dahl, D. (1980) Glial fibrillary acidic protein in monolayer cultures of C-6 glioma cells: effect of aging and dibutyryl cyclic AMP. *Brain Res,* **200,** 225-230.

Reali, C., Pillai, R., Saba, F., Cabras, S., Michetti, F. and Sogos, V. (2012) S100B modulates growth factors and costimulatory molecules expression in cultured human astrocytes. *J Neuroimmunol,* **243,** 95-99.

Reali, C., Scintu, F., Pillai, R., Donato, R., Michetti, F. and Sogos, V. (2005) S100b counteracts effects of the neurotoxicant trimethyltin on astrocytes and microglia. *J Neurosci Res,* **81,** 677-686.

Regan, M. R., Huang, Y. H., Kim, Y. S., Dykes-Hoberg, M. I., Jin, L., Watkins, A. M., Bergles, D. E. and Rothstein, J. D. (2007) Variations in promoter activity reveal a differential expression and physiology of glutamate transporters by glia in the developing and mature CNS. *J Neurosci,* **27,** 6607-6619.

Ribeiro, L. C., Quincozes-Santos, A., Leite, M. C. et al. (2009) Caloric restriction increases hippocampal glutamate uptake and glutamine synthetase activity in Wistar rats. *Neurosci Res,* **64,** 330-334.

Ronzio, R. A., Wilk, S., Rowe, W. B. and Meister, A. (1969) Preparation and studies on the characterization of sheep brain glutamine synthetase. *Biochemistry,* **8,** 2670-2674.

Rose, C. F., Verkhratsky, A. and Parpura, V. (2013) Astrocyte glutamine synthetase: pivotal in health and disease. *Biochem Soc Trans*, **41,** 1518-1524.

Rothermundt, M., Peters, M., Prehn, J. H. and Arolt, V. (2003) S100B in brain damage and neurodegeneration. *Microsc Res Tech,* **60,** 614-632.

Rouach, N., Avignone, E., Même, W., Koulakoff, A., Venance, L., Blomstrand, F. and Giaume, C. (2002) Gap junctions and connexin expression in the normal and pathological central nervous system. *Biol Cell,* **94,** 457-475.

Rustandi, R. R., Baldisseri, D. M. and Weber, D. J. (2000) Structure of the negative regulatory domain of p53 bound to S100B(betabeta). *Nat Struct Biol,* **7,** 570-574.

Salter, M. W. and Hicks, J. L. (1994) ATP-evoked increases in intracellular calcium in neurons and glia from the dorsal spinal cord. *J Neurosci,* **14,** 1563-1575.

Scemes, E. and Giaume, C. (2006) Astrocyte calcium waves: what they are and what they do. *Glia,* **54,** 716-725.

Schliwa, M., Euteneuer, U., Bulinski, J. C. and Izant, J. G. (1981) Calcium lability of cytoplasmic microtubules and its modulation by microtubule-associated proteins. *Proc Natl Acad Sci U S A,* **78,** 1037-1041.

Scott, C. C., Vacca, F. and Gruenberg, J. (2014) Endosome maturation, transport and functions. *Semin Cell Dev Biol,* **31,** 2-10.

Seifert, G., Henneberger, C. and Steinhäuser, C. (2016) Diversity of astrocyte potassium channels: An update. *Brain Res Bull*.

Seifert, G., Schilling, K. and Steinhäuser, C. (2006) Astrocyte dysfunction in neurological disorders: a molecular perspective. *Nat Rev Neurosci,* **7,** 194-206.

Seiler, N., Reid, J. and Knödgen, B. (1990) A sensitive method for the assay of glutamine synthetase. *Neurochem Res,* **15,** 301-305.

Selinfreund, R. H., Barger, S. W., Pledger, W. J. and Van Eldik, L. J. (1991) Neurotrophic protein S100 beta stimulates glial cell proliferation. *Proc Natl Acad Sci U S A,* **88,** 3554-3558.

Simpson, J. E., Ince, P. G., Lace, G. et al. (2010) Astrocyte phenotype in relation to Alzheimer-type pathology in the ageing brain. *Neurobiol Aging,* **31,** 578-590.

Sofroniew, M. V. (2009) Molecular dissection of reactive astrogliosis and glial scar formation. *Trends Neurosci,* **32,** 638-647.

Sofroniew, M. V. (2015) Astrocyte barriers to neurotoxic inflammation. *Nat Rev Neurosci,* **16,** 249-263.

Sofroniew, M. V. and Vinters, H. V. (2010) Astrocytes: biology and pathology. *Acta Neuropathol,* **119,** 7-35.

Soldati, T. and Schliwa, M. (2006) Powering membrane traffic in endocytosis and recycling. *Nat Rev Mol Cell Biol,* **7,** 897-908.

Sorci, G., Agneletti, A. L., Bianchi, R. and Donato, R. (1998) Association of S100B with intermediate filaments and microtubules in glial cells. *Biochim Biophys Acta,* **1448,** 277-289.

Sorci, G., Riuzzi, F., Arcuri, C., Tubaro, C., Bianchi, R., Giambanco, I. and Donato, R. (2013) S100B protein in tissue development, repair and regeneration. *World J Biol Chem,* **4,** 1-12.

Souza, D. G., Bellaver, B., Souza, D. O. and Quincozes-Santos, A. (2013) Characterization of adult rat astrocyte cultures. *PLoS One,* **8,** e60282.

Stadtman, E. R., Shapiro, B. M., Ginsburg, A., Kingdon, H. S. and Denton, M. D. (1968) Regulation of glutamine synthetase activity in Escherichia coli. *Brookhaven Symp Biol,* **21,** 378-396.

Steiner, J., Bogerts, B., Schroeter, M. L. and Bernstein, H. G. (2011) S100B protein in neurodegenerative disorders. *Clin Chem Lab Med,* **49,** 409-424.

Stenovec, M., Kreft, M., Grilc, S., Potokar, M., Kreft, M. E., Pangrsic, T. and Zorec, R. (2007) Ca2+-dependent mobility of vesicles capturing anti-VGLUT1 antibodies. *Exp Cell Res,* **313,** 3809-3818.

Stenovec, M., Trkov, S., Kreft, M. and Zorec, R. (2014) Alterations of calcium homoeostasis in cultured rat astrocytes evoked by bioactive sphingolipids. *Acta Physiol (Oxf),* **212,** 49-61.

Stenovec, M., Trkov, S., Lasič, E., Terzieva, S., Kreft, M., Rodríguez Arellano, J. J., Parpura, V., Verkhratsky, A. and Zorec, R. (2016) Expression of familial Alzheimer disease presenilin 1 gene attenuates vesicle traffic and reduces peptide secretion in cultured astrocytes devoid of pathologic tissue environment. *Glia,* **64,** 317-329.

Szymanski, C. J., Humphries, W. H. and Payne, C. K. (2011) Single particle tracking as a method to resolve differences in highly colocalized proteins. *Analyst,* **136,** 3527-3533.

Tabernero, A., Medina, J. M. and Giaume, C. (2006) Glucose metabolism and proliferation in glia: role of astrocytic gap junctions. *J Neurochem,* **99,** 1049-1061.

Tabuchi, K., Imada, M. and Nishimoto, A. (1982) Effects of cyclic AMP on S-100 protein level in C-6 glioma cells. *J Neurol Sci,* **56,** 57-63.

Thilo, L., Stroud, E. and Haylett, T. (1995) Maturation of early endosomes and vesicular traffic to lysosomes in relation to membrane recycling. *J Cell Sci,* **108 (Pt 4),** 1791-1803.

Tomaselli, K. J., Neugebauer, K. M., Bixby, J. L., Lilien, J. and Reichardt, L. F. (1988) N-cadherin and integrins: two receptor systems that mediate neuronal process outgrowth on astrocyte surfaces. *Neuron,* **1,** 33-43.

Trabelsi, Y., Amri, M., Becq, H., Molinari, F. and Aniksztejn, L. (2017) The conversion of glutamate by glutamine synthase in neocortical astrocytes from juvenile rat is important to limit glutamate spillover and peri/extrasynaptic activation of NMDA receptors. *Glia,* **65,** 401-415.

Tramontina, A. C., Tramontina, F., Bobermin, L. D., Zanotto, C., Souza, D. F., Leite, M. C., Nardin, P., Gottfried, C. and Gonçalves, C. A. (2008) Secretion of S100B, an astrocyte-derived neurotrophic protein, is stimulated by fluoxetine via a mechanism independent of serotonin. *Prog Neuropsychopharmacol Biol Psychiatry*, **32,** 1580-1583.

Tramontina, F., Leite, M. C., Gonçalves, D. et al. (2006) High glutamate decreases S100B secretion by a mechanism dependent on the glutamate transporter. *Neurochem Res,* **31,** 815-820.

Turnquist, C., Horikawa, I., Foran, E., Major, E. O., Vojtesek, B., Lane, D. P., Lu, X., Harris, B. T. and Harris, C. C. (2016) p53 isoforms regulate astrocyte-mediated neuroprotection and neurodegeneration. *Cell Death Differ,* **23,** 1515-1528.

Vaca, K. and Wendt, E. (1992) Divergent effects of astroglial and microglial secretions on neuron growth and survival. *Exp Neurol,* **118,** 62-72.

Van Eldik, L. J. and Wainwright, M. S. (2003) The Janus face of glial-derived S100B: beneficial and detrimental functions in the brain. *Restor Neurol Neurosci,* **21,** 97-108.

Vanhoutte, N. and Hermans, E. (2008) Glutamate-induced glioma cell proliferation is prevented by functional expression of the glutamate transporter GLT-1. *FEBS Lett,* **582,** 1847-1852.

Vardjan, N., Gabrijel, M., Potokar, M. et al. (2012) IFN-γ-induced increase in the mobility of MHC class II compartments in astrocytes depends on intermediate filaments. *J Neuroinflammation,* **9,** 144.

Vasile, F., Dossi, E. and Rouach, N. (2017) Human astrocytes: structure and functions in the healthy brain. *Brain Struct Funct*.

Villarreal, A., Aviles Reyes, R. X., Angelo, M. F., Reines, A. G. and Ramos, A. J. (2011) S100B alters neuronal survival and dendrite extension via RAGE-mediated NF-κB signaling. *J Neurochem,* **117,** 321-332.

Villarreal, A., Seoane, R., González Torres, A., Rosciszewski, G., Angelo, M. F., Rossi, A., Barker, P. A. and Ramos, A. J. (2014) S100B protein activates a RAGE-dependent autocrine loop in astrocytes: implications for its role in the propagation of reactive gliosis. *J Neurochem*.

Vives, V., Alonso, G., Solal, A. C., Joubert, D. and Legraverend, C. (2003) Visualization of S100B-positive neurons and glia in the central nervous system of EGFP transgenic mice. *J Comp Neurol,* **457,** 404-419.

Wang, D. D. and Bordey, A. (2008) The astrocyte odyssey. *Prog Neurobiol,* **86,** 342-367.

Wang, Y., Kudoh, J., Kubota, R., Asakawa, S., Minoshima, S. and Shimizu, N. (1996) Chromosomal mapping of a family of human glutamine synthetase genes: functional gene (GLUL) on 1q25, pseudogene (GLULP) on 9p13, and three related genes (GLULL1, GLULL2, GLULL3) on 5q33, 11p15, and 11q24. *Genomics,* **37,** 195-199.

Wilder, P. T., Lin, J., Bair, C. L. et al. (2006) Recognition of the tumor suppressor protein p53 and other protein targets by the calcium-binding protein S100B. *Biochim Biophys Acta,* **1763,** 1284-1297.

Wilhelmsson, U., Li, L., Pekna, M. et al. (2004) Absence of glial fibrillary acidic protein and vimentin prevents hypertrophy of astrocytic processes and improves post-traumatic regeneration. *J Neurosci,* **24,** 5016-5021.

Wyss-Coray, T., Loike, J. D., Brionne, T. C., Lu, E., Anankov, R., Yan, F., Silverstein, S. C. and Husemann, J. (2003) Adult mouse astrocytes degrade amyloid-beta in vitro and in situ. *Nat Med,* **9,** 453-457.

Xiong, Z., O'Hanlon, D., Becker, L. E., Roder, J., MacDonald, J. F. and Marks, A. (2000) Enhanced calcium transients in glial cells in neonatal cerebellar cultures derived from S100B null mice. *Exp Cell Res,* **257,** 281-289.

Yamamoto, H., Konno, H., Yamamoto, T., Ito, K., Mizugaki, M. and Iwasaki, Y. (1987) Glutamine synthetase of the human brain: purification and characterization. *J Neurochem,* **49,** 603-609.

Yan, S. D., Chen, X., Fu, J. et al. (1996) RAGE and amyloid-beta peptide neurotoxicity in Alzheimer's disease. *Nature,* **382,** 685-691.

Yang, Y., Vidensky, S., Jin, L., Jie, C., Lorenzini, I., Frankl, M. and Rothstein, J. D. (2011) Molecular comparison of GLT1+ and ALDH1L1+ astrocytes in vivo in astroglial reporter mice. *Glia,* **59,** 200-207.

Zhang, L., Liu, W., Alizadeh, D., Zhao, D., Farrukh, O., Lin, J., Badie, S. A. and Badie, B. (2011) S100B attenuates microglia activation in gliomas: possible role of STAT3 pathway. *Glia,* **59,** 486-498.

Zhang, Y., Sloan, S. A., Clarke, L. E. et al. (2016) Purification and Characterization of Progenitor and Mature Human Astrocytes Reveals Transcriptional and Functional Differences with Mouse. *Neuron,* **89,** 37-53.

Zhou, D., Jiang, X., Xu, R., Cai, Y., Hu, J., Xu, G., Zou, Y. and Zeng, Y. (2008) Assessing the cytoskeletal system and its elements in C6 glioma cells and astrocytes by atomic force microscopy. *Cell Mol Neurobiol,* **28,** 895-905.

Zorec, R., Horvat, A., Vardjan, N. and Verkhratsky, A. (2015) Memory Formation Shaped by Astroglia. *Front Integr Neurosci,* **9,** 56.